Murdoch
UNIVERSITY

Thesis

Photobioreactor design for microalgae cultivation using a thermoelectric cooler for temperature control

Author

Vincent Blagotinsek

Supervisor

Dr David Parlevliet

November 2018

Submitted to the School of Engineering and Information Technology, Murdoch University in Partial fulfilment of the requirements for the degree of

Bachelor of Engineering Honours (BE(Hons))

Instrumentation and Process control, Renewable Energy.

Page Intentionally left Blank Page

Authors Declaration

I Vincent Blagotinsek the author confirm that the work presented in paper is my own true work conducted by my own independent study. I am the sole author of the research.

Page Intentionally left Blank Page

Abstract

This thesis aims to design a photobioreactor that has a low capital investment so microalgae cultivation becomes cheaper. Implementation of temperature control is achieved by a thermoelectric cooling (TEC) device by pulse width modulation.

Materials of cheap cost from local vendors are availabe including low thermal conductivity materials like foam insulation and temperature sensors that have accurate measurement. Arduino based sensors of low cost are used to obtain process variable information of the system such as lux intensity, internal ambient temperature, and the temperature of a 500 mL flask of water. Power supplies are used to supply a 12 VDC connection to the LED lights, mixing motor and TEC. Switching of these voltages is done with MOSFETs to achieve a variable voltage.

Understanding the capabilities of a temperature feedback control by implementation of temperature sensors is investigated and it was found that high-frequency feedback signals cause antireset windup and overheating of components. On/off switching is also implemented to negate the high frequency switching issues while PI controller installation is discussed and favours the PBR sensor over the internal ambient temperature sensor.

The lower temperature regions of the PBR are unatainable which results in PV offset and hardly noticable temperature changes that are not desirable. A remedy to solve the issue suggests that materials with high thermal conductivities should provide better heat energy transfers when using TECs. Lux lighting sensor illustrates the maximum achievable LED intensity. Undesirable heat energy generated by the LED lights will increase the internal PBR temperature.

Overall TECs are very costly to run because heatsinks and fans for heat extraction are required for heat removal, while the TEC devices for this research is not efficient enough to get to the lower temperature regions. This research concludes that cheap quality electrical components will achieve strict control of variables while it is possible to create low budget microalgae monitoring systems.

Acknowledgements

First and foremost, I would like to thank my beautiful wife, Crystal. Your continuous encouragement and vigour are what got me through. I watched how hard you worked to ensure I had everything required to complete my degree. Sometimes it was a little unfair that you had to bear so much, but you never complained.

Secondly my family Andrey, Gwen, Dad and Mum, we have all been through a lot, and I am so grateful that Dad is still with us today. My extended family thank you for always being there for me you are all an incredible bunch of people.

My friends for always paying for my dinners when we went out to eat, I owe each one of you a big thanks your friendships are genuinely one of a kind.

Dr David Parlevliet my supervisor, I thank you for your guidance and support through this final chapter it was a delight to work under you. Salman thank you for the support to get me started. Jeff Laava thank you for being a kind spirit and assisting with ordering the parts; you're passing is a shock, it was always a delight to come see you… goodbye friend.

Page Intentionally left Blank Page

Dedication

Dearest Chloé, there is much to learn, and what we set our path to is never easy. All I wish for you, is to do something that is good for you and that it makes you incredibly happy, never give up on that.

Love always Daddy :)

Table of Contents

List of Figures

List of Tables

Nomenclature

LED	Light-emitting diode	**PCB**	Printed Circuit Board
RGB	Red, Green, Blue	**COP**	Coefficient of performance
PAR	Photosynthetically active radiation	**PFD**	Photon flux density
PWM	Pulse Width Modulation	**MV**	Manipulated Variable
TEC	Thermoelectric cooler	**PID**	Proportional Integral Derivative
RPM	Rotations / Revolutions per minute	**LIFA**	LabVIEW interface for Arduino
PBR	Photobioreactor	**MV**	Manipulated variable
IP Rating	Ingress Protection Rating	**PV**	Process variable
PCB	Printed Circuit board	**MOSFETs**	Metal oxide semiconductor field effect transistor
SP	Setpoint		

Chapter 1. Introduction

Microalgae generally aquatic based and complex have many influencing factors affecting their growth, while benefits like high-value products for dietary supplementation, renewable energy and treatments of hazardous contaminants are of high interest because of its many unique properties [1], [2], [3], [4], [5].

Microalgae commercial farming has seen many changes since the late 19th century and today cultivation methods of microalgae consists of optimising the growth rates for higher biomass yields that are economically viable [2], [6]. This is done by closed or open cultivation methods like tanks or ponds to simulate the natural habitat at the optimal conditions [6]. The tanks are known as photobioreactors (PBRs) and are arranged in a closed system. Materials that PBRs are constructed from is glass, plastic or metals.

Closed PBRs are used for tight control that can monitor, maintain and protect microalgae culture from environmental conditions [7], [8], [9]. Typical designs include Tubular which is better known as manifold PBRs (horizontal) or Serpentine PBRs (vertical), Flat Panel PBRs and column PBRs, each of them has one advantage over the other [7].

Effective photosynthesis can be performed when PBRs are designed around concepts that are efficient in light capture, and the distribution of the light to the microalgae. Precise control of the variables like temperature also encourage cell growth and offer the user the ability to experiment and implement conditions that promote cell growth [10], [11].

Closed PBRs have the advantage of better temperature control over a wide range of species as mentioned by M. Borowitzka [12], and asserts that a broad range of algal species can be cultivated [12]. M. Borowitzka further suggests that temperature control can be done by a heat exchanger or evaporative cooling [12].

As the microalgae inside the photobioreactor begins to grow, the density of the culture begins to increase, this affects the light intensity and causes a reduced effect on the exponential growth phase [13]. Some of the factors explored today are the photoperiod duration and light intensity that can have a positive or negative effect on the growth rates of microalgae [14]. For example, *Nannochloropsis sp* was cultivated over a 9-day period and exposed to three different

photoperiod regimes and three different light intensities (50, 100 and 200 μmol/m^2 s) with (12:12,18:06 and 24:00) respectively. Results concluded that 100 μmol/m^2 s with an 18:06 light:dark ratio performed the best.

Microalgae species usually have the optimal growth temperature between 20 ºC to 25 ºC [15]. While other temperature ranges that microalgae species experience is between 15 ºC to 30 ºC suggesting that microalgae species are different and broad [15]. Microalgae that grow over a broad range of temperatures are usually economically viable. Selection of geographical locations that attest to microalgae's optimal temperatures will enable the microalgae to flourish and produce products that are of high value [16].

The motivation for this research is to design a microenvironment around some of the parameters that can cultivate microalgae as close to the optimal photosynthetic yields at a low budget.

The aims the project outline is, build a closed microenvironment to understand the economic viability of thermoelectric coolers and if they are effective at cultivating microalgae with the emphasis of the design to keep capital cost low. Implement a control scheme under the pulse width modulation (PWM) and compared with on/off control highlight the most effective control logic.

The thesis is structured in the following way. Chapter 2 methods illustrate the required equipment and online citations to the datasheets. While design builds on the constraints and construction of the housing including software design, controller design, sizing and electrical layout. In chapter 3 the results will obtain temperature information, calibration curves and lux intensity. Discussion summarised the findings and justification into the results are postulated. The paper concludes on the overall progress and suggests further research methods. Appendices are provided, and the reader will be notified when to view the appropriate sections.

1.1 Literature review

Microalgae generally aquatic based have been cultivated for development and studies [1],[2]. Microalgae is complex and has many influencing factors that are immensely crucial for growth and production [5].

Murdoch University Algae R&D Centre requires a design that a temperature range of 15 ºC – 30 ºC can operate within. The PAR range in the wavelength must be adjustable with data logging capabilities.

The purpose of this research is for engineers who need to understand the factors affecting growth and in doing so, gain a better understanding of the variables that influence growth rates. Microalgae is complex, many researchers have already pioneered years of research, this paper does not fulfil every aspect of microalgae research, it is a brief overview mainly focused on variables that influence high growth rates.

Various journals and databases were visited using the Murdoch university library which includes the latest algae research books from the vast selection at Murdoch University Perth W.A. Two significant sections explore the literature ahead. Firstly, the variables affecting growth; a broader review is emphasised on light intensity, wavelength and temperature. While the nutrients topic illustrates other variables that affect the growth rate of algae. Secondly algae cultivation; Effective photobioreactor design is deeply investigated and suggested methods of temperature control is reviewed.

Therefore, the objective of this literature review aims to address the following; what are the immediate variables that influence maximum biomass production and what variables can the designer control to enhance the production.

1.2 Variables affecting growth rates

1.2.1 Light intensity and wavelength

The amount of light exposure stimulates algae growth, too much light at high intensities can create irreversible oxidative damages [5]. B. Cheirsilp et al. [17], found that increasing the light intensity from 2000 up to 10,000 lux a noticeable decline in growth rate could be observed [17]. Photosynthetically active radiation (PAR) is defined as the energy flux in the waveband between 400-700nm as depicted in **Figure 1-1** [18]. W. Lunche et al. [19], asserts this amount of solar electromagnetic radiation is what plants require in order to perform photosynthesis [19].

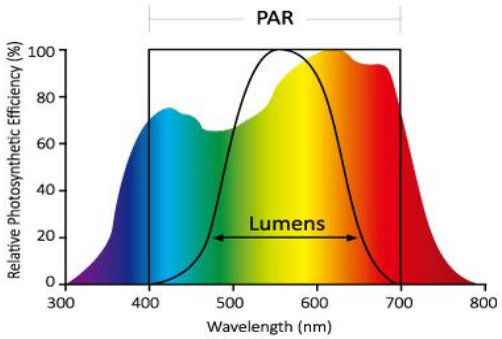

Figure 1-1 Wavelength in nm, a visible location of the PAR region Photosynthetic active region of plants and algae [20].

Controlled and measured illumination has been the preferred method when it comes to increasing the productivity of algae biomass [21]. Light emitting diodes (LEDs) can exhibit various types of colours compared to their counterparts; the more traditional white light [22]. H. Tang et al. There are many ways to measure light effectivity, one method is to measure light using a light metre to obtain readings over the PBR then average them out [23].

Studies by P. Das et al. [24] reveal, specific growth rates (μ) for *Nannochloropsis sp*, under blue LED light (470 nm) with exposures of 800 – 1000 lux produces the highest biomass growth rates compared to its other colour spectrums of green, red, yellow and white. The results found that light with shorter wavelengths has a much more significant impact on the photosynthetic efficiencies [24].

On the other hand, T. Mooij et al. [25] claims that exposure of 1500 μmol photons / m^2 s of yellow wavelength light on *Chlamydomonas reinhardtii* a single cell green alga had a low biomass yield

[25]. Supplementing 50 μmol-photons/m^2 s of yellow light with blue light and still maintaining a total combined yellow and blue exposure of 1500 μmol photons / m^2 s, the biomass yield recorded had increased [25]. The paper reveals a possible cause is the wavelength deficiencies that white, yellow or green light emit [25].

W. Gruszecki et al. [26] asserts that blue light has considerable effects towards growth rates and triggers mechanisms for metabolic regulation like light harvesting for photosynthesis. Also, C. Ra et al. [27] mentions that blue LED light could enhance the production of *chlorophylls* algae because they have two absorption bands at blue (400-500 nm) [27].

The second experiment does not support the idea that yellow light yields more algae growth compared to blue light because; 50 μmol photons / m^2 s of the yellow light was supplemented with blue light [25]. Both experimental results have different conditions towards the light, and different algae strains have different characteristics, although yellow light supplementation was used the common factor between both experiments exists that, blue light plays a vital role in algae productivity [24],[25].

Optimal light cycle experiments reveal that various light intensities ranging from Photon flux density (PFD) 70 – 273.1 μmol photons / m^2 s had increased growth on the microalgae, *Neochloris oleoabundans* as the biomass culture began to densify [13]. Results in **Figure 1-2** concluded that regardless of other factors that contribute to biomass concentration, PFD of 91.2 – 177.8 μmol photons / m^2 s is chosen because of the photosaturation which occurs before 200 μmol photons / m^2 s [13].

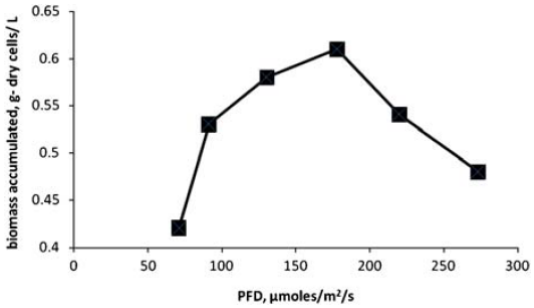

Figure 1-2 Effect of various Photon Flux densities on culture growth
Increasing the light intensity as biomass concentration increases show growth of concentration. Photosaturation occurs at 180 μmol photons / m^2 s [13].

1.2.2 Light absorbance and transmittance

Microalgae require a right amount of light for growth, low levels of light will reduce the growth rates whereas too much light will cause photoinhibition [28]. Linear increases in photosynthetic activity is observed when light exposure is low, and by the time the light begins to intensify, maximum photosynthetic rates are observed [29].

Q. Bechet et al. [30], defines three types of models categorised on their ability to account for light gradients [30]. Type II models is defined over a range of design and operational conditions that can accurately predict the algae production [30]. Type II models outlined in this research included Lambert-Beer Law, a simplified two-flux model and the radiative transfer equation (RTE) [30].

J.F. Cornet et al. [31], reported that Two flux model leads to very complex partial differential equations to resemble the field of radiation with two opposite fluxes F_z^+ and F_z^- [31]. While W.G. Houf et al. [32], established five methods to calculate RTE that take into account the aqueous suspension and the variables acting upon it; such as optical depth, incident radiation and scattering [32].

W. Balken et al. [29] maintains that Lambert-Beer Law is the simplest of all three mentioned above although light absorption is taken into account; still, Beer's law can be improved by including scattering of light [29].

Beer's law describes how optical absorbance (A) is measured in relation to the optical path length (l) of the concentration $([C])$ where (ε) is described to be the molar absorption constant [33].

$$A = \varepsilon l[C] \tag{1}$$

Eq. (2) the transmittance (T) which is a ratio of the light intensity that has already passed through the concentration (I_{tr}) and light intensity that entered the concentration sample (I_{inc}) [33].

$$T = \frac{I_{tr}}{I_{inc}} \tag{2}$$

By combining Eq. (1) and (2), Lambert-Beer law is obtained which relates the absorption and the transmittance, Eq. (3) [33].

$$A = -\log\left(\frac{I_{tr}}{I_{inc}}\right) \tag{3}$$

F. Fernandez et al. [34] claim that that successful estimation of biomass concentration is possible as the attenuation increases, it is shown by proposing the hyperbolic model, Eq. (4) [34]. (At), Maximum attenuation achievable (A_{tmax}), and (Kat) constants which has been derived from a table of figures [34]. Illustrated below in **Figure 1-3** biomass concentration with attenuation on the Y-axis.

$$At = \frac{A_{tmax} \cdot [C]}{Kat + [C]} \tag{4}$$

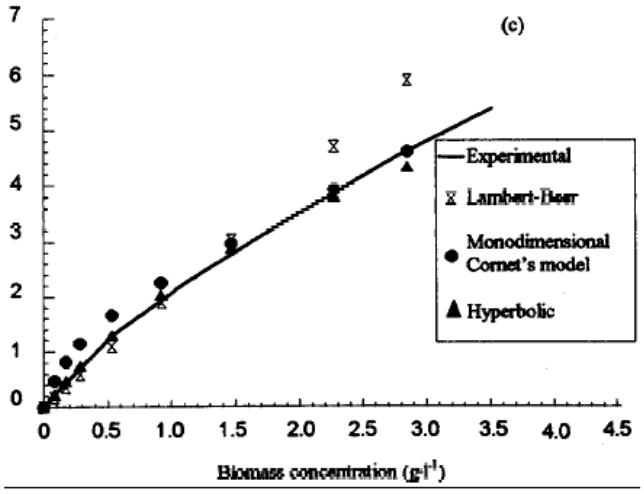

Figure 1-3 Hyperbolic equation predicting attenuation over high biomass concentrations
Inconsistent solar light patterns throughout the day combined with high concentrations of microalgae in outdoor cultivation units show that the hyperbolic equation derived from experimental results would closely detail the attenuation. Y-axis: Attenuation [34].

Recent studies outlined by C. Hung et al. [28] show that beer's law was used to find maximum transparent rectangular chambers (TRC), to understand the best light exposure to microalgae cultivating inside [28].

$$I(z, C_b) = I_0 e^{-K_b C_b \cdot z} \tag{5}$$

Eq. (5) illustrates the irradiance inside the culture by $I(z, C_b)$, biomass concentration (C_b), length of the optical path (z), (I_0) the measured irradiance on the culture surface and the extinction coefficient (K_b) which is how equipped a culture can absorb a given wavelength input [28]. The purpose of this research was to explore which type of the three designs exhibit maximum light penetration into dense microalgal culture to encourage growth [28].

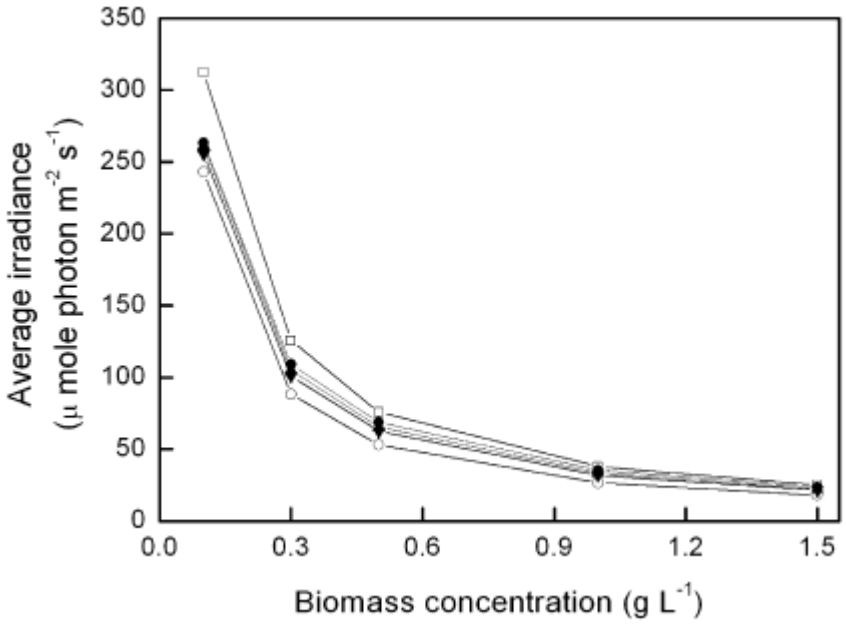

Figure 1-4 Photobioreactor designs for maximum light penetration
(▼) TRC1. (▲): TRC2. (●) TRC3. Bioreactors examined in microalgae production with the ability to conduct light to dense cultures, as concentration increases irradiance decreases [28].

In contrast, both papers affirm that beer lamberts law can account for attenuation of light when biomass concentrations are low [34], [28]. On the other hand, F. Fernandez et al. [34] found that Beer-Lamberts law only responded well to low biomass concentrations. Whereas Eq. (4), adjusted well to higher biomass concentrations. It should also be noted that **Figure 1-3** accounts for 3 g / L whereas **Figure 1-4** accounts for 1.5 g / L suggesting that biomass cultures greater than 1.5 g / L will require further development of Beers law.

1.2.3 Photoperiod

Photoperiod is known as the Earth's rotation around the sun and the daylengths which are measured in a 24h cycle and is also known as a light-dark ratio (light:dark) [35]. Cyanobacteria have developed their photoreceptors which allows measurement of light to anticipate the seasonal variations [35].

S. Wahidin et al. [14] asserts that photoperiod duration and light intensity has a positive effect on the growth of microalgae production [14]. Cultivations of *Nannochloropsis sp* was grown over a 9-day period under three different photoperiod regimes with three different intensities of light exposure (50, 100 and 200 μmol / m^2 s) with (12:12,18:06 and 24:00). Results from this study concluded that 100 μmol / m^2 s with an 18:06 light:dark ratio performs the best.

While Z. Khoeyi et al. [36] demonstrate growth characteristics of *C. vulgaris* in its three growth stages by varying the light intensity and the photoperiod (37.5, 62.5 100 μmol / m^2 s) with (08:16, 12:12 and 16:08h) [36]. Maximum biomass production recorded was when 62.5 μmol / m^2 s and 16:08 h ratio was used [36]. While Too much light intensity and longer photoperiods can be too stressful for growth conditions, the opposite can also have a positive effect [14].

R. Anderson [37] outlines that light:dark regimes for algae growth to be around the 12:12 to 16:08 for a majority of algae cultures. Productive photosynthesis relies on a light: dark regime including lighting conditions: the duration and intensity [14].

Two different studies from S. Wahidin et al. is summarised below in **Figure 1-5**, while studies from Z. Khoeyi et al. **Figure 1-6** respectively.

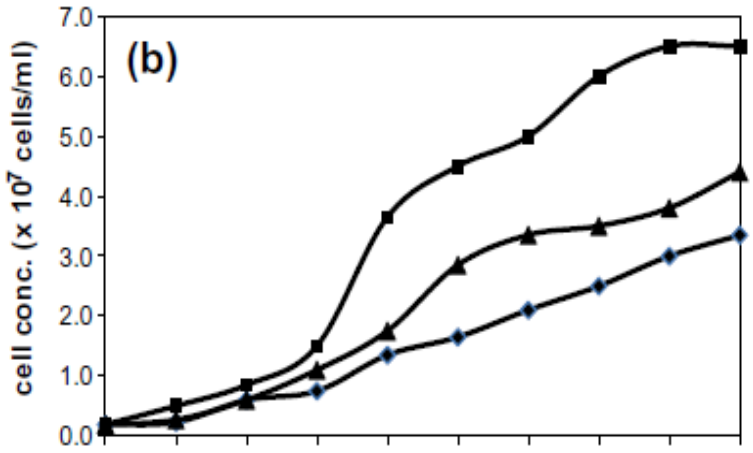

Figure 1-5 Light Intensities and Photoperiod study 1
100 µmol m^{-2} s^{-1} of light intensity Including the photoperiod: (■) 18:06. (▲) 24:00 (♦) 12:12 (b). [14].

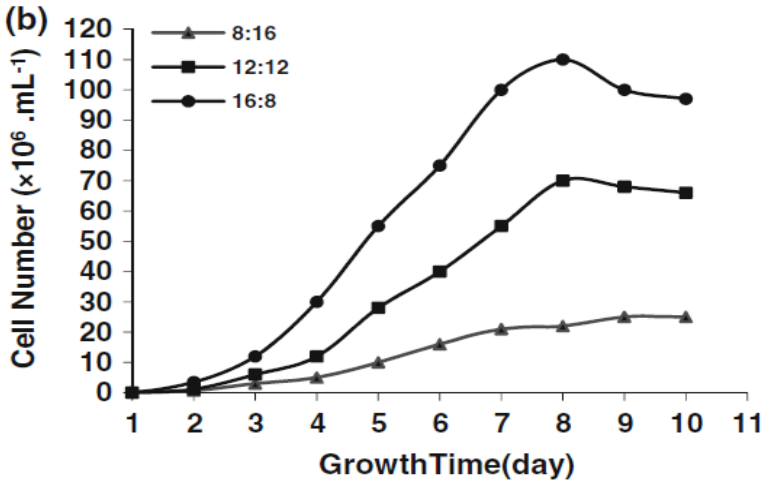

Figure 1-6 Light intensity and Photoperiod study 2
62.5 µmol / m^2 s of light intensity including photoperiod with the best growth rate experienced with 16:08 Light: Dark ratio [36].

1.2.4 Temperature

Algae that can survive over a broad temperature range are considered to be more suitable for culture cultivation, primarily when the fatal temperature is increased a little more compared to their optimal growth temperature [16]. Typical effects of Increasing temperature range affects the algae in the following way, the ability for the algae to perform photosynthesis which leads to the lack of oxygen production and causes damage within the cell membrane [15]. Page (11) **Figure 1-7** depicts algae strains exposed to temperature variations.

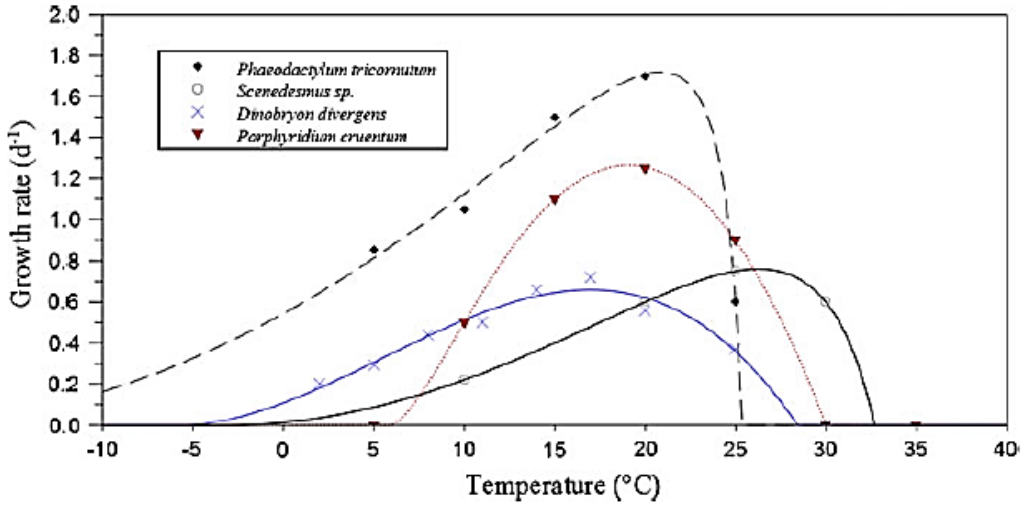

Figure 1-7 Growth rate behaviour resulting from temperature variations of four algae species and their growth rates expressed. As temperature increases, the algae growth rate reaches a max and then begins to diminish [15].

Thermophytic algae are known best where the fatal temperatures can exceed 85 ºC in temperature, *Cyanidium caldarium*, *Synechocystis* and *Phormidium* are just some of the thermophytic algae strains [38]. While eurythermal strains like *Chlorella* have had much success overgrowth ranges from 4 ºC to 38 ºC, other algae strains such as *Navicual glaciei* showed decreased growth rates as optimal growth temperature is increased beyond 4 ºC [39].

A paper presented from "Effect of temperature and light on the growth of algae species" Presents optimal temperatures for particular species of algae [40]. The information in **Table 1-1** illustrates some of the temperature ranges for various algae species [40].

Table 1-1 Optimal temperature ranges for Algae

Algae species	Colour	Temperature range (ºC)
Chlorella. minutissima	Green	10-30
Spirogyra species	Green	10-17
Chaetomorpha valida	Green	17-29
Heterosigma species	Red	16-30
Chattonella species	Red	17.5-30
Porphyra species	Red	Optimal at 15
Sargassum horneri	Brown	Optimal at 25
Euglena gracilis	Brown	27-31
Ostreopsis cf. ovata	Brown	18-30

Below in **Figure 1-8** depicts that not only does light intensity have a considerable effect on growth rate but so does the temperature [6]. Below the results by M. Huesemann et al. showing algae growth rates as a function of temperature and lighting intensity [6].

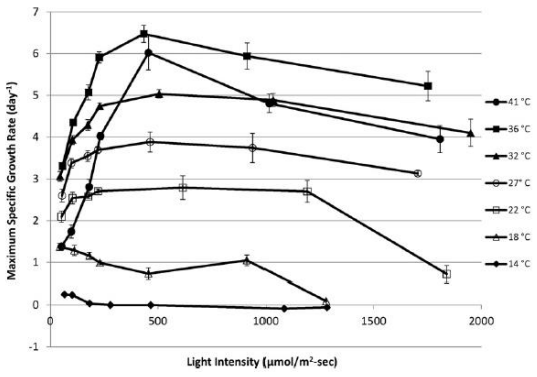

Figure 1-8 Effects of growth rates with Light intensity and temperature
Chlorella sorokinian performed the highest growth rate temperature of 36 ºC and around 500 µmol / m^2 s [6].

Microalgae species but not all are known to experience growth from temperatures over a wide band between 15 ºC -30 ºC however, the optimal conditions usually lie between 20 ºC -25 ºC [15].

As the primary goal is to control the growth by increasing yield, strict control of temperature is also necessary [41]. A study to the growth of bacteria (*Rhodobacter capsulatus*) used phase change materials (PCMs) was conducted, the product acts as a temperature absorber that takes the heat in during the day and reduces the stored energy during the night [42]. Selection of the PCM included the temperature profile of the location, including the phase change two times per day. Experimental PCMs used are, Decanoic (organic) and Glauber's salt (inorganic) both with melting points of 32 ºC [42]. The PCM was part of one of the three photobioreactor arrangements in **Figure 1-9**.

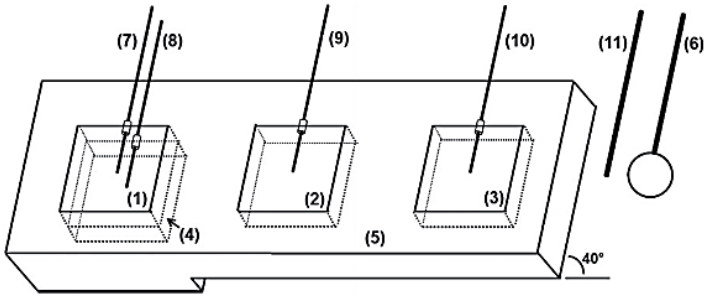

Figure 1-9 PCM experimental design for temperature control
(1-4) Compartments with (4) being the PCM. (6-11) Various sensors temperature and light [42]

Experimental results reveal that; *Rhodobacter capsulatus* the species of interest, generates heat because of the metabolic behaviours and light absorption. System (1) PCM and bacteria reach a maximum temperature of 50 ºC. Compared with the system (2) the bacteria in water with no PCM was 60 ºC and system (3) with only water 40 ºC. The overall temperature change observed was only a marginal difference per hour, 8.7 down to 6.4 ºC with a maximum temperature of 60 ºC to 50 ºC, not enough to keep the bacteria alive for the growth setpoint of <40 ºC [42]. Although this is a more nonconventional range of temperature control, studies concluded that energy required for cooling was reduced by 52% [42]. The temperature behaviours concerning the PCM arrangement is illustrated below **Figure 1-10**.

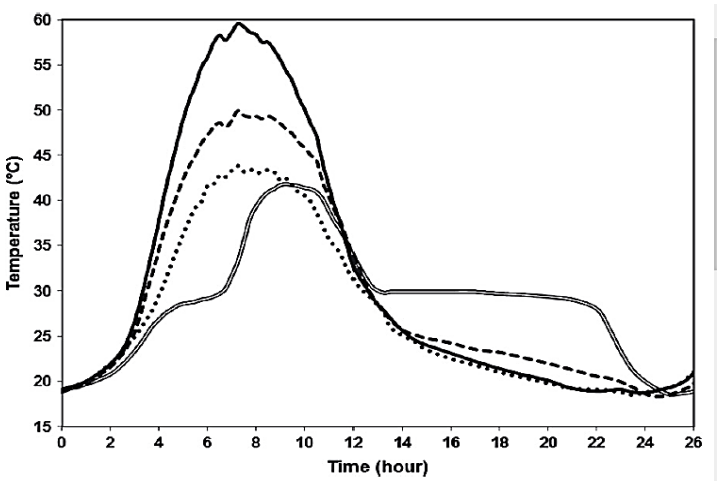

Figure 1-10 Temperature of various cultures with PCM
To regulate the temperature towards setpoint shows promising results but still fail to reach the desired temperature. The compartment with water (3) compared to the compartment with bacteria (2) shows how much energy generated causes the system to increase temperature [42].

Algae cultivation must be suitable for the geographical location and have a broad growth temperature to be economically viable to produce high-value products [16]. It is shown that producing astaxanthin from *H. pulvialis* is not economically viable when cultivated at its optimal growth range temperature of 20 ºC [43]. Experimental temperature ranges from 20 ºC - 30.5 ºC where evaluated with an economic assessment [43]. Results concluded, maintaining the optimal 20 ºC temperature required more energy compared to 27 ºC, so a location of Kobe in Japan, would be much favourable because of the colder climates [43].

1.2.5 Nutrients

Studies established by C. Hsieh et al. [44] show that batch cultivation has to result in improved lipid growth. By feeding algae, the correct nutrients like nitrate, ammonia, and urea; which is a white crystalline water-soluble solid that is a source of nitrogen [45], [44]. Studies involving a semi-continuous process show that lipid productivity in the early stationary phase can be increased. By timing the amount of urea feed (0.025 g / L) to *Chlorella sp* in doing so the urea deficient condition is replaced [44]. Below the findings.

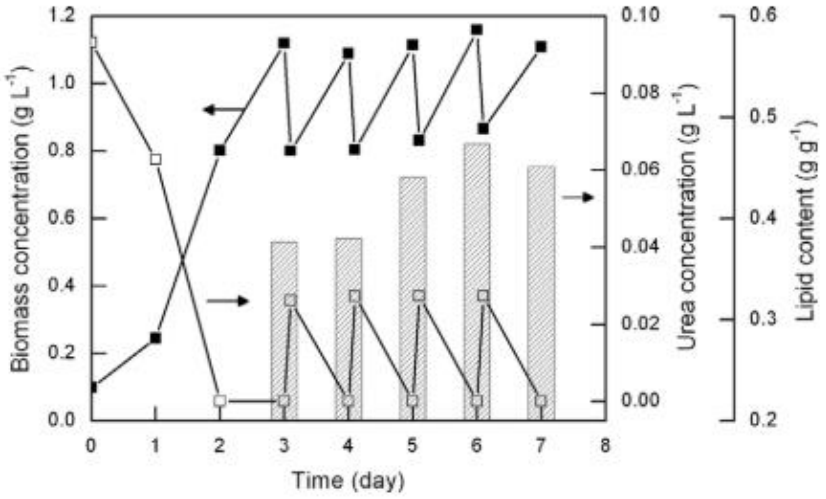

Figure 1-11 Urea feed times concerning growth rates
(■): Biomass concentration. (□): Urea concentration. After a feed of 0.025 g / L on day three biomass concentration is increased again [44].

Minerals are often part of a cultivation recipe and sometimes include potassium, sodium, calcium, sulfate, magnesium, and phosphate [46]. It has been shown that limiting the phosphate in *Scenedesmus Obliquus* increases lipid accumulation [47]. G. Iyer et al. [48] shows that green algae *Chlorolobion braunii* and *Coelastrella oocystiformis* can absorb various concentrations of potassium: (200, 400, 600, 800, 100 and 2000 ppm) [48]. When *Coelastrella oocystiformis* is exposed to 400 ppm of potassium the algae concentration was found to absorb 75.8% of the total potassium. While *Chlorolobion braunii* is exposed to 400 ppm of potassium it could uptake 40.66%; other concentrations yield had less uptake [48].

While some of these nutrients are useful for the lipid growth, algae such as *Chlorella vulgaris* and *Chlorella salina* have promising results in contamination reduction [49]. When algae are exposed to these contaminants, the reduction in pH was noticed including, total dissolved solids [49]. Biological oxygen demand and chemical oxygen demand measures of water toxicity had reductions of both algae strains including heavy metal contamination [49]. **Figure 1-12** on page 16 summarises the findings, as shown *C. Vulgaris* yields the most promising results.

The study is further confirmed by E. Salama et al. [50], that nitrate, phosphate, urea ammonia and various trace elements are the building blocks for microalgae growth, but further suggests that ratios of N or P should be considered when using wastewater for algae nutrients [50]

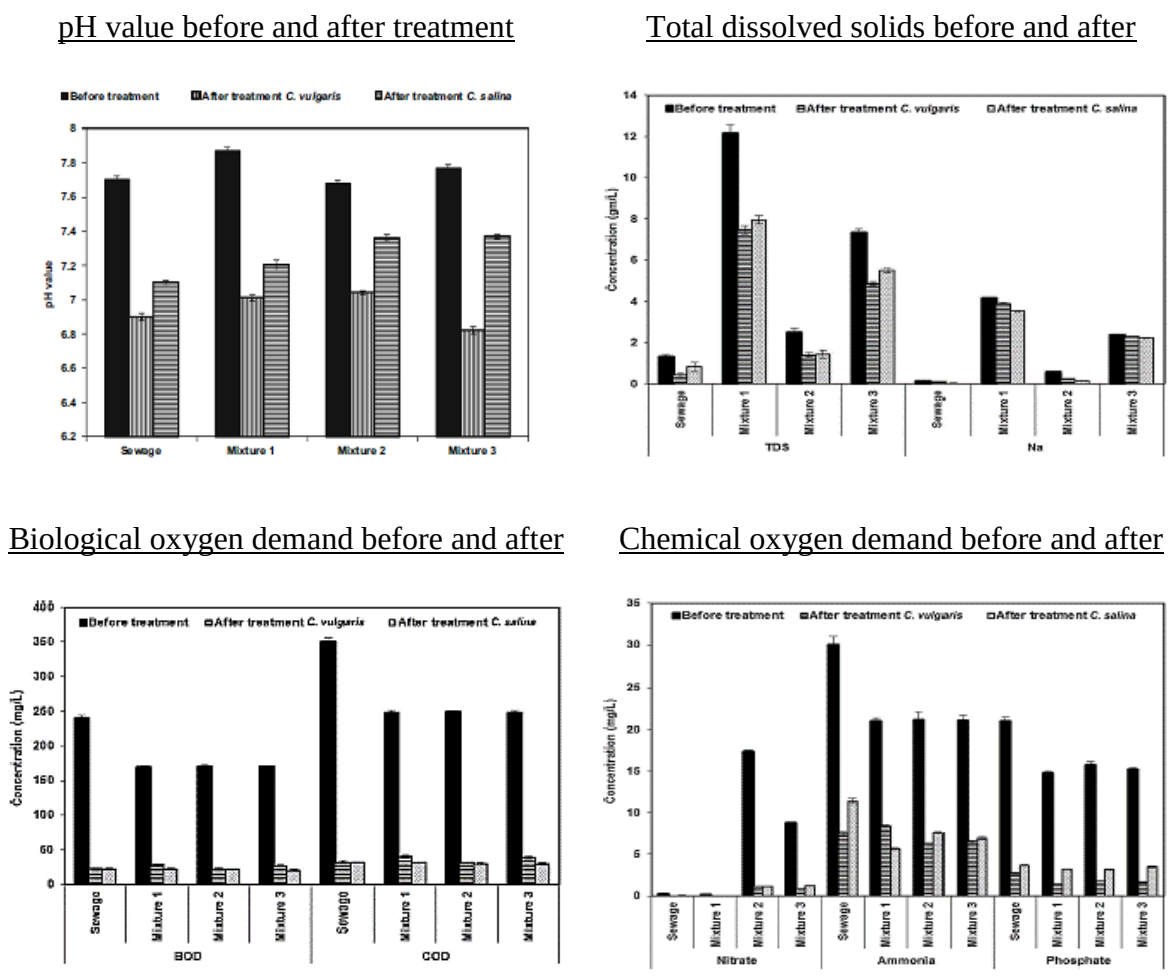

Figure 1-12 Microalgae treatment in polluted water
The dark black columns are before treatment followed by *C vulgaris* and *C salina* respectively. A before and after measurement was taken to show how the algae strains can improve the water quality [49]

1.2.6 Salt concentrations

Halophytic is known for its very high salinity conditions where algae can grow. *Stephanoptera*, *Eherenbergii*, *Ulothxix*, *Dunaliella salina* and *Oscillatoria* are known to be some of many algae which can tolerate these conditions [38] [8]. These algae strains are particularly useful when biofuel production require water and land. Therefore microalgae can be grown in the rich saline ground, and fresh water can be spared for agricultural food crops [16].

A current study suggests a two-phase method which aimed to increase the lipid content *Dunaliella tertiolecta* [51]. The first phase of the method is to incorporate 2,4-Dichlorophenoxyacetic acid (2,4-D) into the culture medium at the early stage which increases the significant accumulation of biomass by 40-50% [51]. This was done in combination by adding Auxin (plant hormones) at the beginning and end. At the stationary phase; delivering NaCl is added to rapidly increase the salinity from 0.5 mol L^{-1} (M) to 2 M [51]. A reasonable elevation in growth and the production of lipids was recorded. Results from this study below **Figure 1-13**.

Salt stress causes algae to consume more glucose by doing so the accumulation rate of biomass can be prolonged and increase for a period reported by T. Wang et al. [52].

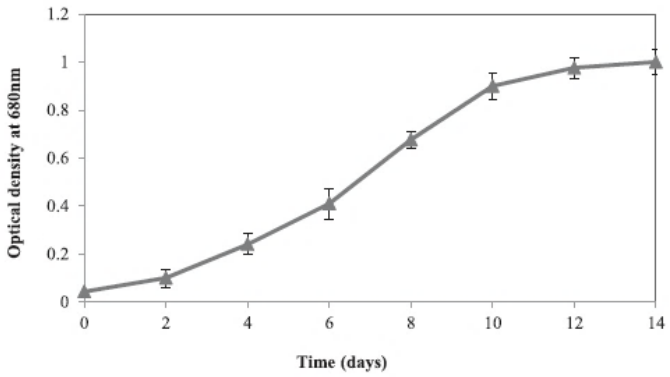

Figure 1-13 *D. tertiolecta* growth phase over 14 days
while exposed to an optical density of 680 nm, NaCl is used on the growth of *D tertiolecta*. Exponential to linear growth is observed between 0-10 days, by day (12-14), 1 M NaCl shows the growth tends towards stationary stage [51].

1.2.7 CO2 and microalgae growth

CO_2 Fixation by biological means is well known as, biofixation by the application of microalgae to reduce the impact of CO_2 [53]. In order to increase biomass production and perform photosynthesis, algae require a carbon source such as CO_2 gas or chemical bicarbonate [54].

In 2017 the PBL Netherlands Environmental Assessment Agency reports that; global greenhouse gas emissions (GHG) increased towards the 49.3 gigatons [55]. Increase in renewable energy usage and the decrease in coal consumption continues to play a role, and it was reported that 2016 that the increase had slowed by 0.5% [55]. The emissions consist of about 72% carbon dioxide (CO_2), Methane, Nitrous oxide and various other gases known as fluorinated gases which make up the remainder [55]. Whereas the annual emissions in Australia for December 2017 were recorded at 533.7 Mt CO2-e which was a 1.5% increase from the previous year [56].

Theoretically, 513 tonnes of CO_2 can be consumed by microalgae, and 9% of the solar input energy is converted into 280 tonnes of dry biomass yield per hectare per [53]. While K. Kadman [57] argues that a 50 MW power plant could approximately generate 414 000 t / yr of CO_2, as a result implementing a microalgae cultivation system which consumes 1000 ha of land could mitigate 210 000 t / yr of the CO_2, based on data conducted from San Juan power plant in New Mexico [57].

High microalgae growth rates have been reported by M. Morais et al. [58] when CO_2 was introduced to algae (*Scenedesmus obliquus* and *Spirulina sp)* and cultivated at a temperature of 30 ºC with a 12:12 h light dark ratio consisting of 3200 lux illumination [58]. The study considers bioreactors in a column arrangement with aeration supplied from a compressor arrangement [58]. To compare the results of both species, three bioreactors have different concentrations of the CO_2 respectively 0%, 6% and 12%. The first bioreactor consisting of 0% CO_2 shows that the specific growth rates (μ_{max}) for *Spirulina sp* to be 0.33 / d while *S. obliquus* to be 0.15 d^{-1} [58]. While the μ_{max} recorded with 6% CO_2 fixation was 0.44 / d and 0.22 / d respectively and when 12% CO_2 fixation was introduced, μ_{max} observed was 0.33 / d and 0.22 / d respectively [58]. The results concluded that *Spirulina sp* and *S. obliquus* had the highest μ_{max} when 6% of CO_2 was introduced, contributing to a maximum of CO_2 biofixation per day of 53.29% and 45.61% [58].

1.2.8 pH

pH of large values can affect the lipid growth and cause triacylglycerol (TAG) accumulation [59]. TAG protects the algae when over energisation occurs and is a response mechanism when stressful conditions arise [60]. It has been shown by M. Bartley et al. [61] *Nannochloropsis salina* that the optimum growth rates when pH was between 8-9 and by the addition of 400pm of CO_2 via air stone aerators, a pH below 8 could be maintained [61].

While N. Moheimani [62] reports that *Tetraselmis suecica* and *Chlorella sp* have separate pH conditions at night and day. Results of this experiment reveal that *Tetraselmis suecica* increase in pH from 7.6 - 8.7 on daytime when no CO_2 is added and a reduction in pH at night time to 7.9 [62]. *Chlorella sp, on the other hand,* increased pH 7.6-9 at daytime and decreased back to 7.6 at night time [62]. Reducing the pH for *Tetraselmis suecica* and *Chlorella sp* to 6 and 5 respectively found that the algae cells would clump or stick to the glass walls of the PBR's until the optimal pH to previous values were obtained [62].

R. Munzo et al. [4], mentions that a possible cause to a rise in pH is the microalgae uptake of CO_2 and asserts that in cultivation systems the pH balance is easy to control [4].

1.2.9 Respiration

Respiration is a process that algae perform for some biological activities such as, production and consumption of oxygen [63], [64]. Photorespiration is a process in C_3 plants which reduces the efficiency of photosynthesis; this is known to occur when CO_2 levels are low [65]. Although an essential process, respiration and photorespiration effects can be reduced by limiting the concentration of oxygen, in doing so the oxygen is not catalysed by the enzyme known as Rubisco [64]. The decline in respiration has considerable effects on algae growth rate of biomass overnight from light and temperature fluctuations from dark respiration [16], [6].

Exposure to light experiments where conducted and it was found seasonal variations *L. corallioides* has maximum respiration in the summer compared to the winter [66]. Influencing factors include salinity and the season; including temperature requirements for photosynthesis and

respiration [66]. Below the gross production affected by irradiation and respiration inhibiting growth.

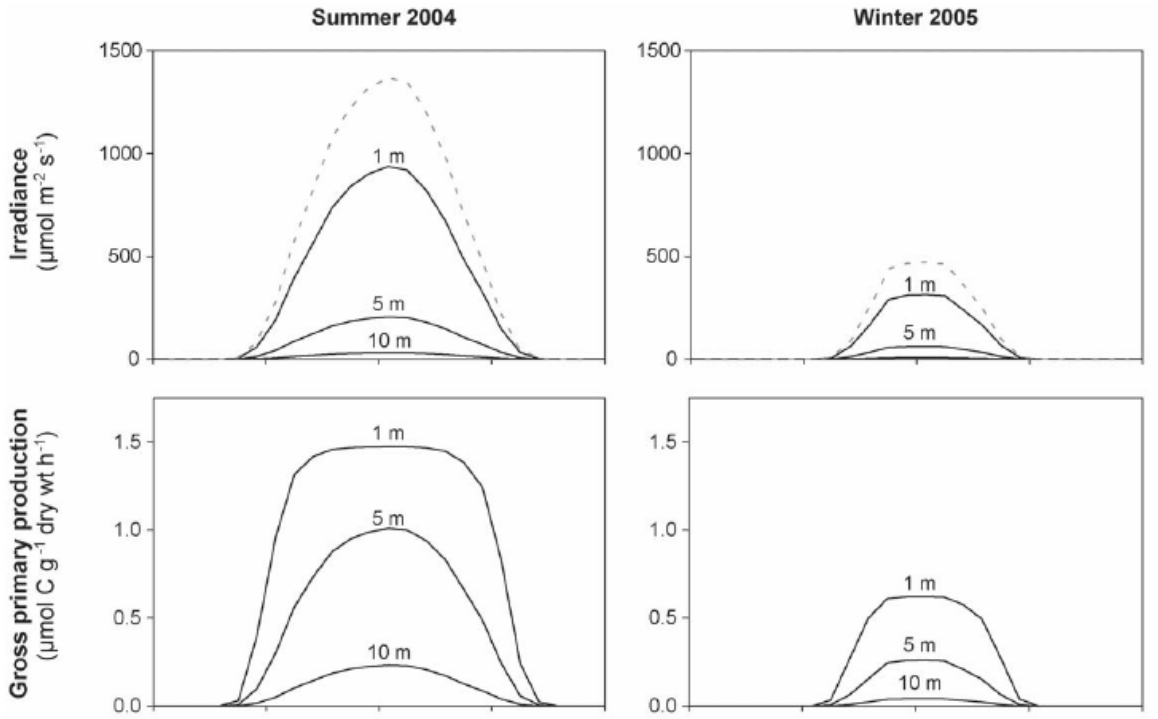

Figure 1-14 Irradiance and daily estimated production of algae Lithothamnion corallioides. The dotted line is the surface of the water and the solid line, underwater irradiances. This figure represents the variations over the summer and winter of the production [66].

1.3 Microalgae cultivation

Efforts into laboratory scale of microalgae and the commercial farming of microalgae have been around since the late 19th century and can be dated back further in time. Cultivation since has been evolving and optimised into what it has become today as closed, vertical or open methods of cultivation [2]. With a clear goal to create an economically viable microalgae process, and produce high biomass daily yields [6]. On the other hand selection of algae, strains must flourish under all conditions in the environment and outcompete other algae strains that may cause cross contamination which is why open and closed cultivation methods have existed [41].

Small-scale laboratory experiments are not always viable on larger upscale designs because room temperatures and lighting intensities will not guarantee that these microalgae cultures will flourish under daily variations in a seasonal outdoor environment [6]. The growth of microalgae is so

closely related to the temperature conditions and the lighting available that the design and operation of culture environments must be taken into account [15].

1.3.1 Open culture environments

Facilities that operate on a large scale are more concerned with the high rate of production and are outdoor arrangements known as open ponds [8]. Open ponds are less labour intensive to design and are constructed with channels of water known as a raceway [67]. Raceway designs also come in the shape of an oval and are circulated with a paddlewheel which also assists in moving the algae around raceway while mixing it [7].

Typical surface areas of a raceway can be maximised by the following equation below (ρ) is density algae broth (P) is the length p/q is a ratio and is recommended that it should be larger than 10, if the ratio is too small bends in the raceway cause disturbances [7].

$$A = \frac{\pi q^2}{4} + \mathrm{p}q \tag{6}$$

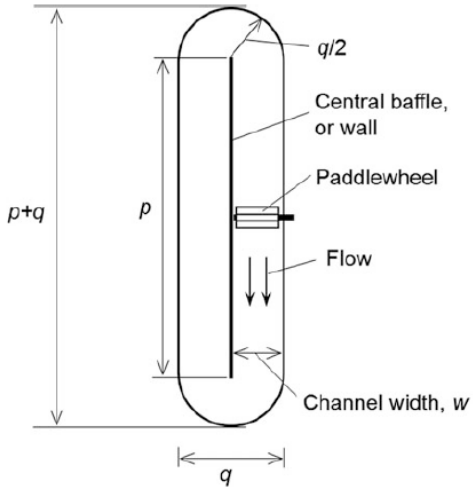

Figure 1-15 Raceway pond from the top view down
(ρ) is density algae broth: (P) is the length [31].

V_L is the working volume which relates the surface area with the depth of the algae culture broth.

$$V_L = Ah \tag{7}$$

Turbulent flows in the raceway enable the algae cells to mix and enhance the removal of the oxygen which has been generated when photosynthesis occurs [54]

The Reynolds number *Re* is determined by (ρ) density of the algae broth, (u) the velocity, (d_h) hydraulic diameter, and (μ) is the algae viscosity below the Reynolds number.

$$Re = \frac{\rho u d_h}{\mu} \tag{8}$$

Below, **Figure 1-16** illustrates the open cultivation methods.

(A) Photo credit: V. Blagotinsek, (B) Photo credit Cognis nutrition and health [38]. (C) Photo credit D. Sahoo [38].

Figure 1-16 Open Culture environments
(A) Paddlewheel raceway design at Murdoch R&D Centre, Perth W.A. (B) Dunaliella Salina production in Australia. (C) Raceway Pond.

1.3.2 Closed culture environments

Photobioreactors (PBRs) best described as a closed system that comes in many different arrangements. Constructed from glass or plastic they are used when carrying out closed culture cultivation that is not exposed to contamination or environmental conditions [7],[8], [9]. These arrangements come in the form of; Tubular which is better known as manifold PBRs (horizontal) or Serpentine PBRs (vertical), Flat Panel PBRs and column PBRs, each of them have one advantage over the other [7].

Tubular PBRs although very different from column PBRs are covered in detail by [68]. These PBRs use mechanical means by pumps or sequestration to inoculate the exchange of CO_2 and O_2

for the culture medium. Tubular type PBRs reduce the energy lost when dealing with pipes due to head losses and allow lower oxygen concentrations to occur which is favourable in commercial practices to upscale [7], [9]. Flat plate PBRs can be tilted and orientated towards the light and are designed for high efficiencies when accelerated photosynthesis is needed [7], [9]. Column PBRs are designed in a vertical arrangement with air-lift suspension. Some even have two columns; one inside the other which is designed for high-density algae cultures that require more light [9], [7]. Below Page 23 **Figure 1-17** illustrates the typically closed culture environments.

(A) Photo credit: D. Sahoo [7].

(B) Photo credit: AlgoFilm University of Nantes, France [54].

(C) Photo credit: The company Plexiglass [9]

(D) Photo credit Prof. E. Molina Grima [9].

Figure 1-17 Closed Photobioreactor arrangements
Typical closed cultured environments and their different methods of cultivation: (A): Tubular Manifold (B): Flat plate PBR, (C): Column PBR. (D): Serpentine PBR.

Table 1-2 Cultivation methods overview

Open/outdoor represents the outdoor cultivation method which is exposed to the atmosphere, while closed represents closed environments, outdoor or indoor. This overview is a broad spectrum of the immediate pros and cons of each method, not so much the individual aspects of each cultivation method.

S.No.	Cultivation type	Cultivation Name	Pros	Cons
1.	Open culture / outdoor environments	Raceway Pond, Paddlewheel design, Mixed ponds, Shallow Lagoons	-Less complex to build -High Production -Less complex to operate [67]. -Low energy consumption -Cheaper maintenance [1]. -Not so susceptible to overheating [54].	-Temperature control difficult [40]. -High risk of contamination [54]. -Consumes a lot of lands [69]. -Poor biomass productivity [70]
2.	Closed culture /outdoor or indoor environments	Tubular PBRs, Column PBRs, Flat plate PBRs, Laboratory scale PBRs.	-Prevent evaporation -No cross contamination -Limit CO_2 Loss [8] -Better control overgrowth -Produce high-value products [8] -High Illumination surface area [70]	-Fouling formation on inner walls which can have effects on photosynthesis [54]. -Expensive on a large scale [70] -The difficulty for cleaning and maintenance

1.4 Effective Photobioreactor design

PBRs should be efficient in light capture and the distribution of the light to the algae so effective photosynthesis can be performed it should also offer the user the ability to perform precise control of the variables so that cell growth can be optimised [10], [11]. As the algae inside the photobioreactor begin to grow the broth begins to increase density, this affects the light intensity that causes a reduced effect on the immediate growth rates [13].

1.4.1 Mixing

Mixing of the culture is one option to improve the exchange of PFD to the algae culture. However, it noted that aggressive amounts of mixing cannot be tolerated by all species [71], [13]. Studies suggested by N. Moheimani et al. [72] that the different mixing speeds influence the growth of *P. carterae* [72]. Varying the Reynolds number between 15,979 and 79,866 respectively (100 rpm)

and (500 rpm), growth rates would decrease as the Reynolds number was increased past 31,927 (200 rpm) [72]. Experiment results conclude that as a range of 0 – 200 rpm is maintained algae culture growth rate performs best [72]. Below **Figure 1-18** shows the results.

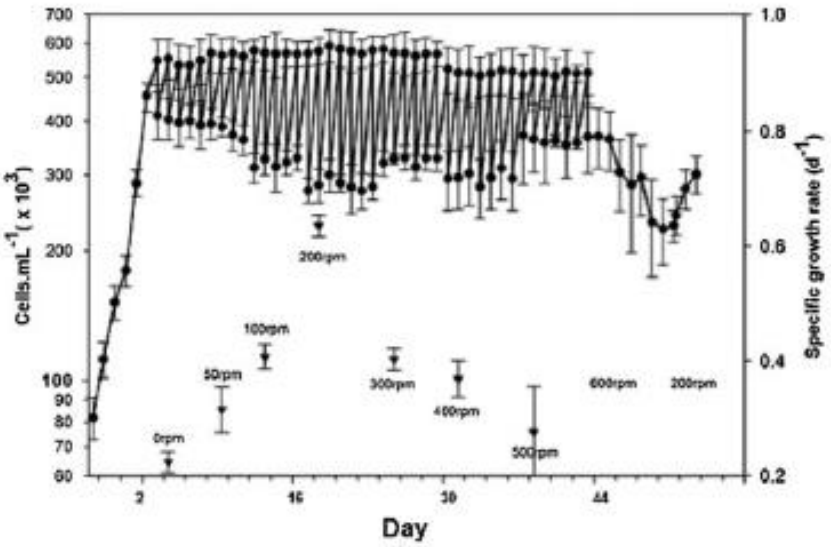

Figure 1-18 Growth rate of P. carterae with various mixing speeds
Effect of growth rate as the rpm of the mixing bar was increased, optimal growth conditions were experienced between 0 – 200 rpm [72]

M. Leupold et al. [73] confirms that applying a sheer force of a smooth nature can produce better growth characteristics. While photosynthetic changes can be observed even when small changes on the tip speed are regulated [73]. While Q. Huang et al. [74] asserts speeds of 1m s^{-1} have the potential to produce micro eddies that are detrimental to cell growth.

1.4.2 Light

Microalgae's natural habitat is outdoors, however Q. Huang et al. [74] assert that the primary cause for temperature rise in cultivation is the radiance applied to microalgae outside of the PAR range while ultraviolet is detrimental for cell development [74]. This is affirmed by R. Munoz et al. [4], where photoinhibition is observed as the solar irradiance is at its peak [4].

1.4.3 Temperature

Closed bioreactors have the advantage of better temperature control over a wide range of species as mentioned by M. Borowitzka [12] that confirms, a broad range of algal species can be cultivated [12]. M. Borowitzka further suggests that temperature control can be done by a heat exchanger or evaporative cooling [12].

To date, 35,000 microalgae species have been identified [16]. **Table 1-1** highlights the temperature ranges of microalgae are very wide and different. While B. Uyar et al. [42] established that PCM could absorb 76.4 W h, it suggested that a more convenient method would be to use a heat pump that has a coefficient of performance (COP) of 3 [42].

Thermoelectric refrigeration involves the Peltier effect of transforming electrical energy into heating or cooling methods [75]. Cooling is achieved when a voltage difference is applied to dissimilar metals at the junction increasing the temperature at one junction and cooling down the junction at the other [76].

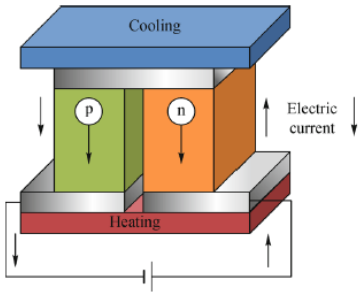

Figure 1-19 Thermoelectric module
Peltier effect creates a temperature difference on each side of two semiconductor materials n-type and p-type. When DC voltage is applied across the two semiconductors the heat plates on both sides, absorb and remove heat [76].

Microcontrollers have been used to control the temperature output of a thermoelectric cooler (TEC) [76]. Controlling the temperature of the system is done by switching the relay on or off based on the temperature that was set within a range [76]. While recent studies found this method was by far the least efficient; stored energy in the heat exchanger will flow back towards the cooler side of the Peltier module when switched off [77]. This scenario causes power consumption costs,

reduced COP and temperature oscillations as shown in **Figure 1-21**, so other methods should be investigated such as Proportional integral and derivative (PID) control [77].

Temperature control via pulse width modulation (PWM) has been implemented by using off the shelf PID controllers MAXIM (MAX1978) © specific for TEC temperature regulation [78]. Results showed that the temperature was maintained around a steady state of 25.069 ºC with 4-watt power consumption as shown in **Figure 1-20** on page 27 [78].

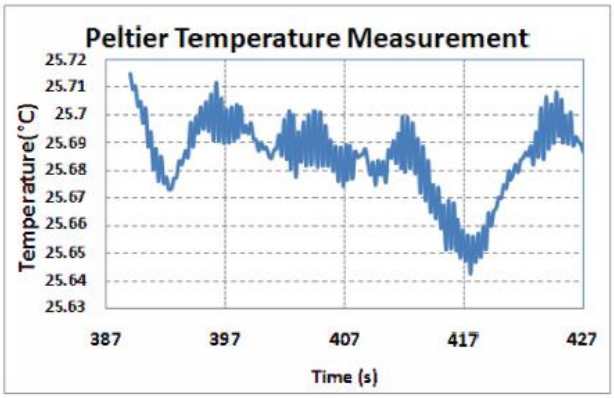

Figure 1-20 Steady State temperature of Peltier with PID control
Once the temperature reached a steady state after 387 seconds, it is shown that 25.069 ºC is maintained [78]

Reviewing the case for both results and comparing **Table 1-1**, precise temperature control would be not required because of the optimal growth range of algae [15]. While issues of heat flow towards the cold end when switched off mentioned by A. Martinez et al. [77], can be solved by extracting the heat from the hot side of the TEC with a fan to minimise the heat flow towards the cold side of the TEC [79].

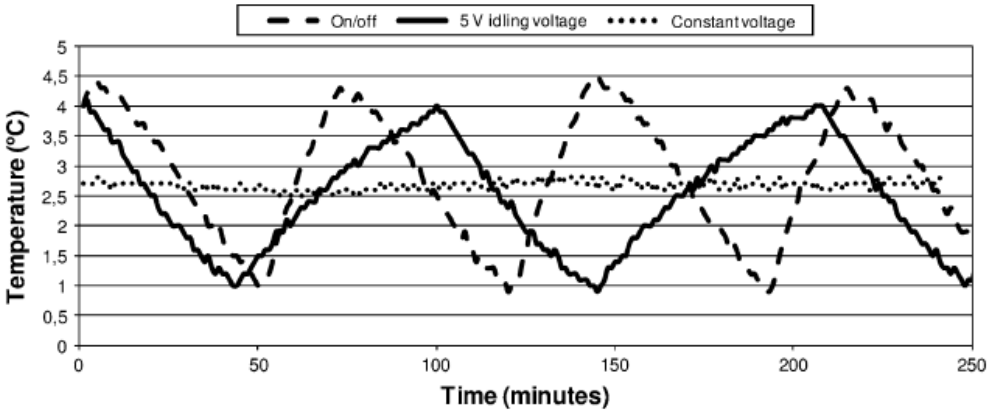

Figure 1-21 Temperature control with TEC on/off Control
Setpoint bounds cause the oscillations of the temperature when TEC on/off switching is involved. Switching a full 12 V is represented by (---) whereas the idling voltage of 5 V (-) was used to switch the TEC. Notice the 5V has a longer time constant compared to the full 12 V range. While PID (⋯) asserts its position as optimal control logic [77].

1.5 Literature review conclusion

Microalgae growth is affected by the amount of light intensity received within the PAR range that is not always dependent of solar irradiance but also come from artificial sources. Microalgae concentrations increase as growth rates increase causing the density in biomass concentrations to become thick for light to reach the inner solution. It is also realised that the importance of the photoperiod has a crucial role on the development of culture and a reasonable amount of consideration into photoperiods must be investigated.

Temperature plays an essential role for growth, and the fatal temperature of algae must be understood before attempting to cultivate the biomass for research purposes. As nutrients are an important factor for microalgae growth, considerations into how much salt, carbon sources and the pH level will improve growing conditions.

Microalgae cultivation is the best way to improve strain quality while open and closed culture both have their pros and cons. Controllability of the variables that influence growth will enhance microalgae production. If optimal control is required, use PID control while simple on-off control can be advantageous for simple processes.

Chapter 2. Materials & Design

The design for a PBR system needs to be a closed system where the temperature can be maintained constantly. Because microalgae require light for growth the use of LED lighting will be installed inside the PBR while the various PAR ranges can be explored through controllability of the LED light. The agitation motor will be installed below the PBR flask on the outside of the system while a magnet housing will be designed, and 3D printed.

To ensure the system can maintain a constant temperature, insulation will be cast around the complete housing to ensure no heat energy can enter the system. A thermoelectric cooler will be installed by conduction onto the aluminium housing and a heat sink with fans will be provided to remove any excess heat energy generated by the thermoelectric cooler.

The controllability of the PBR is done by sensors by Arduino temperature and LUX while the pulse width modulation provided on the micro controller will output the appropriate voltage for the thermoelectric cooler.

Cost effective design of PBRs are needed in order to offset the high production costs associated with biomass production when compared to agricultural or forest biomass [10]. The research conducted in this thesis will provide a foundation for future works that will facilitate a low budget high production cultivation unit that is efficient.

Below in the following section is the materials used for the design and a reference for each component is provided. All the components in this design are accessible to the public domain.

2.1 Materials

All materials are directly sourced from local stores around Perth. To illustrate the materials used for this design while all links are supplied in the reference section for each component. All the parts for this design are accessible to the public domain and are purchased online.

2.1.1 Microcontrollers and instrumentation

Microcontrollers

All microcontrollers and sensor accessories are a hobby-based product which is purchased from Jaycar electronics. Two Duinotech XC 4410 microcontrollers consist of 14 digital input/output pins that include 6 digital pins denoted by the symbol (~) for the PWM signal, and 6 analogue pins A0-A5 [80]. Controllability of the variables will give the advantage of temperature control and allow algae species over a growth range to be cultivated and experimented with [12].

Temperature and humidity sensor

DHT11 Temperature and humidity sensor sensitivity range operates between the humidity range of 20% to 80% ± 5% and temperature range of 0 ºC to + 50 ºC ± 2 ºC [81]. The advantage of this product is that the humidity and the temperature are displayed by a single sensor.

Temperature sensor

LM335Z is the second temperature sensor used in this project. The operation range of the sensor is between -40 ºC to +100 ºC ± 0.3 ºC with the output of 10 mV $^{o}K^{-1}$ [82]. It is used for the ambient internal temperature

Temperature sensor for PBR water

The sensor used for the PBR flask and is a waterproof digital temperature sensor DS18B20. It has a ±0.5 °C between -10 °C to 85 °C. It is used to establish a temperature reading of the PBR culture [83].

Lux Sensor

Appropriate lux sensor used is the TSL2561, this sensor allows the Arduino platform to communicate and program the lux sensor. The operating temperature is between -30 ºC to + 80 ºC with the Lux range of 0.1 to 40,000 Lux [84].

Some algae can experience high growth ranges when a blue and yellow light is mixed [25]. Because of the various colour spectrums of light microalgae can grow in, it is advantageous that the operator of the system can input the PAR range and the intensity.

2.1.2 Power supplies and switching

Power supplies

Two power supplies where purchased, the first one is a two-channel power supply constructed by Mean Well part number RID - 125. Channel 1: 12 VDC, 9.2 A channel 2: 5 VDC, 3 A [85]. The second power supply constructed by POWERTECH, part number MP-3165, a single channel 12 VDC, 3.5 A [86].

MOSFET switching

To switch power for the auxiliary equipment logic-based, N-Channel MOSFET model number STP60NE06 is used for two reasons. Firstly, high voltage and current carrying capacities 60 V, 60 A make this MOSFET suitable to operate over a broad range. Secondly, the microcontroller output voltage from the digital side PWM is 0 VDC to 5 VDC, this allows the gate to tolerate a voltage between 0 VDC to 5 VDC and does not limit the power input to the devices [87], [88].

Solid state relay

SSR-25-DD allows high powered applications without exceeding the maximum power rating. A 3-32 VDC signal can switch a higher voltage 5 to 60VDC [89]. Solid state relays are excellent when high power switching is required.

2.1.3 Thermoelectric cooler and heat removal

TEC Peltier

Many electronic stores sell the Peltier TEC devices. It has efficient voltage V_{max} of 15 VDC and a maximum of 8.5 A, with the $Q_{max} = 68\ W$ [90]. Achieving a maximum Qc of a Peltier correspond to the optimal voltage and currents applied.

The Seebeck coefficients are essential for determining the TEC characteristics however, the mathematical equations which are used in determining the available power and COP are ambiguous from make to model. The main reason is, manufactureres data sheets do not mention what type of coefficients the n-type and p-type semi conductor constants are. This makes it difficult to calculate the TEC correctly. Seebeck coefficients do exist for Peltier devices but without knowing what this data is the information cannot be quantified. Supplied data sheets are more than enough to correctly quantify the heat energy absorbed per power input and is expanded upon in the latter [91].

Basic operation of a TEC works by applying a voltage to the positive and negative conductors, creating a temperature difference on each side of the plates. The low temperature Q_c side and heat rejected being the higher temperature side Q_h.

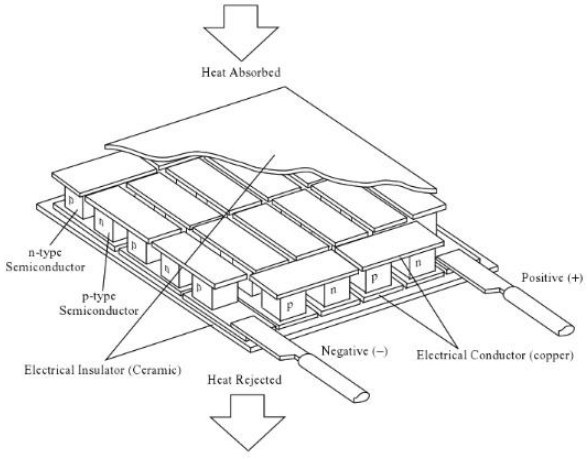

Figure 2-1 TEC arrangement with p and n-type semiconductors
The heat absorbed side and the heat rejected side with the positive and negative conductors [92].

Heatsink

Purchase of a heatsink has the unit dimensions of 0.2 m x 0.01 m x 0.015 m. The aluminium construction has a low thermal resistivity of 0.48 ºC/W and is used for the hot side of the TEC. The heatsink will reduce the flow of any heat energy flowing back towards the cool side of the TEC [77].

Heatsink Fans

Two fans model number YX-2521 is for extraction of heat from the heatsink both with 0.9 m x 0.9 m. The fans maximum operating condition is 12 VDC, 320 mA. Both fans have a maximum of 3000 RPM with a maximum volume of 0.028 m^3/s. The fans will enable a greater heat energy removed from the heatsink [79].

2.1.4 Thermal enclosure

Black Polyethylene Bucket

A 20 Litre black bucket has the diameter of 0.2285 m with a thickness of 0.003 m.

Polyurethane Foam fill

Fomofill ™ is a self-expanding polyurethane foam produced by Ramset. It has a density of 25 kg/m^3 to 35 kg/m^3 and thermal conductivity of 0.04 W/m °C. The long-term operating temperature range is -40 °C – 90 °C [93].

Epoxy glass base

An epoxy glass used for the base of the thermal enclosure has a thermal conductivity of 0.29 W/m °C and sourced from any local hardware store [94]. Aluminium would have been attractive to use because of the high thermal conductivity properties, but the correct sizing for a base is difficult cut and weld which requires skilled labour.

Internal aluminium enclosure

Aluminium housing forms the internal enclosure it has an inner diameter is 0.173 m and 0.001 m thick the mass is 0.411 kg and a total length of 0.265 m.

Thermal paste

Thermal paste used for all heat joints is Nano Diamond Thermal Compound ™. The volume required, and cost determine which thermal paste is suitable for the application.

2.1.5 Microalgae PBR agitation

Hydrodynamic bearing case fan

A case fan with dimensions 0.12m x 0.12m x 0.025m bearing fan is used. The fan speed is 1000 RPM with a maximum power consumption of 12 VDC, 80 mA. Microalgae species cannot tolerate large amounts of vigorous mixing therefore control of mixing will be determined by the user [71].

3D printed fan housing magnet holder

The magnet holder attachment is designed on the dimensions of the fan for agitation. Further details of the schematics for the magnet holder in Appendix A.1 illustrate the dimensions. The purpose of this design is to reduce the magnetic field induction that the magnets will cause on the fan motor reducing the output RPM. A calibration curve is obtained to quantify the speed of the motor.

Magnets

Two Neodymium block magnets establish the magnetic field to the inside compartment. Dimensions of this magnet are 25mm x 12.5 mm x 3.5 mm consisting of a pull force of 4.7 kg and N38 magnet grade.

2.1.6 PAR range LED RGB lights

12 VDC, 0.6 Amps/m LED RGB lights has the PAR range of 475 nm to 630 nm. The user will have control over the amount of intensity within the chamber to favour the microalgae's optimal growth regions [23]. There are higher LUX intensity options of RGB lights on the market with input voltages of 24 VDC but consideration to purchase the 12 VDC is based on cost. The user data sheets do not display how much heat energy the lights create.

2.1.7 Software programs

Arduino

C++ is the Arduino is the open source programming language, the version used for this design is 1.8.5 [95].

LabVIEW

LabVIEW is the interface medium between the user and the process. Since the microcontroller is open sourced Arduino a communication language must establish both platforms so controllability of the system from the user input is possible.

2.2 Design

Adopting the following notation in the coming chapters is displayed below.

$$Q > 0 : Energy\ transfered\ to\ the\ system$$

$$Q < 0 : Energy\ removed\ from\ the\ system$$

$$W > 0 : Work\ done\ to\ the\ system$$

$$W < 0 : Work\ done\ by\ the\ system$$

2.2.1 Thermoelectric cooling and selection

The opposite of a Seebeck effect can describe TECs, that is instead of generating a voltage when two dissimilar metals are touched they can generate a cold temperature on one side and a hot temperature on the other side known as ΔT_{TEC} [96]. This is done when applying a DC electromotive force to the semiconductors arranged by n-type and p-type configurations [96]. Advantages TECs offer are the reduced size, weight, simplicity and no moving parts or refrigerant [97].

Design calculations for the TEC are based on the ambient temperature of the external environment 30 °C. The ambient temperature for this design is chosen because a worse case scenario will highlight how well the PBR operates at a worse case scenario. The internal system must maintain

a final temperature where T_f = 15 °C. 15 °C is chosen as the worse case design criteria that the PBRs minimum temperature must reach. The temperatures mentioned are chosen to reflect the microalgae growth ranges 15 ºC + 30 ºC [40]. Below the calculations illustrate the total amount of energy required to keep the PBR at a steady state temperature of 15 ºC. Complete work and calculations is provided in Appendix A.3.

$$Q_{aluminium} = \rho_{aluminium} \cdot V \cdot C_p \cdot \Delta T = 64.51\ Wh \quad (9)$$

$$Q_{air} = \rho_{air} \cdot V \cdot C_v \cdot \Delta T = 0.2437\ Wh \quad (10)$$

$$Q_{water} = \rho_{water} \cdot V_{water} \cdot C_{water} \cdot \Delta T = -5.80\ Wh \quad (11)$$

$$Q_{total} = -Q_{aluminium} - Q_{air} - Q_{water} = -70.34\ Wh \quad (12)$$

TEC selection depends on $\Delta T_{TEC} = (T_H - T_C)$ on each side of the TEC device. T_H is the hot side of the TEC and T_C the cold side [92]. This temperature gradient will reduce the TECs ability to operate efficientley.

Determining the ΔT_{TEC} requires information from the amount of heat the heatsink can dissipate, the ambient temperature and the internal heat energy that will be removed. ΔT_{TEC} is calculated by the thermal resistivity of the heatsink, Q_{Total} in Eqn. (12) and the ambient temperature 30 ºC. Below the results by a similar method adopted from [98].

$$T_H = 0.48\ ℃/W \cdot (70.34\ Wh) + 30\ ℃ \approx 64\ ℃ \quad (13)$$

$$\Delta T_{TEC} = T_H - T_C = 64℃ - 15℃ = 49℃ \quad (14)$$

All the information gathered is organised into three cases presented in **Table 2-1** below.

Table 2-1 TEC design working parameters
Three different values of Qc is explored. To achieve a lower Tc the coefficient of performance will reduce because Q_c will reduce as ΔT_{TEC} increases.

S. No	T_H (ºC)	T_C (ºC)	ΔT_{TEC}(ºC)	Voltage (V)	Current (A)	Q_c (W)	COP_{TEC}
1	64	15	49	12	5.5	25	0.378
2	64	10	54	10.6	5	20	0.377
3	64	0	64	9.2	4	0	0

Three conditions have been characterised with S.No 1 the most desirable result. The decision that S.No 1 is decided upon, Q_c represents the amount of heat absorbed, which is much higher value compared to the other S. No. Although it is attractive to have a much lower temperature of $T_c = 0$ ºC, the diminishing returns of Q_c produce 0 Wh of energy absorbed, not enough to remove the required energy in Eqn. (12).

The coefficient of performance (COP_{TEC}) corresponds to how well the TEC can operate; while some well-equipped heat pumps are 6.8 [42], [99]. This Tec has a COP below 1 meaning, the TEC is very inefficient.

$$Q_c = +25\ W \tag{15}$$

$$COP_{TEC} = \frac{Q_C}{P_{TEC}} = 0.378 \tag{16}$$

Low COP results are expected because the amount of input power required to keep the TEC at 15 °C is 66 W, which is considered a significant input for such a small output Qc removed [100]. Obtaining a higher COP is achievable when Q_C output can attain a much higher energy absorbed, while the opposite is exact, reducing the input power will increase the COP. Neither condition is possible because the operating characteristics of TECs are limited.

The maximum amount of deliverable power to the TEC must not exceed the TEC rated power. The chosen power supply for the TEC module was illustrated in section 2.1.2. It has the output power of 12 VDC and 9.2 A. It is essential that the TECs limitations are not exceeded this will consequently destroy the equipment. Below, P_{max} is the maximum output of the power supply and P_{TEC} is the amount required to obtain values of Q_c.

$$P_{max} = 110\ W \tag{17}$$

$$P_{TEC} = 66\ W \tag{18}$$

$$P_{max} > P_{TEC} \tag{19}$$

2.2.2 Heat sink selection and design

Extended surfaces such as fins enable the heat energy transfer to occur more effectively [96]. Heat sink selection is a function of the TEC Q_h. For example, the more heat energy output of the TEC, the more heat energy the heat sink needs to remove therefore increasing the heat sink capacity.

The viability of this design requires the heatsink to remove all the heat from the TEC denoted as Q_H. To determine the heatsink capacity for the design the amount of Q_H removed from the thermal housing is the sum of input power and Q_c. The value of Q_H must not be larger than the maximum calculated value of heat sink Q_{hsmax}. Eq. (13) calculated the hot side of the TEC, T_H as 64 °C while section 2.1.3 illustrated the dimensions of the heatsink. Considering all the information at hand Q_{hsmax} is calculated below while the full workings is provided in Appendix A.4.

$$Q_{hsmax} = n \cdot \left(Q_f + Q_b\right) = 260\ W \tag{20}$$

Qf and Qb denote the heat transfer from the fins and base of the heat sink while the number of fins is n. Q_H is now finalised and shows that the heat sink Q_{hsmax} is sufficient for heat removal.

$$Q_H = Q_C + P_{TEC} = 91\ W \tag{21}$$

$$Q_{hsmax} > Q_H \tag{22}$$

A typical design approach followed is the use of forced convection to improve the transfer of heat energy [96].

Heatsink installation

The cold end of the TEC is pressed firmly against the aluminium core, and thermal paste is applied to both sides to form a seal. Once the thermal paste is applied the heatsink is placed onto the aluminium housing. 5mm nuts and bolts are screwed in place to hold and clamp down the TEC between the aluminium core and heat sink. fans are used as forced convection to remove any heat, to ensure the fans are attached firmly, screws are used to hold the fans in place. **Figure 2-2** below illustrates the design steps.

a) Thermal Pase

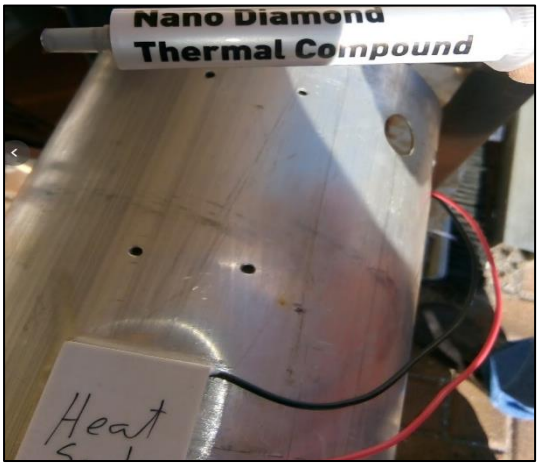

b) TEC with thermal paste and in position

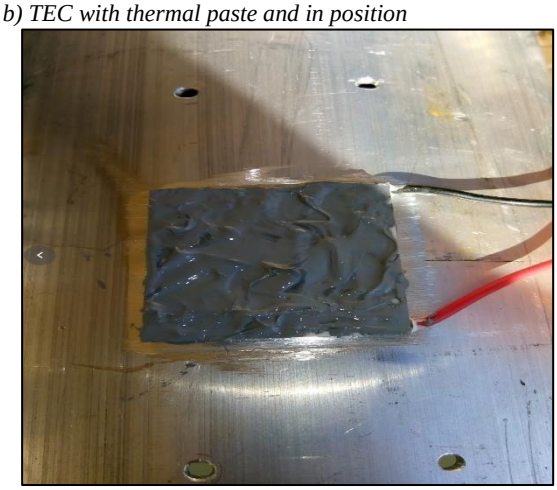

c) Heatsink with wall plugs

d) Fans mounted onto heatsink

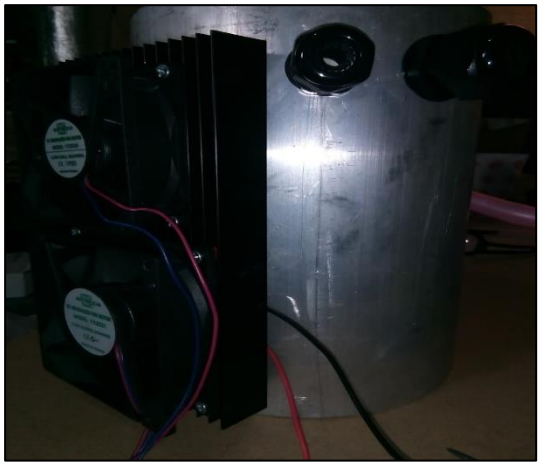

Figure 2-2 Heat sink mount

2.2.3 Photobioreactor design and modelling

A small enclosure is built for practical reasons; firstly, TEC output power is costly, and to build a larger chamber will require more TEC modules and larger power supplies.

To ensure the thermal housing is adequate and a method is followed American Society of heating, refrigeration and air-conditioning engineers (ASHRAE) has strict guide principles that apply to building codes and are reviewed [101].

Thermal insulation is assembled on the walls using Fomofill to reduce the air gaps. This will ensure that the walls reduce heat flow into the core and that the interior maintains an input steady state temperature. The internal aluminium housing is in direct contact with the TEC while the heatsink and insulation provides the thermal protection to the internal chamber.

Thermal mass is created around the aluminium chamber to ensure the absence of heat is maintained. Fomofill is suitable for this application because it is a polyurethane polymer with a low thermal conductivity property [102]. Fomofill is cast around the aluminium enclosure carefully, while the black bucket preserves the adequate layer to a minimum wall thickness of 0.047 m [103]. Thermal mass is the result, encasing the aluminium chamber with a low thermal conductivity material.

ASHRAE describes a thermal bridge section by a location where higher heat transfer may occur; increasing energy use and moisture build-up [101]. Perspex plastic on base the section of the thermal housing represents a thermal bridge section. The thermal bridge in this design is a necessity; it assists in allowing the magnetic flux from the motor housing to reach the internal PBR flask for agitation. Fomofill is placed around the thermal bridge to reduce external heat transfers.

Located next to the sensor cables is a second point entry, this is provisions for CO_2, pH which allows already operational devices platform onto the PBR once other services are placed through this opening minimal heat transfers will occur.

To reduce the impact of Fomofill entering the heatsink section metal is cast around the heatsink and the gaps are filled with thin cardboard to reduce the creep of Fomofill into the gaps and removed when dried.

For the base section to sit flat, the Fomofill is smoothed off at the point where it is about to about to set. The placement of fomofill in this section reduces the chances of any expansion from the Fomofill when curing times are in place as the Fomofill can expand to 3 times is volume.

Figure 2-3 Below is the thermal housing design from top left (A) Aluminium housing and the heatsink. (B) Entry holes for auxiliary sensors and pipes for CO_2 and PH. (C) heatsink. (D) Thermal insulation by Fomofill.

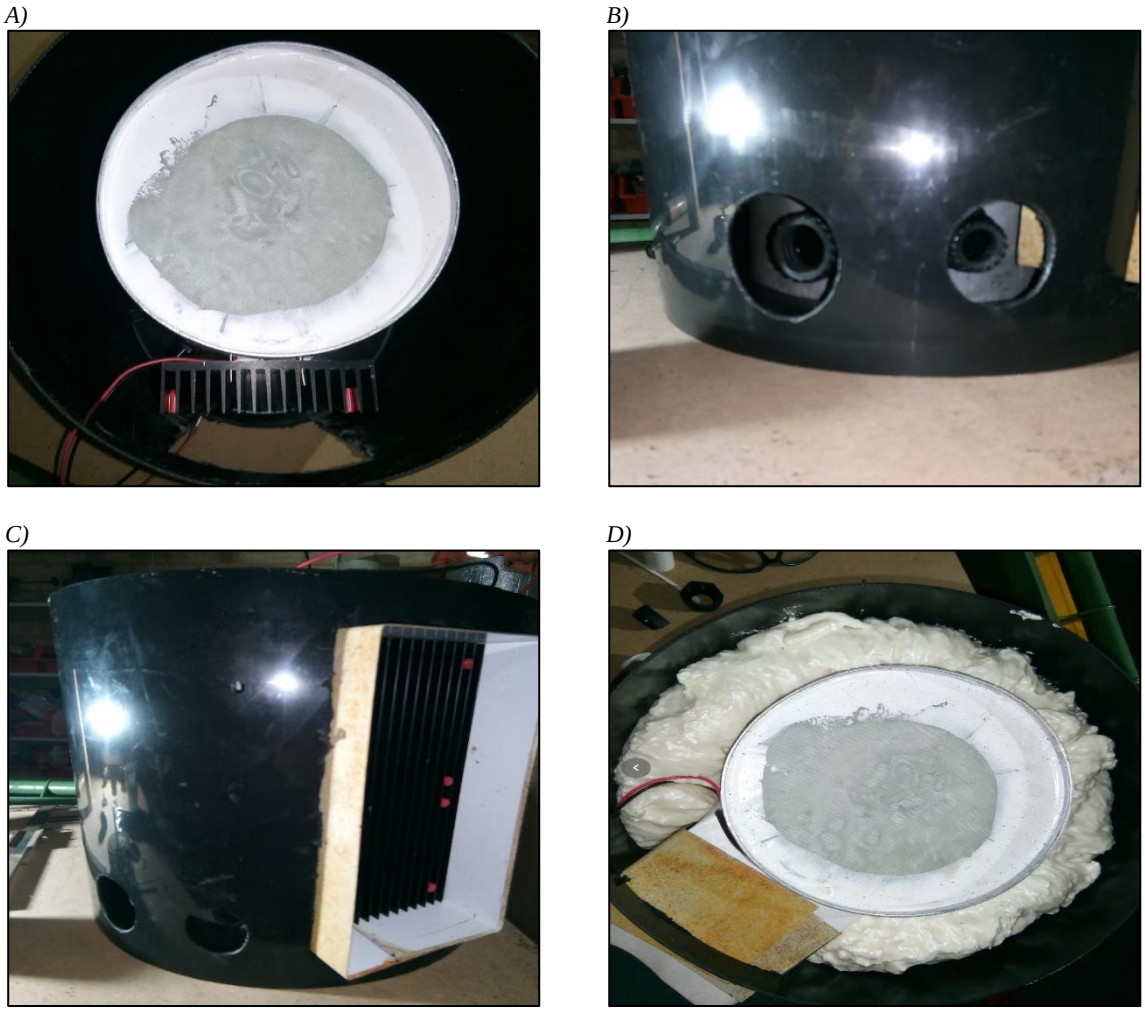

Figure 2-3 Design steps of Thermal housing

Heat transfer model

Q_{in} is the total heat transfer between the external environment and the internal section. To determine the heat transfer from the outside ambient temperature +30 °C to the desired internal steady state temperature of +15 °C is calculated below in **Figure 2-4**, while the full equations and calculations are provided in Appendix A.5.

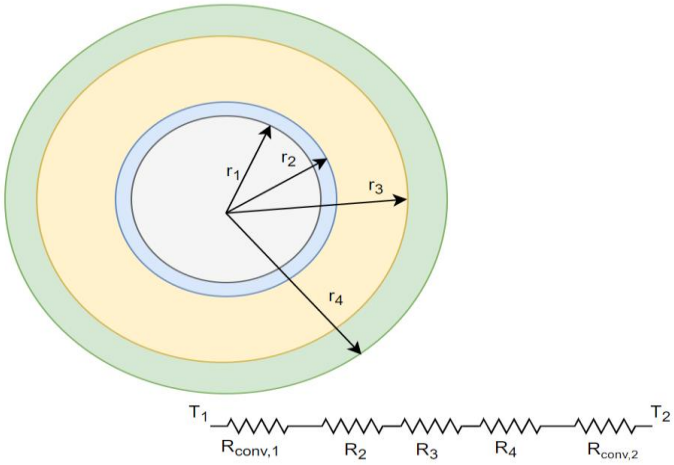

Figure 2-4 Thermal resistance of the PBR
Three layers, Light blue: The aluminium with r_1 radius. Yellow the polyurethane with r_3 radius and green the plastic mould with r_4 radius. $R_{conv1-2}$ are the convective heat transfers while R_{2-4} are the resistances of each layer.

The amount of heat energy required to keep the system at 15 ºC is Q_{in}. Q_{in} accounts for the thermal convection and conduction [104].

$$Q_{in} = -2.37\ Wh \tag{23}$$

Coefficients h_1 and h_2 is the heat transfer coefficients that are obtained from Y. A Cengel et al. [99] illustrating that 2 to 25 W/m^2 ºC is typical for free convection. Although h_1 and h_2 is not a property of the material, other factors like surface roughness, geometry, temperature and pressure determine what the heat transfer coefficient is [105]. To stay on topic, the coefficients of h_1 and h_2 are used from Y.A Cengel et al. The highest value of 25 W/m^2 °C is used for the worse case.

Figure 2-5 illustrates the overall thermal housing with the given water temperature from a tap at 25 °C while the TEC initial condition is 15 °C from the datasheet. Assumptions for the model is, the internal environment that being the aluminium housing is already at 15 °C. Therefore, the water

inside the 500 mL flask is assumed to reach the same temperature at steady state. In **Figure 2-5**-a, the change in water temperature of the flask is expected to reach its steady state condition after 25 minutes, if the temperature of the aluminium and the internal environment is already 15 °C. **Figure 2-5**-b shows the erratic oscillations coloured in Magenta; a result that the aluminium is already at a steady state temperature of 15 °C. As shown in **Figure 2-5**-c-d, after 200 minutes the inner insulation will reach the temperatures lower than originally set. Low thermal conductivities of polyurethane attest to the ability to maintain low temperatures.

a) Change in PBR water temperature

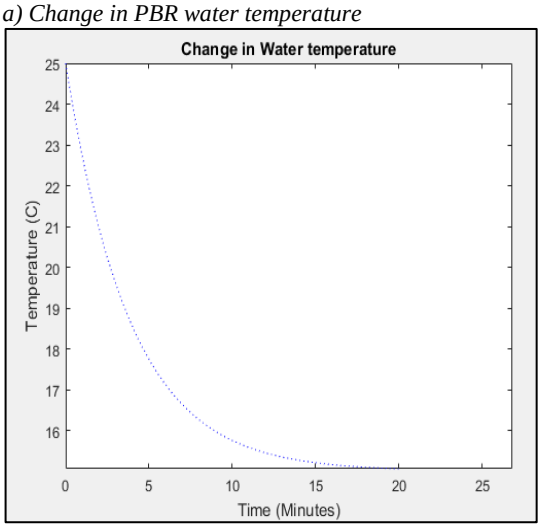

b) Change in Aluminium temperature housing

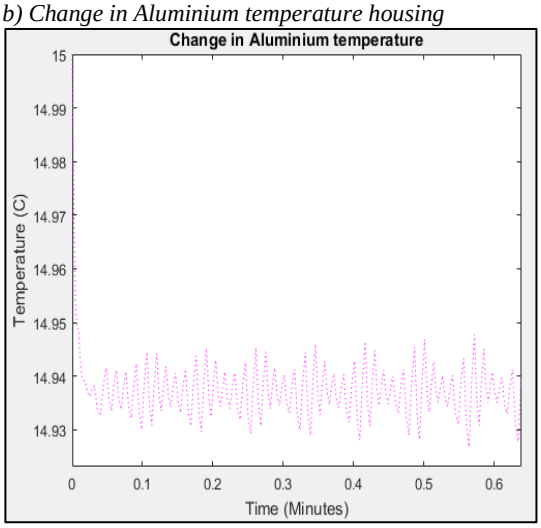

c) Change in Polyurethane temperature housing

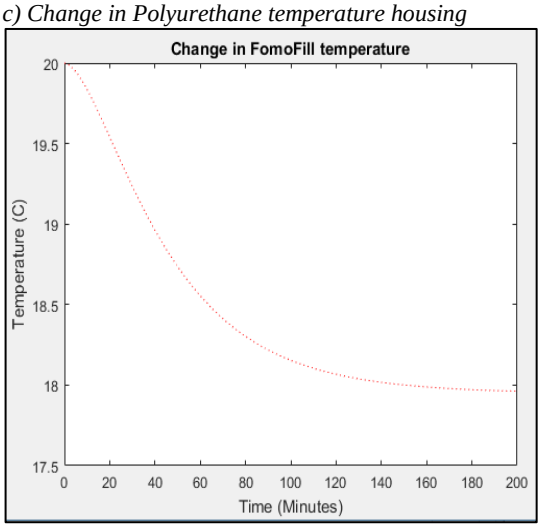

d) Change in Polyethylene housing

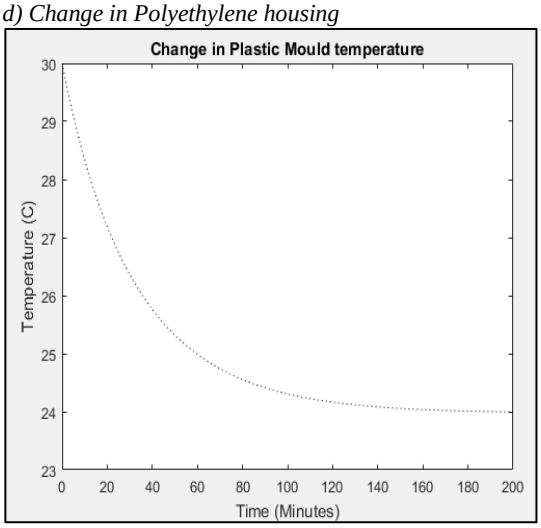

Figure 2-5 Heat flow through each of the layers in the housing
The above figure depicts each layer of the thermal housing and how tolerable the insulation is when the outside temperature is 30 ºC and the inner compartment is 15 °C. This steady state condition is the TEC delivering a temperature of 15 °C to the aluminium housing while the water temperature initital condition is T_{water} = 25 °C.

The heat transfer rate from the external section of the system to the internal is calculated using the methods highlighted in [106], [104]. Appendix A.6 illustrates the workings in full description.

The previous sections established the total Q_{in} and Q_{tot} from Eq. (12) and (23). To this point Q_c is 25 W, since total heat energy has been considered for all parts of the design the amount of time Q_c will operate for can be determined. $Q_{f,}$ the amount of total heat energy that is accounted for is shown below illustrates the total amount of heat energy that must be removed from the system.

$$Q_f = -Q_{tot} - Q_{in} = -72.71\ Wh \tag{24}$$

While the amount of heat absorbed from the TEC Q_c is +25 W, suggests that 25 W of power is not enough to remove Q_f. However, because the TEC is a heat pump, the device will need to operate for a total of 3 hours to have a noticeable effect on the heat removal of Q_f , the findings are expanded upon in the discussion.

$$Q_C = 25\ W \times 3hrs = +75\ Wh \tag{25}$$

2.2.4 Microcontrollers and instrumentation

The temperature sensor must be installed in locations that provides the most accurate data. The top section consists of the temperature and humidity DHT11 and the lower section the LM335Z temperature sensor both of the sensor data is averaged out and displayed in LabVIEW. The DHT11 sensor is not waterproof, so the precedence to install the sensor in the upper section is decided upon to improve the longevity of the instrument [107]. The Light sensor TS2561 is placed as close as possible towards the PBR section, this will ensure the light exposure values are as close to what the microalgae will receive.

Serial port data exchange by a single microcontroller was not possible. LabVIEW write back function block to the Arduino could not establish a link because the string data from LabVIEW to Arduino is difficult to implement. The serial data from LabVIEW in string format could not communicate with the PWM ports on the microcontroller. Every time the output of two or more commands from the LabVIEW interface was sent to Arduino microcontroller, intermittent faulting would cause a delay of information.

LIFA for Arduino is used to communicate with LabVIEW. The software addition for LabVIEW allows fast connection to each PWM and enables the exchange of data from the LabVIEW interface to the Arduino microcontroller effortlessly. A major drawback for this software, Murdoch university does not operate extra software for LabVIEW. The new communication uses two com ports, com port 3 and com port 4. Sensor data is sent from com port 4 while com port 3 controls the PWM outputs.

2.2.5 Electrical schematic diagram

Electrical schematic drawing

The electrical schematic diagram in Appendix D.2 **Figure 5-5** illustrates each connection point for the PBRs connections. The MOSFETs control the operability of each field device and is essentially responsible for sending outputs to the field devices. PWM 6 connects the MOSFET to the agitation motor which is supplied by (MP-3165) power supply unit. The power supply and MOSFET combination allow voltages of 0 V to the maximum of 12 V to the motor enabling variable speed control. Mixing is particularly useful when microalgae culture increases in density and the need to improve light capture on the culture is essential [13].

12 V power source (MP-3165) supplies power to the LED RGB spectrum lights. Connected to each colour red, green, and blue is three MOSFETs PWM ports 11, 10 and 9 respectivley. The advantage of using three MOSFETS is red light can be mixed with green light to create yellow light, or all lights can operate together to create white light. The alternative is possible for example; using a single PWM port will allow more direct experiments like blue light, which is vital for experimentation in algae growth [24].

The TEC PWM port is 5 and is part of the control feedback loop that enables the control of the temperature by voltage to operate the TEC proportionally from 0 W to 25 W the stand-alone power supply is connected to the MOSFET and the PWM port on the microcontroller.

PCB design

Hobby based Arduino boards and sensors have short cables that are plug in pin-based connectors. A solution is required that enables the length of the cables to connect to the PBR and the terminal enclosure without changing the pin conductors on the microcontroller.

A PCB board is designed and ordered online from china. The connections of the microcontroller and sensors can connect to each field device without the need for soldering.

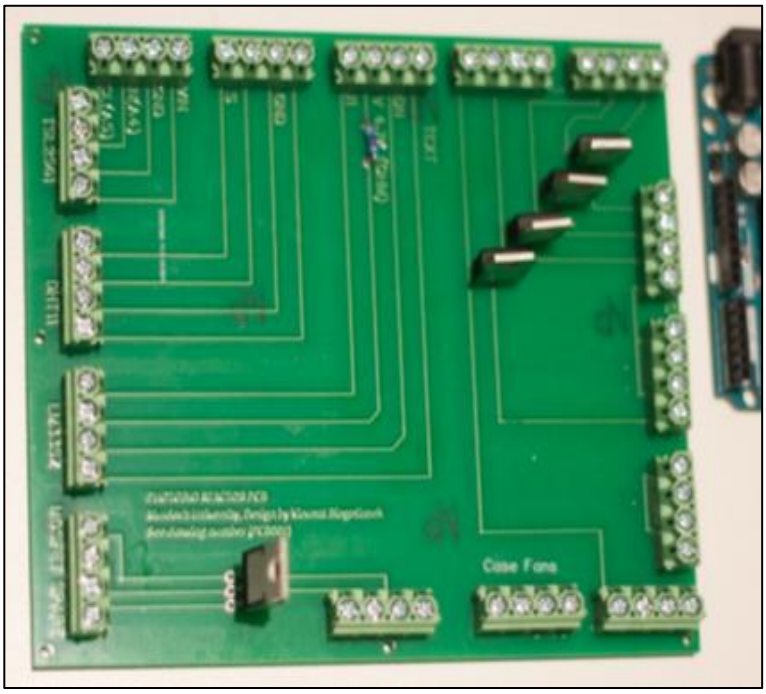

Figure 2-6 PCB Board
designed by Vincent Blagotinsek, manufactured in China by JLCPCB.

This PCB offers extra connection points for a separate MOSFET connection and the ability to connect and control a relay if necessary. Cooling fans will also connect to the PCB where a section is designated that act as the junction supply for each fan. The electronics section and fans for the cooling of the heat sink are all connected at their labelled sections within the PCB so anyone willing to build similar products can connect new systems easily.

2.2.6 Agitation design

The purpose of Agitation design is to create a system where the user can manipulate the speed of agitation and in turn, find the optimal range where microalgae can experience a maximum growth rate. It is known that too much agitation in the PBRs can cause shear stress to microalgae, this, in turn, reduces the growth rates [72].

Fusion 360 is a free online 3D printing software is used when designing the magnet housing [108]. Dimensions of the fan is used and transposed onto the software and a magnet housing is designed and printed. The functions of the 3D printed mould is to hold the magnets, account for the thickness of the PBR base, and mitigate any magnetic fields that will reduce the speed of the fan. Appendix A.1 provides the design of the magnet housing. **Figure 2-7** shows the fan housing.

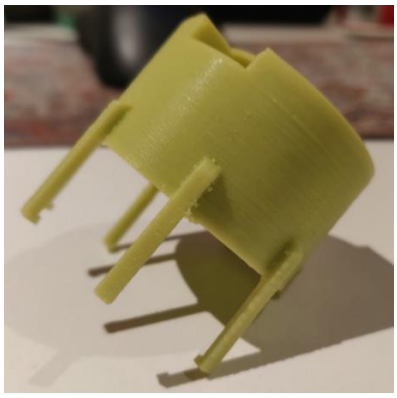

Figure 2-7 3D Printed fan arrangement

A fan motor rotates the flask stiring bar. The magnetic housing attatched to the fan agitates the PBRs fluid by magnetic flux to the bar stirrer. One of the main issues when working with such a device is magnetic fields and the interferences on the overall RPM of the motors from the magnets [109].

Although no instruments are used to determine the magnetic field strength similar experiments are conducted to find where the field was the strongest. C. Ravadulla et al. [110] illustrate that 2-3 cm apart the magnetic field range of Neodymium magnets are measured. The magnetic field strength (mT) illustrates that values between 150 – 200 mT, and anything closer will have a greater mT value. The magnetic strength for this design is conducted by field testing and reducing the gap to a minimum of 2.5 cm increased the field strength for the mixing bar inside the flask.

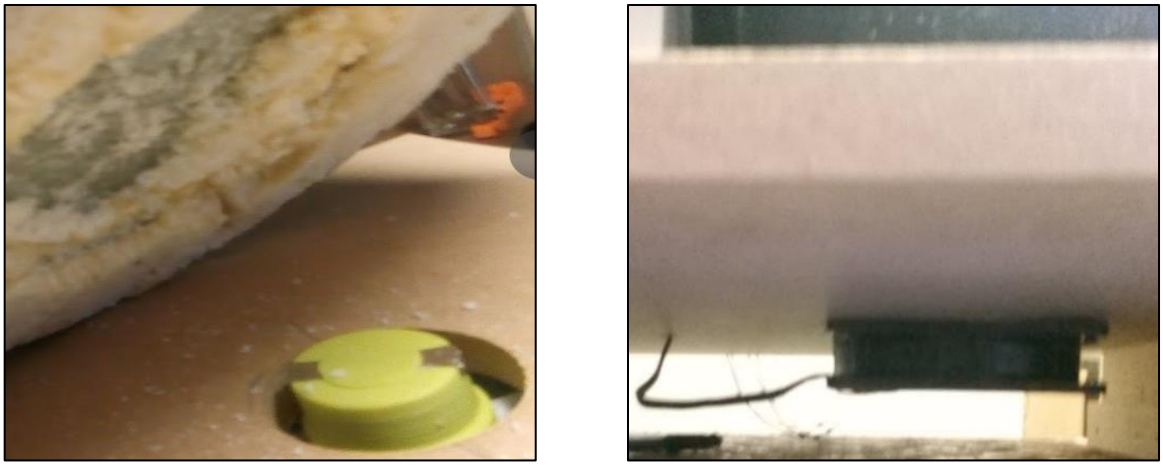

Figure 2-8 Magnet Housing overlay
Left, the final design of magnets with the cut-out. The thermal enclosure is sealed down above it. Right, Underneath mounting of the fan motor. Source: (The author)

User input allows the enables the speed control of the motor. The overlay in LabVIEW allows the user to input desired values into agitation motor values, in turn, causing the motor to turn. A cheap but not so accurate representation of the speed curve is the calibration curve. The calibration curve is implemented in LabVIEW as a cheap RPM metre, so some idea of the RPM is displayed on the overlay. Illustrated in **Figure 5-4** Appendix B.1 is the calibration curve.

2.2.7 LED lighting

LED lighting will assist in microalgae photosynthesis. The LED lighting is installed inside the aluminium section. The lights are fastened inside the aluminium housing by applying the sticky side of the LED inside the chamber. Supply voltage of the lights is 12 V and is connected to the main PCB where three separate MOSFET's allow control of red, green and blue light. The address of each light is then embedded into the LabVIEW software so that the operator can select the required light.

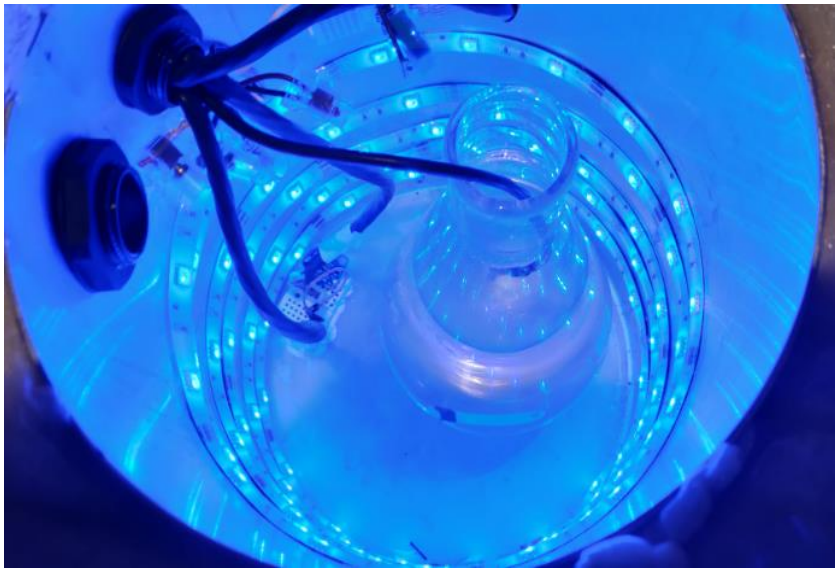

Figure 2-9 LED installation inside the PBR

Light dark ratio

A problem occurs when a case loop consisting of a timer is used to control the duty cycle of the RGB lights. Delays in process speed occur, and the Arduino output fails to operate fluently. Therefore no light:dark ratio will be implemented

2.2.8 Software user interface

Arduino

Sensors compatible by Arduino are very common and cheap, some of these sensors require libraries to operate. A good example is the lux sensor, it requires a library download and operates in conjunction with the Arduino language. The sensors which require a library are DHT11, TSL2591 and the LM335Z.

Calibration of the lux sensor is achieved in the Arduino program this enables finer adjustments of lux ranges sensitivity of the range is viewed in Appendix E.1.

For PWM signals to communicate with LabVIEW from Arduino; LabVIEW interface for Arduino (LIFA) is used. This enables the PWM signatures a communication line between the LabVIEW software and Arduino effortlessly. LIFA is a LabVIEW additional software that can be

downloaded free of charge and is designed by national instruments. LIFA blocks are used for the LED lights and the PBR mixer.

LabVIEW

LabVIEW is the user interface where the user can change the intensity of a single LED light or a combination of all three ranges together RED, GREEN and BLUE. Experimentation of motor speed indicators and the visual representation of the complete process. The user can download excel data over a period and investigate the influencing growth parameters.

The temperature sensor and lux information is sent by VISA read by string array and is displayed on the interface overview. Temperature setpoint allows new temperature conditions while humidity PBR temperature and inside ambient temperature is displayed on the temperature analysis section.

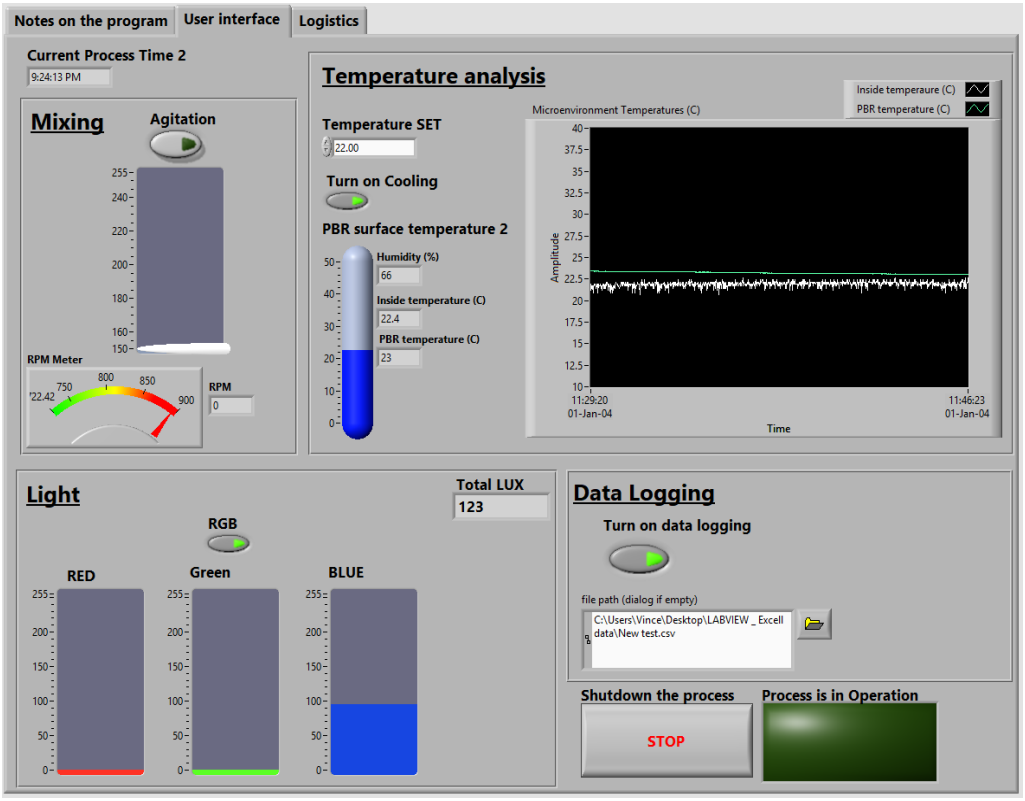

Figure 2-10 LabVIEW user interface

The data logging section on the user interface saves the LED light intensity, mixing RPM and the humidity, temperature and the PBR temperature into an excel spreadsheet. By selecting the folder, new files or old files are accessible.

2.2.9 Feedback PI control for Thermoelectric coolers

At this stage, it is not yet clear which is the more advantageous process variable that the PI controller will be installed on. The same MV influences both the internal ambient temperature and the PBR. Therefore, the internal ambient temperature and the PBR water temperature will be experimented on individually to find the best matching. A typical control pairing is to select the directly acting MV to influence the behaviour of the PV [111].

Temperature control for the TEC is created in LabVIEW. The following PI control law is adopted in the time domain form following the methods outlined by D. Seaborg et al. [112].

The derivative term from the PID controller is negated because the temperature sensor LM335Z produces very fine temperature ranges that are calculated to the accuracy of two decimal places, including a derivative term will cause more oscillations and unwanted behaviour [111]. Eq. (27) is the PI algorithm from the time domain into the discretised Velocity form Δv_k.

$$u(t) = K_c \left[\varepsilon(t) + \frac{1}{\tau_I} \int_0^t \varepsilon(t) dt \right] \tag{26}$$

$$\Delta v_k = K_c \left[\varepsilon(k) - \varepsilon(k-1) + \frac{\Delta t}{\tau_I} \varepsilon(k) \right] \tag{27}$$

The second choice of a discretised PI controller called the position form is available to implement. However it is not suitable for this process. Implementing velocity form has many advantages such as the change in controller output is calculated directly. This change in output is particularly useful for the PWM output which primarily drives the TEC and can be advantageous in controlling the antireset windup [112].

Estimated errors of antireset windup will occur when the temperature is close to the setpoint, this will cause the threshold of the output to reach the maximum of 12 V on the TEC. The obvious is expected of 0 V within seconds of each other occurring constantly.

Small spikes in the temperature could increase the PWM signal to a maximum of 5 V which will equate to around 12 V on the TEC side. Consequently, this will dramatically reduce the life of the TEC and cause overheating of the MOSFET [111], [113]. Certainly, tuning methods of the gain and integral terms of the PI controller will reduce some of these spikes, and these ideas will be expanded upon in the results section.

Figure 2-11 shows is the function block diagram of the implemented PI controller. Here it is illustrated that the PWM port 5 will send the signal to the TEC to switch on or off depending on how small the error calculation. The block diagram illustrates the control logic flow that is used to invoke the temperature change inside the microenvironment.

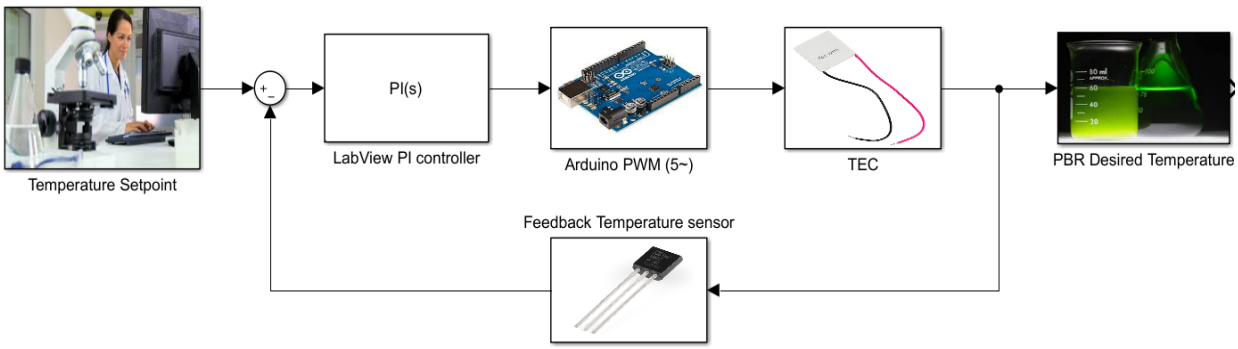

Figure 2-11 PI Block diagram of Microenvironment

Software handshaking

Information is processed from the sensors and sent to the microcontroller. This microcontroller sends the information by the serial communication protocol to LabVIEW where the PI controller in velocity form is implemented.

The summing point for the implemented controller is a point of interest; this is how the error for the PI controller in LabVIEW is generated. Creating the error is done by subtracting the temperature process variable from the initial setpoint temperature change. The error iteration is calculated at t = 0 and the second error iteration is sent back to the controller when t = 1, thus the difference in control action multiplied by the gain K_C [111]. As the controller calculates the required control action the information is sent to the calibration curve equation so that the characteristics of the PWM input to the TEC is preserved and not mismatched.

The slope of the gradient at the output vs the input is created so that the microcontroller can output 5 VDC to the MOSFET, suggesting that the microcontroller receives the PWM signal in the form of 0 to +255. Essentially this voltage is stepped up and is what regulates the Qc of the TEC by the proportional supply voltage. **Figure 2-12** below illustrates the LabVIEW PI and the calibration curve equation Appendix B.2 shows the calibration curve workings.

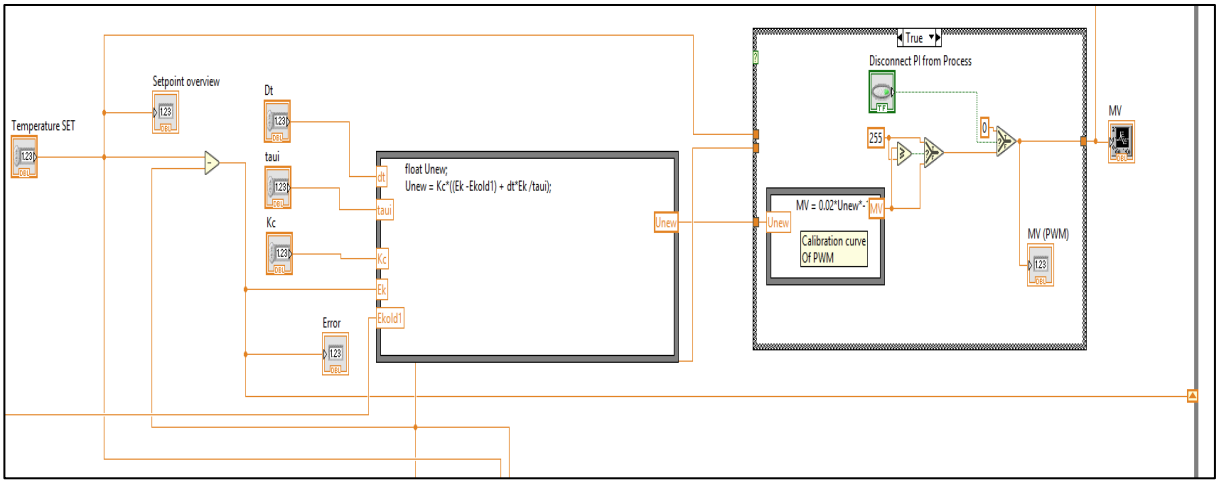

Figure 2-12 PI and PWM calibration data
Above is the PI controller in LabVIEW. The far left is the setpoint the subtraction block is the error which is sent to the Equation block where the PI in velocity form is implemented.

The internal ambient temperature and the PBR water temperature will have separate instances where the PI controller will be installed on the water temperature sensor and the ambient temperature sensor individually. Therefore the same treatment as the above chapter is implemented on the PBR water temperature PV also.

PI control tuning parameters

Quantitative approaches such as Ziegler-Nichols tuning methods is difficult to implement. The difficulty lies in obtaining a transfer function to obtain the proportional controller gain K_c and the ultimate period P_u. Pushing the temperature ranges beyond the point of instability to allow the system to oscillate and obtaining the P_u value is not realisable. The time constants between each temperature iteration will take hours while a similar outcome implementing relay tuning is also expected.

Other quantitative methods of process characterisation is visited such as Cohen-Coon, first order model characterisations in MATLAB and least squares method in excel. Both methods are not realisable because the process variable data from the sensor is reading too many points within two decimal place and causes model mismatch when exported to MATLAB or excel. When Cohen-Coon is trailed the response from the process reaction curve takes hours to reach the setpoint. When implementing the τ and α from the obtained curve, very large time constant and the signal distortion is too noisy from the poor-quality sensor.

The qualitative approach by trial and error is used. The main control objective is, the MV should not operate at such a high switching frequency. Observing the MV response as the PV moves closer to the setpoint. By reducing or increasing the proportional term first the controller output signal must not behave so aggressive. The integral terms is then adjusted so no overshoot will occur.

On off control

This control logic that will enable the TEC output to behave less aggressive. When the temperature increases past setpoint the TEC will turn on with a PWM of 255 which is 100% of the full load supplied to the power supply. The opposite is expected, if the temperature moves below the setpoint the TEC will turn off sending a signal of 0 that corresponds to 0%.

PWM signature of 255 will correspond to 5 V at the microcontroller and 12V at the TEC. Although the TEC operates at a maximum voltage of 12V a PWM signal of 255 is chosen because the solid-state relay operates between 3 to 5 VDC and will always supply the maximum voltage to the load.

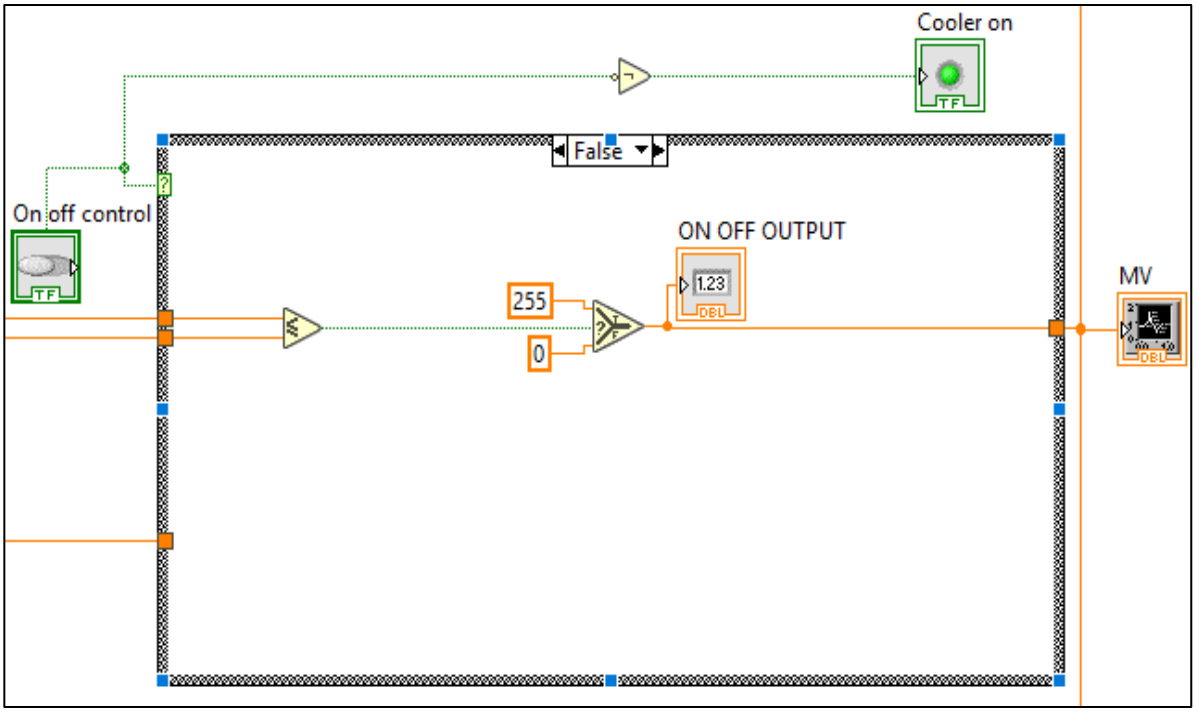

Figure 2-13 On / Off control
On/off control when the setpoint is lower than the incoming temperature the TEC will switch on and remove heat energy from the environment.

Implementation of on/off control is now in operation with the utilisation of a solid-state relay to deal with the high-frequency switching. This high-frequency switching is still apparent, and while the PV moves close to the setpoint, the error sent to the MV will not change as much and cannot be corrected without further analysis or filters.

The advantage a solid-state relay has compared to a new MOSFET is the solid-state relay can handle a higher frequency switching, and no risk of electronic components being damaged can occur.

Chapter 3. Results

3.1 Temperature

Within this chapter multiple testing was done when the ambient temperature of the room was at different temperature ranges, therefore, some results may vary for example the ambient temperature in the design phase was 30 °C. The following figures labelling will relate the internal ambient temperature of the PBR as ***Inside temperature***. This notation is adopted on the legend to reserve less space; both terms are used interchangeably.

Model validation

A step input from 26 ºC to 24 °C is implemented. After 30 minutes the temperature of the PBR and the internal ambient temperature will reach the steady state condition of 24 °C.

Modelling the temperature was illustrated in the design chapter **Figure 2-5**. The assumptions of the model are; if the internal temperature of the PBR is set to the same steady state temperature as the PBR water flask temperature, then the PBR flask water temperature model will reach the same steady state condition as the internal temperature as shown below in **Figure 3-1**, the inside temperature and the model PBR water temperature.

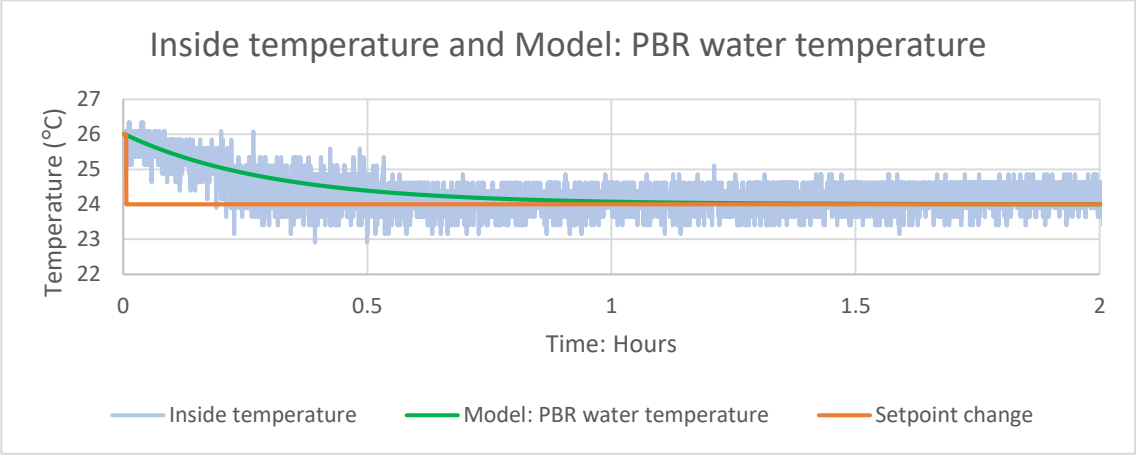

Figure 3-1 Inside temperature and PBR water temperature

3.1.1 Temperature control: internal ambient temperature

PI control on ambient temperature sensor

When in the testing phase it is required to observe how the PWM output will react when a setpoint change is implemented. Although the deviation from PV and setpoint at 0 – 10 seconds is observed on **Figure 3-2**-a, the figure illustrates how the controller reacted when a setpoint change is implemented when the PV is close to the setpoint.

Antireset windup occurs when the setpoint is close to the PV, tedious error signals are generated and cause the PWM signal to send higher voltages than required. The MOSFET was destroyed by overheating and is the result of high-frequency switching. Below on page 58, **Figure 3-2** depicts the process variable and the corresponding PWM output.

a) Process variable and setpoint change

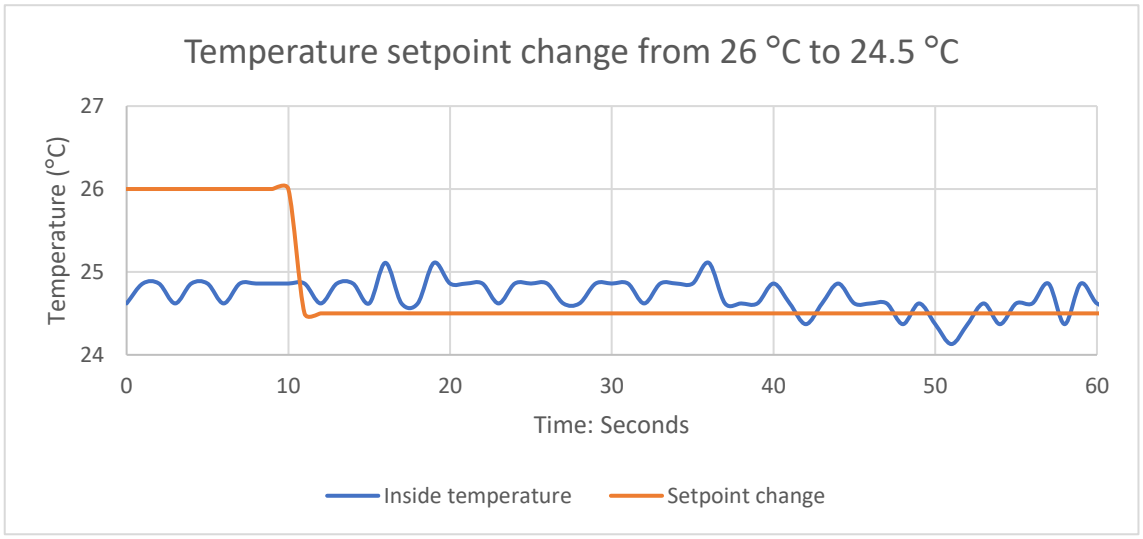

b) MV from LabVIEW to Arduino

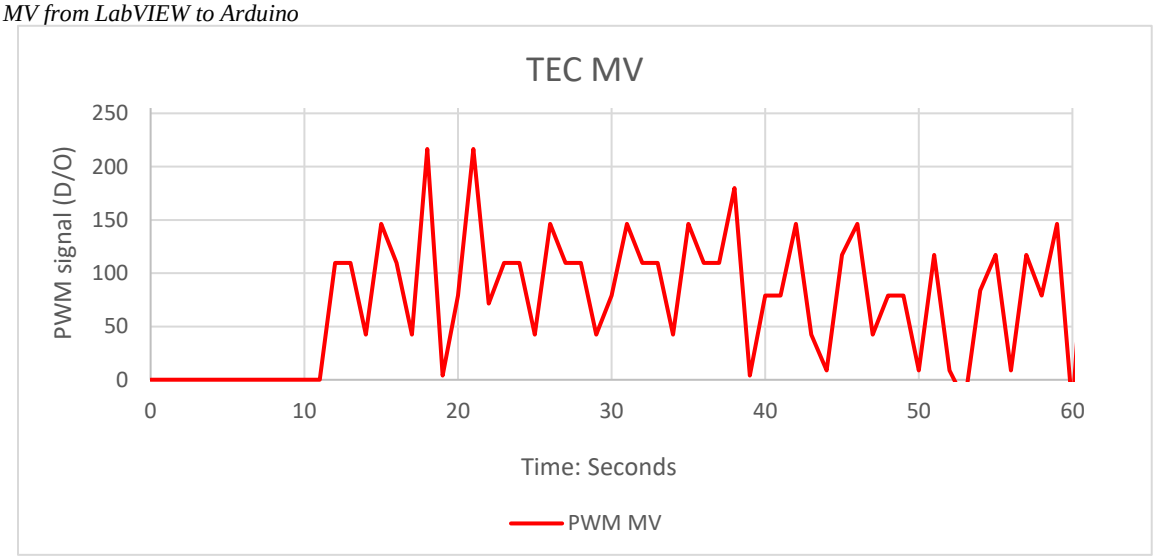

Figure 3-2 PWM output to TEC

In the design phase, the PWM signature was tested, (a): temperature setpoint change from 26 °C to 24.5 ºC, (b): PWM manipulated variable.

The behaviour of the PI control in **Figure 3-2**-b establishes that when the input step is change from 26 ºC to 24.5 ºC is implemented depicts how poorly the controller operated. After 10 seconds the MV behaves so aggressive sending this signal value to the TEC voltage supply.

The feedback signal from the sensor verifies how low-quality components can destroy a MOSFET. From this point onwards, a solid-state relay is implemented immediately to remedy the MOSFET issues.

Field validation

Below on page 60, **Figure 3-3** represents the PV and MV characteristics of the microenvironment under PI control with the MOSFET now replaced with the solid-state relay. 2 hours 13 minutes after the setpoint change is implemented the MV starts to operate as the PV begins to cross the setpoint boundary **Figure 3-3**-b illustrates how the MV is operating.

A setpoint change from 21 °C to 20°C was implemented and minimal temperature change was observed over a total of 2 hours and 30 minutes while the PBR water temperature experiences very little change in temperature. One thing to note is the high frequency switching is still observable because the controller is still installed on the internal ambient temperature sensor while the solid-state relay is now in service to replace the MOSFET while still under PI control.

a)

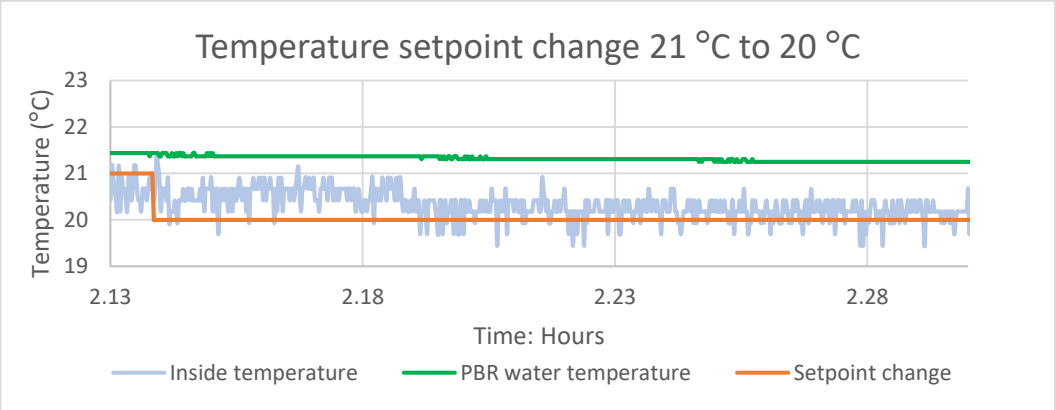

b)

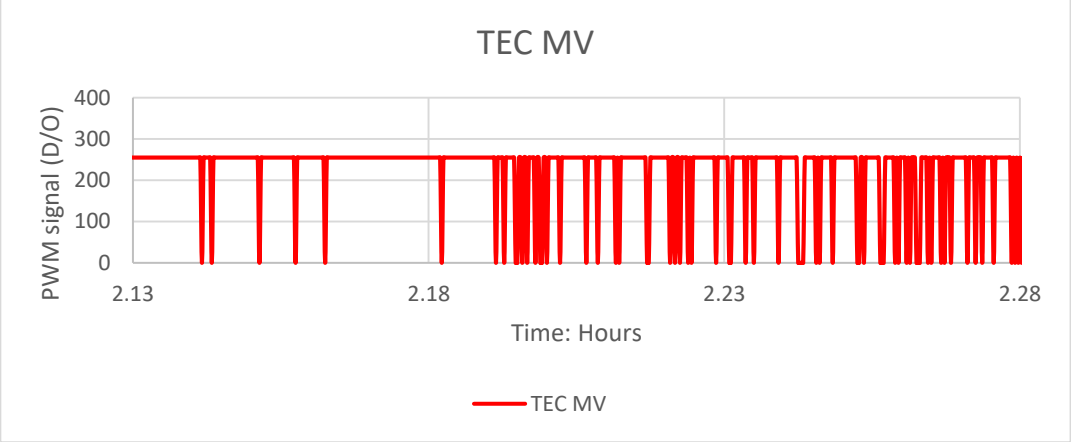

Figure 3-3 Field testing the PBR
The PWM signal is set to the value of 255 to reduce the full load capacity on the power supply. Notice a setpoint change at t = 0 is implemented while the temperature after 3 hours is 22 °C. This asserts that the TEC is too small for the application.

Effect of light

Below on page 61, **Figure 3-4** shows temperature runaway in the system. When a temperature setpoint change from 25 °C to 15 °C is implemented with 650 lux of red light, the TEC does not have enough power to remove the heat energy produced by the RGB lights. After 1.5 hours of service time the temperature of the internal system does not move towards the intended setpoint target. This is not a desirable response.

a)

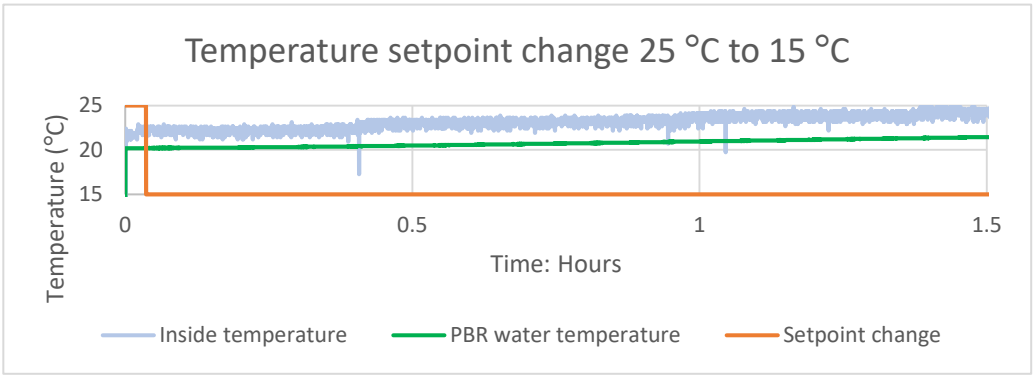

b)

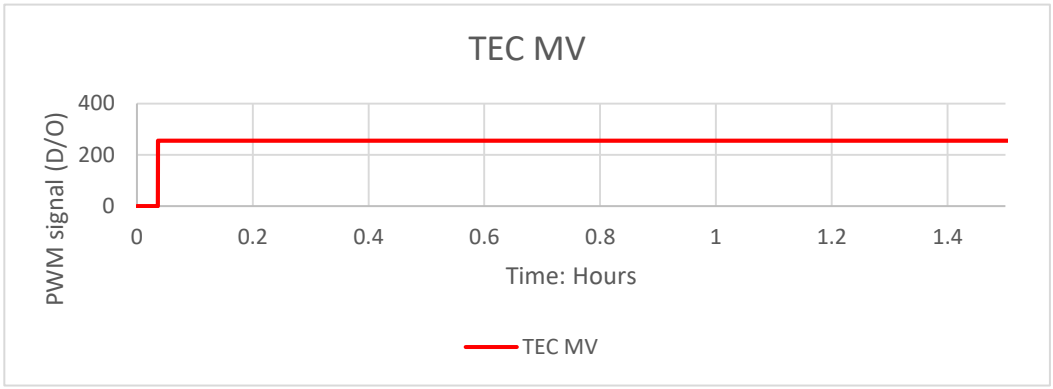

c)

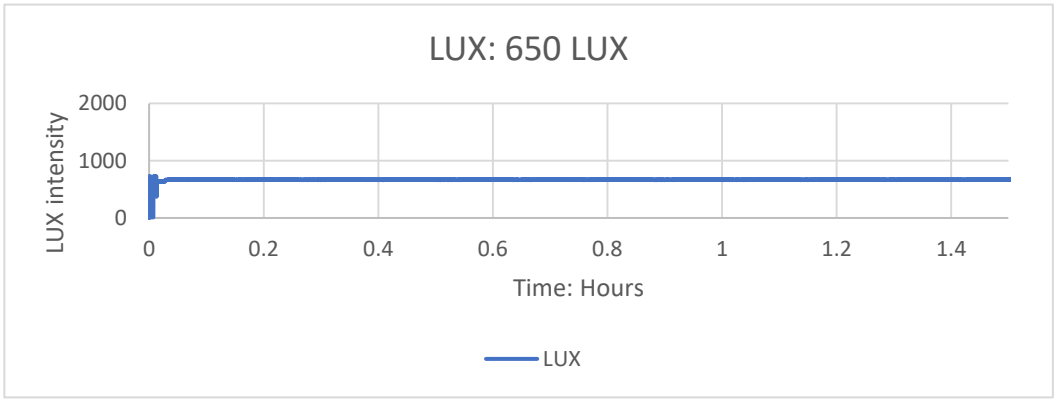

Figure 3-4 Temperature and LUX interference

A noticeable change of temperature occurs when the RGB lights are on. A LUX reading of 650 creates enough heat that it causes the temperature to rise. Figure a) illustrates how the temperature can rise causing the setpoint to become unattainable.

Setpoint change to lower temperatures

Figure 3-5 illustrates a temperature setpoint change from 20 ºC to 15 ºC while applying a full 12 VDC to the TEC. To illustrate how inefficient the TEC is, a small change in temperature is observed after 2.5 hours of service time. The large offset shows that the PBR temperature will never reach 15 ºC.

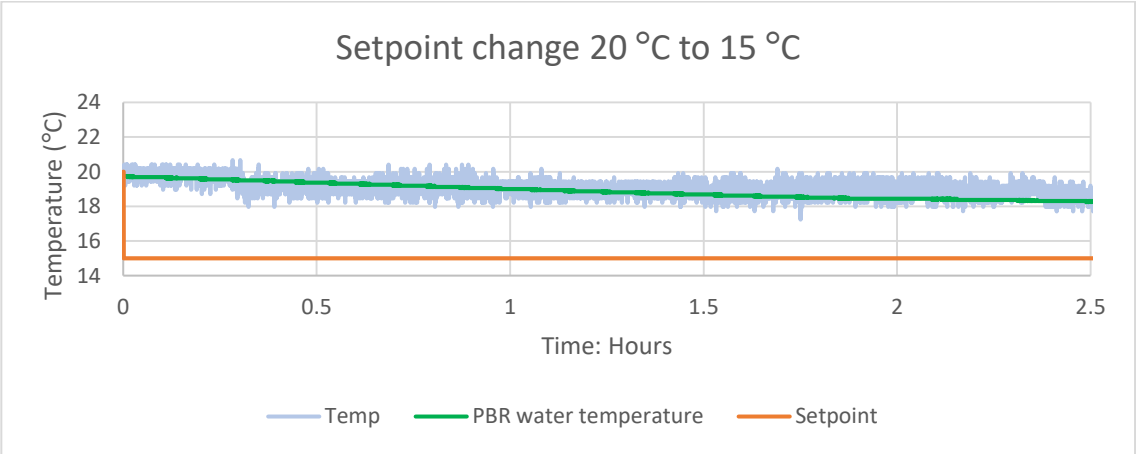

Figure 3-5 Contrasted model and field results
At t = 1 a setpoint change from 20 ºC to 15 ºC is implemented. No change in temperature occurs over the given period.

3.1.2 Temperature control: PBR water temperature sensor

On / off control

On / off control is installed on the PBR water temperature sensor. Below **Figure 3-6** Illustrates two setpoint changes the first change is implemented at t = 0 and the second change is implemented after 3.5 hours.

At exactly 2 hours, the PV crosses the setpoint boundary. In **Figure 3-6**-b illustrates that there is no high frequency switching present. After 2 hours the MV switches off and the water temperature drops another 1 °C. The final setpoint change of 15 °C is implemented and the MV increases to full power as noted in **Figure 3-6**-b between 3.5 hours and 4 hours.

Figure 3-6-b shows there is not enough power for the TEC to remove any more heat energy after 4.5 hours. A total of 4.5 hours in service time logged and a total change in 6 °C in temperature.

a)

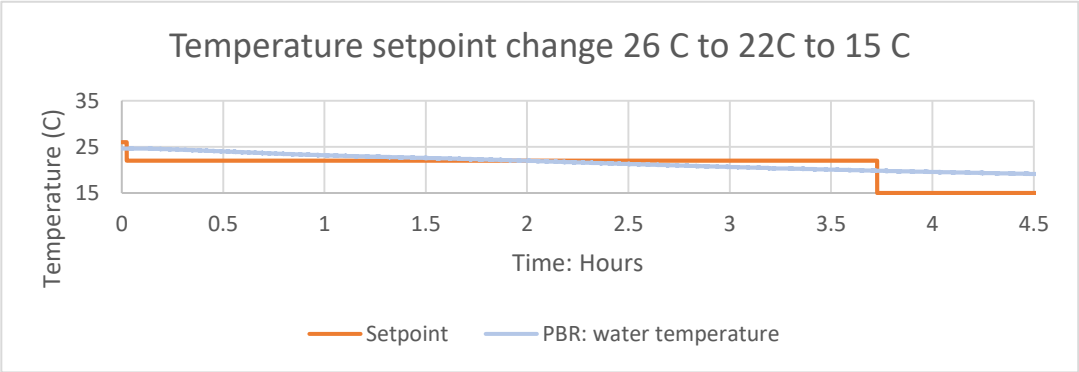

b)

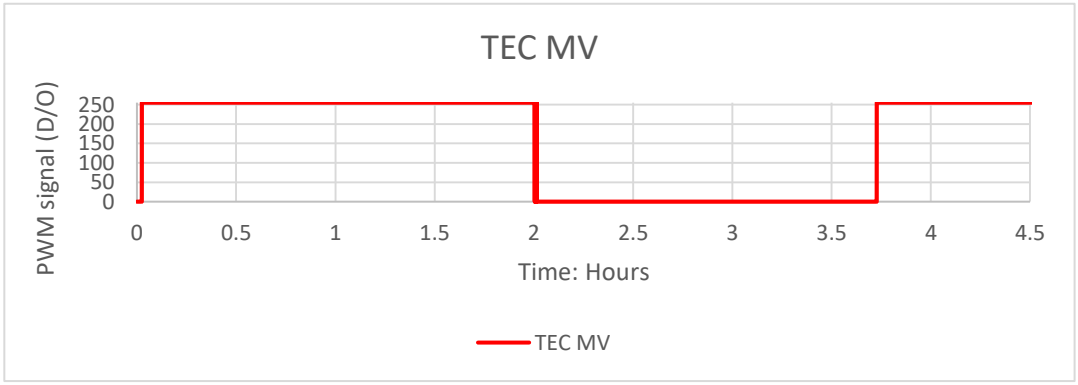

Figure 3-6 PBR water temperature with on/off control

3.2 Agitation mixing curve

Digital Tachometer (DT-48) obtained the values for the calibration and was implemented by steps of 10% for a PWM output. The response of the FAN is only observed after 60% of PWM input and any RPM value below 60% is considered 0 RPM. The before and after effect of installing the magnetic housing is displayed in Appendix B.1, **Figure 5-4**.

Table 3-1 Agitation motor RPM before and after results

% Input	PWM input	RPM Before	RPM after
60	153	760	730
70	178.5	796	772
80	204	840	816
90	229	860	852.6
100	255	910	878.7

3.3 Lighting sensor and RGB light

By changing the single RGB lighting lux intensities are obtained for each separate instance. Red is 950 lux, Green is 770 lux, Blue is 335 lux and the total lux with all intensities is set to the highest value, that is 1850 lux. This test is conducted by changing the sliders on the user interface in LabVIEW and observing the change.

Other various colours are obtainable by mixing red, green and blue spectrums from the user interface.

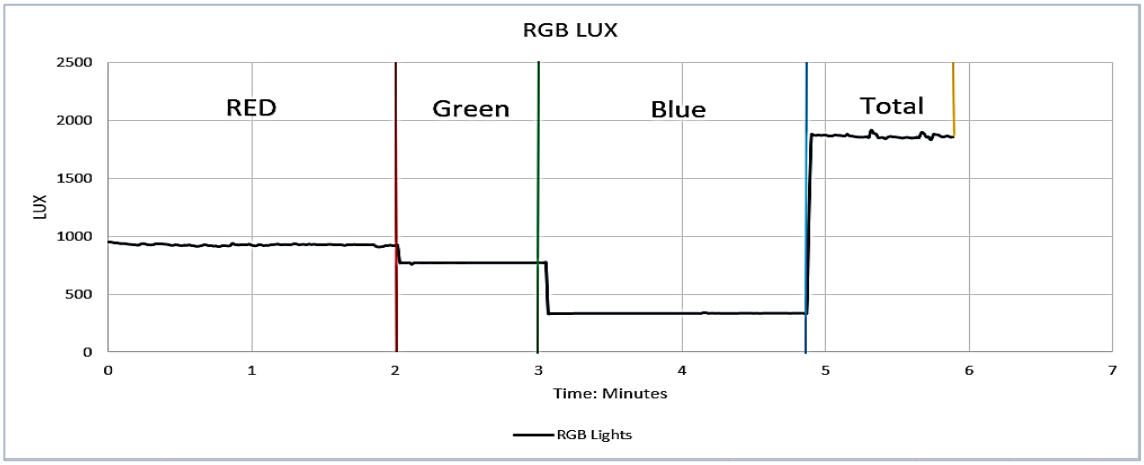

Figure 3-7 RBG LUX intensity

3.4 LabVIEW and Arduino communication

LabVIEW and Arduino communicate effectively using the LIFA software. The PWM ports are accessible to any pin located on the microcontroller. By using the toggle sliders on the interface, the intensity of lights or the speed of the agitation motor is accessible.

Figure 3-8 Illustrates how the PWM signal and the corresponding LIFA block operates. A value of 138.39 is sent to port 10 on the Arduino controller, and the output field device receives this signal and operates at the PWM value of 138.39.

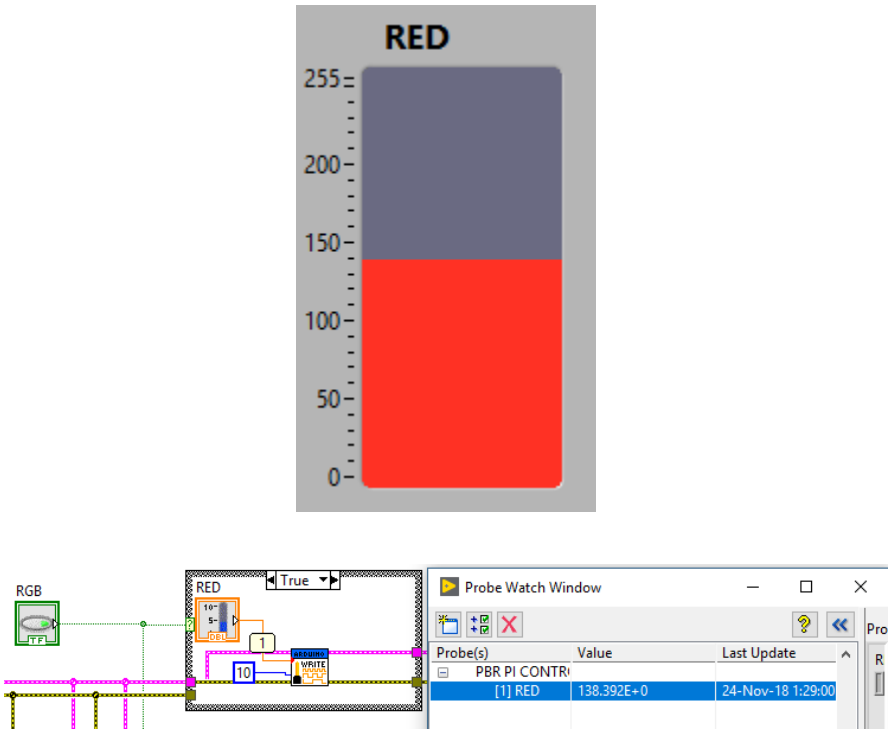

Figure 3-8 Red LED PWM signal in LabVIEW

Chapter 4. Discussion

4.1 Temperature control and setpoints

The noticeable change over 2.5 hours of time in **Figure 3-5** suggests the internal heat energy is too much for the input power and is related by the first law of thermodynamics which states: the change in internal energy U of the system is equal to the sum of energy transferred across the PBRs boundary by heat and work Eq. (28) below where ΔU is the change in internal energy, W is the total work and Q is the heat by the notation adopted from [114].

$$\Delta U = W - Q \tag{28}$$

Eq. (24) on page 44 illustrated that there is -72.71 Wh of energy which needs to be removed and Eq. (15) confirmed the amount of work that the TEC could output was +25 W. Eq. (29) below illustrates the internal energy possessed by system boundary still requires -47.71 Wh of energy that must be removed from the system.

$$\Delta U = 25 - 72.71 = -47.71\ Wh \tag{29}$$

Eq. (25) asserts that running the TEC for a total of 3 hours could eliminate such issues when subtracting Eq. (24) from Eq. (25) suggesting that minimum temperature ranges used in the model is attainable.

$$Energy\ reserve = +75\ Wh - 72.71\ Wh = +2.29\ Wh \tag{30}$$

TEC installation is conductive, and the heat transfer along the material will flow from a higher temperature to a lower temperature providing conduction is continuous along all metals. Water inside the glass flask at room temperature receives little conduction because the thermal bridge material is made from epoxy and possesses a low thermal conductivity 0.29 W/m °C [115], [94]. The TEC must now overcome the work required to conduct through the low thermal conductivity the glass and finally the water. Mostly this is where and why the considerable time constants are present.

Cool air by convection would have been the better option. However, installation costs to perform convection should be managed better by a refrigerator which is a cheaper option compared to buying three TEC devices for faster time constants or modifying the design to create convective heat transfers.

This further implies that the TEC thermal bridge should be metal and consist of a much higher thermal conductivity [115].

Temperature control

As expected, the PWM signature was arbitrary with high-frequency switching. To get around this problem, there are three solutions.

The first solution; design a first order low pass filter circuit. Low pass filters (LC) consist of a capacitor and an inductor designed to reject high frequencies, essentially allowing only lower frequencies to pass [116]. For the stage of this project, the author does not see it a viable option, although a possible cheap option for future research if the designer can build their own PI controllers with LC circuits specific for TEC application considering the purchase price is about $700 from the RS store [117].

Second choice is to purchase a high powered MOSFET. High power MOSFETs can operate at higher temperatures and higher switching frequencies however they are much more costly [118].

While the third option was to implement the on/off switching successfully. The main drawback, the control scheme only allows 0 or 12 VDC output to the TEC. **Figure 3-3**.b. illustrated the on/off switching over a period of 10 minutes and the solid-state relay experienced no overheating but high frequencey switching is observable on the ambient temperature sensor.

On/off control is not as accurate as PI control. The main reason being, the significant time constants in temperature are a problem between the switching on and off stages. These time constants cause the PV to deviate away from the setpoint, and temperature fluctuations become apparent. Economic feasibility is not particularly good when the interest of high value biomass is a requirement, to keep overhead costs down the optimal photosynthetic yield must be maintained [119].

Process variable selection for controller installation

Advantages and disadvantages for both controller locations are summarised from the results. Internal ambient temperature under PI controller caused the MOSFET to overheat from the sensitivity of the LM335Z temperature sensor. Fine temperature readings oscillating between the setpoint cause the error sent to the controller to output high PWM values, switching 5 to 8 times in 10 seconds as depicted in **Figure 3-2**.

The PBR water temperature signal is digital this means it does not receive such an oscillatory feedback signal when it is used for control and therefore is an optimal solution when implementing control schemes that require a smooth input signal such as PI or on/off as illustrated in **Figure 3-6**.

Although both temperatures are controlled by the same MV, the PV that closely relates the installation of the PI controller is the PBR's water temperature. The sensor is directly in contact with the water inside the PBR by conduction. Although aforementioned that the thermal conductivity by conduction is less then substantial, direct manipulation of the PV always advantageous and is why the control loop is placed around the PBR water temperature [120].

Because the PBRs water temperature sensor does not exaggerate small changes in temperature the PI velocity form controller was put back into service but not tested because logic based MOSFETs are no longer available for purchase within the stage of this project.

Inadequate temperature setpoint targets

Figure 3-5 affirms that no change of the water temperature is observable after a setpoint change was implemented from 20 ºC to 15 °C. This shows that the TEC is unable to attain temperatures in the lower regions and can be related to **Table 2-1** where TEC working parameters are illustrated. This table provides examples of different Qc values that are absorbed and obtaining a lower temperature difference across the TEC provide a better cooling capacity.

Microalgae that survive over a wide temperature range are attractive and suitable for culture cultivation. This is primarily of importance when the fatal temperature is increased a little more compared to their optimal growth temperature and the species remain unaffected [16]. Increasing temperature range disrupts the algae in the following way, microalgae cannot perform photosynthesis and leads to the lack of oxygen production and causes damage within the cell

membrane [15]. This affirms that if the microenvironment maintains a setpoint between 15 ºC to 30 ºC then some microalgae species but not all can experience growth. However optimal conditions usually lie between 20 ºC to 25 ºC [15].

Figure 3-6 illustrates the operational results of the TECs MV, operating for over 2 hours consuming 132 Wh to remove 4ºC of heat energy while driving up the cost of operation is not viable. These devices should be avoided altogether if large batches of microalgae are a target, effective cultivation methods should be investigated.

4.2 LabVIEW software and Arduino

Microcontrollers

A single microcontroller should be implemented to receive input data simultaneously with output data and operate fluently. Lack of the Arduino C/C++ knowledge caused the author to use LIFA to keep the experiment going and complete the required research. It has been mentioned to the author that Murdoch university does not allow additional installation products to their LabVIEW software, and therefore is a contributing factor for offsite testing.

4.3 Optimal growth rates

Lighting sensor characteristics

Low lux values with a maximum of 1850 lux suggesting that the LED lights for the task are not effective enough for growth cultivation of microalgae.

Oxidative damages occur when light intensities are beyond the microalgaes photosynthetic limits while the opposite is true and the correct ammount received can stimulate growth. [5]. B. Cheirsilp et al. [17], affirm that marine Chlorella and Nannochloropsis experience low growth rates when exposed to light intensity from 2000 up to 10,000 lux [17].

Maximum growth rates with lights have been experimented using blue light and W. Gruszecki et al. [26] asserts that blue light has positive influence in growth rates and triggers metabolic regulation mechanisms like light harvesting for photosynthesis.

Agitation mixing

Calibration curves obtained in **Figure 5-4** illustrate that RPM value of the fan will have a maximum of 890 RPM and the minimum below 750 RPM. The stirring bar RPM will be a lot slower as the density of culture is to increase and should be calculated independently if culture density is known.

Agitation and mixing the culture improves the exchange of PFD to the algae culture. While aggressive amounts of mixing is not favoured by all microalgae [71], [13]. N. Moheimani et al. [72] experimented with different mixing speeds and observed the influence on the growth of *P. carterae* [72]. By varying the Reynolds number between 15,979 and 79,866 respectively (100 rpm) and (500 rpm), microalgae growth rates were found to decrease as the Reynolds number was increased past 31,927 (200 rpm) [72].

4.4 Established photobioreactor comparison

Within the market there is already devices operating efficiently with similar capabilities but better-quality components and construction at a very high cost. Cost effective technologies, production per hectare of land are some of the many obstacle that determines if cultivation of microalgae is economically viable [121], [12].

These components are designed and produced by companies like Photon systems instruments and have a range of cultivation vessel capacities from 0.4 litres to 3 litres [122]. Their capabilities include temperature control from 15 ºC to 55 ºC and depending on the model selected red-blue or red-white LED panels produce a maximum of 3000 µmol/m^2 s [122]. Depending on the storage capacity of microalgae the cost of the units range from $18,864 to $31,440.20 a very large capital cost for such a small cultivation method. While magnetic stirring and mixing can be purchased for $5,347 and mixes 5 solutions per time.

The designed microenvironment attests to its value in cost to construct. The cost of this build was $775. Cheap design methods and understanding make it possible to engineer cost effective designs and is one of the challenges faced when effective cultivation methods are needed. Small 12 VDC fans are accessible for $30 and 3D printed manifolds with magnet housings can be attached to them, suggesting over 170 mixers can be constructed.

Universities have access to products such as LabVIEW which allow immediate interfacing. This gives universities vast potential to design cost effective cultivation methods and operate close to their optimal yields.

The internal aluminium housing of this system is 6.3 litres and has a total energy consumption of 1466.24 kWh/year costing $415.39 assuming the system operates 24 hours per day as illustrated in D.1 [123]. A heat pump consisting of 425 L has an average energy consumption of 474 kWh/year, considering the current Western Australian cost per kWh of electricity is 28.33 cents the operational cost of this system would be $134.30 per year [124], [123].

Chapter 5. Conclusion and future work

TEC devices have very low coefficients of power and should not be used for microalgae cultivation when profit yield is of interest. The amount of heat energy moved per power input makes TEC devices only good for small applications where low heat energy input or output is required.

TEC devices produce a negative temperature gradient that dramatically reduce the heat removed when the hot side of the TEC becomes too hot. This heat must be removed by a heatsink and will increase capital expenditure because requirements such as, power supplies and fan motors are needed to remove the heat energy.

Increasing the life span of the components is more advantageous when purchasing higher quality sensors in comparison to the time spent filtering. The better response from the sensor is the PBR water temperature sensor this is because it was in direct measurement with the process temperature and does not produce noisy signals.

Velocity form PI control is the better option for PWM signals however MOSFETs of low quality should never be used for switching. The use of a solid-state relay with the velocity form PI control still has high frequency switching and the PWM signature will only operate at high or low values. Therefore on / off control is used to substitute the PI controller altogether and opt for a simpler control scheme.

Large time constants in the temperature of the PBR including, undesirable offset of the temperature process variable suggests that the TEC is too small for the task. Two contributing factors highlight these issues, firstly thermal conductivity of the material between the system boundaries and secondly, the TEC for this application has reached its maximum attainable heat absorbed value.

Operating the RGB lights to maximum intensity increases the internal energy of the PBR, temperature run away is observable when high lux values are present in the system, but low lux values do not affect the internal energy of the system.

This research highlights that adopting some of the cultivation methods in this paper for microalgae can be done at a cost-effective margin compared to the already established designs on the market while careful consideration into sensor components will reduce some of the issues in this paper.

Suggested future research

Future developments and improvements to attain the lower temperature ranges can be solved. The TEC should be in direct contact to the base of the internal flask and PI control installed on the digital temperature sensor to remove noisy signals. This will cause shorter time constants of the water temperature and remove any observable offset where lower temperatures are concerned.

Knowledge gained from this research illustrates that TECs are not effective at removing heat energy and are more suitable for small scale applications where cost is of no concern. Other devices that have a higher COP such as a heat pump are perfectly capable of removing this heat energy.

Learnings from this study should build on the experimentation of this thesis and transpose these ideas into refrigeration units that have better COP to overcome the heat released from LED lighting and heat generated from microalgae cultivation [38]. Mixing and agitation by a similar design will reduce capital costs so funds could be spent elsewhere. Higher quality LED lights should be installed inside with extra provisions for nutrients so already established feeding and pH methods can hybridise onto these refrigerators. Monitoring of the system could be paired with off the shelf microcontrollers and feedback information displayed on LabVIEW for strict control to optimise yield. a mock up design has been illustrated in Appendix F Hybrid refrigerator.

Programming effectively are some issues that should be fixed by a computer system engineer. Arduino is a C/C++ function language and when serial data of PWM commands from LabVIEW is received, arrays of data must allocate this information to the correct output pins on the microcontroller. Essentially this will allow a single microcontroller and negate the need for Murdoch university to install additional platform software into LabVIEW. Other upgrades should include, light dark ratio on a timer loop so that the RGB spectrum lights can operate on a timed cycle.

.

References

[1] D. Sahoo and P. Baweja, "General Characteristics of Algae," in *The Algae World*(Cellular Origin, Life in Extreme Habitats and Astrobiology, 2015, pp. 3-29.

[2] M. A. Borowitzka, "Algae for biofuels and energy " in *Developments in applied phycology*, M. A. Borowitzka and N. R. Moheimani, Eds. (A Short History), New York: Springer, 2013, pp. 1-10.

[3] M. L. Garciaa, K. Adjalléb, S. Barnabéb, and G. S. V. Raghavana, "Microalgae biomass production for a biorefinery system: Recent advances and the way towards sustainability," *Renewable and Sustainable Energy Reviews,* vol. 76, pp. 493-506, 2017.

[4] R. Munoz and B. Guieysse, "Algal-bacterial processes for the treatment of hazardous contaminants: a review," *Water Res,* vol. 40, no. 15, pp. 2799-815, Aug 2006.

[5] M. A. Borowitzka, M. A. Borowitzka and N. R. Moheimani, Eds. *Algae for biofuels and energy* (Developments in applied phycology, 2013). New York: Springer, 2013, p. 288.

[6] M. Huesemann *et al.,* "A validated model to predict microalgae growth in outdoor pond cultures subjected to fluctuating light intensities and water temperatures," *Algal Research,* vol. 13, pp. 195-206, 2016.

[7] S. S. Devi and D. Sahoo, "The Algae World," vol. 26, D. Sahoo and J. Seckbach, Eds. 1st ed. (Cellular Origin, Life in Extreme Habitats and Astrobiology, Netherlands: Springer, 2015, pp. 564-570.

[8] M. A. Borowitzka and N. R. Moheimani, "Biomass and Biofuels from Microalgae," in *Advances in Engineering and Biology*, vol. 2, N. R. Moheimani, M. P. McHenry, K. d. Boer, and P. A. Bahri, Eds. Switzerland: Springer International Publishing, 2015, pp. 1-15.

[9] G. C. Zittelli, N. Biondi, L. Rodolfi, and M. R. Tredici, "Handbook of microalgal culture," in *applied phycology and Biotechnology*, R. Amos and H. Qiang, Eds. 2 ed. West Sussex: John Wiley & Sons, Ltd, 2013, pp. 229-250.

[10] B. Wang, C. Q. Lan, and M. Horsman, "Closed photobioreactors for production of microalgal biomasses," *Biotechnol Adv,* vol. 30, no. 4, pp. 904-12, Jul-Aug 2012.

[11] J. Willmen, F. Zijffers, M. Janssen, J. Tramper, and R. H. Wijffels, "Design Process of an Area-Efficient Photobioreactor," *Marine Biotechnology,* vol. 10, no. 4, pp. 404 - 415, Sep. 2007.

[12] M. A. Borowitzka, "Commercial production of microalgae: ponds, tanks, tubes and fermenters," *Journal of Biotechnology,* vol. 70, pp. 313-321, 1999.

[13] S. Wahal and S. Viamajala, "Maximizing algal growth in batch reactors using sequential change in light intensity," *Applied biochemistry and biotechnology,* vol. 161, no. 1-8, pp. 511-22, May 2010.

[14] S. Wahidin, A. Idris, and S. R. Shaleh, "The influence of light intensity and photoperiod on the growth and lipid content of microalgae Nannochloropsis sp," *Bioresour Technol,* vol. 129, pp. 7-11, Feb 2013.

[15] M. Ras, J.-P. Steyer, and O. Bernard, "Temperature effect on microalgae: a crucial factor for outdoor production," *Reviews in Environmental Science and Bio/Technology,* vol. 12, no. 2, pp. 153-164, 2013.

[16] M. A. Borowitzka and N. R. Moheimani, "Algae for biofuels and energy," in *Developments in applied phycology,* vol. 5: Springer, 2013, pp. 77-85.

[17] B. Cheirsilp and S. Torpee, "Enhanced growth and lipid production of microalgae under mixotrophic culture condition: effect of light intensity, glucose concentration and fed-batch cultivation," *Bioresour Technol,* vol. 110, pp. 510-6, Apr 2012.

[18] K. J. McCREE, "Test of current definitions of photosynthetically active radiation against leaf photosynthesis data," *Agricultural Meteorolog,* vol. 10, pp. 443-453, Dec. 1971.

[19] L. Wang, W. Gong, Y. Ma, B. Hu, and M. Zhang, "Photosynthetically active radiation and its relationship with global solar radiation in Central China," *Int J Biometeorol,* vol. 58, no. 6, pp. 1265-77, Aug 2014.

[20] A. Breslin and A. Montwill, *Let there be light: the story of light from atoms to galaxies,* 2nd ed. Imperial College Press, 2013.

[21] W. Blanken, M. Cuaresma, R. H.Wijffelsa, and M. Janssena, "Cultivation of microalgae on artificial light comes at a cost," *Algal Research,* vol. 2, pp. 333-340, Sep. 2013.

[22] Ruiqing Ma, Ningfang Liao, Pengfei Yan, and K. Shinomori, "Categorical color constancy under RGB-LED light sources," *Color Res Appl,* pp. 1-18, 2 May 2018.

[23] H. Tang, M. Chen, K. Y. Ng, and S. O. Salley, "Continuous microalgae cultivation in a photobioreactor," *Biotechnol Bioeng,* vol. 109, no. 10, pp. 2468-74, Oct 2012.

[24] P. Das, W. Lei, S. S. Aziz, and J. P. Obbard, "Enhanced algae growth in both phototrophic and mixotrophic culture under blue light," *Bioresour Technol,* vol. 102, no. 4, pp. 3883-3887, Feb 2011.

[25] T. de Mooij, G. de Vries, C. Latsos, R. H. Wijffels, and M. Janssen, "Impact of light color on photobioreactor productivity," *Algal Research,* vol. 15, pp. 32-42, Jan. 2016.

[26] W. I. Gruszecki *et al.*, "Blue-light-controlled photoprotection in plants at the level of the photosynthetic antenna complex LHCII," *J Plant Physiol,* vol. 167, no. 1, pp. 69-73, Jan 1 2010.

[27] C. H. Ra, C. H. Kang, J. H. Jung, G. T. Jeong, and S. K. Kim, "Effects of light-emitting diodes (LEDs) on the accumulation of lipid content using a two-phase culture process with three microalgae," *Bioresour Technol,* vol. 212, pp. 254-261, Jul 2016.

[28] H. C. Hung and W. W. Teng, "A novel photobioreactor with transparent rectangular chambers for cultivation of microalgae," *Biochemical Engineering Journal,* vol. 46, no. 3, pp. 300-305, June. 2009.

[29] W. Blanken, P. R. Postma, L. de Winter, R. H. Wijffels, and M. Janssen, "Predicting microalgae growth," *Algal Research,* vol. 14, pp. 28-38, 2016.

[30] Q. Bechet, A. Shilton, and B. Guieysse, "Modeling the effects of light and temperature on algae growth: state of the art and critical assessment for productivity prediction during outdoor cultivation," *Biotechnol Adv,* vol. 31, no. 8, pp. 1648-63, Dec 2013.

[31] J. F. Cornet, C. G. Dussap, and G. Dubertret, "A structured model for simulation of cultures of the cyanobacterium Spirulina platensis in photobioreactors: I. Coupling between light transfer and growth kinetics," *Biotechnology and bioengineering,* vol. 40, no. 7, 1992.

[32] W. G. HoufF and P. Incropera, "An assessment of techniques for predicting radiation transfer in aqueous media," *Journal of Quantitative Spectroscopy and Radiative Transfer,* vol. 23, no. 1, pp. 101-115, 2005.

[33] R. R. Pethig and S. Smith, "Introductory bioelectronics: for engineers and physical scientists," Wiley, 2012, p. 481.

[34] F. G. Acien Fernandez, F. Garcıa Camacho, J. A. Sanchez Perez, J. M. Fernandez Sevilla, and E. M. Grima, "A Model for Light Distribution and Average Solar Irradiance Inside Outdoor Tubular Photobioreactors for the Microalgal Mass Culture," *Department of Chemical Engineering,* pp. 701-714, Jan. 1997.

[35] U. Lagercrantz, "At the end of the day: a common molecular mechanism for photoperiod responses in plants?," *J Exp Bot,* vol. 60, no. 9, pp. 2501-15, 2009.

[36] Z. Amini Khoeyi, J. Seyfabadi, and Z. Ramezanpour, "Effect of light intensity and photoperiod on biomass and fatty acid composition of the microalgae, Chlorella vulgaris," *Aquaculture International,* vol. 20, no. 1, pp. 41-49, 2011.

[37] R. A. Andersen, *Algal culturing techniques*. Elsevier/Academic Press, 2005.

[38] D. Sahoo and J. Seckbach, *The Algae World,* 1st ed. (Cellular Origin, Life in Extreme Habitats and Astrobiology). Netherlands: Springer, 2015.

[39] M.-L. Teoh, S.-M. Phang, and W.-L. Chu, "Response of Antarctic, temperate, and tropical microalgae to temperature stress," *Journal of Applied Phycology,* vol. 25, no. 1, pp. 285-297, 2012.

[40] S. P. Singh and P. Singh, "Effect of temperature and light on the growth of algae species: A review," *Renewable and Sustainable Energy Reviews,* vol. 50, pp. 431-444, 2015.

[41] M. A. Borowitzka, "Algae for biofuels and energy," in *Developments in applied phycology, 2013*, vol. 5, M. A. Borowitzka and N. R. Moheimani, Eds. (Species and Strain selection), New York: Springer International Publishing, 2013, pp. 80-81.

[42] B. Uyar and N. Kapucu, "Passive temperature control of an outdoor photobioreactor by phase change materials," *Journal of Chemical Technology & Biotechnology,* vol. 90, no. 5, pp. 915-920, 2015.

[43] L. Giannelli, H. Yamada, T. Katsuda, and H. Yamaji, "Effects of temperature on the astaxanthin productivity and light harvesting characteristics of the green alga Haematococcus pluvialis," *Journal of Bioscience and Bioengineering,* vol. 119, no. 3, pp. 345-50, Mar 2015.

[44] C. H. Hsieh and W. T. Wu, "Cultivation of microalgae for oil production with a cultivation strategy of urea limitation," *Bioresour Technol,* vol. 100, no. 17, pp. 3921-6, Sep March. 2009.

[45] H. Robert and M. Elizabeth, *A dictionary of Biology,* 7th ed. (Science and technology, Life Sciences). 2018.

[46] F. Bux and Y. Chisti, *Algae Biotechnology* (Green Energy and Technology). Switzerland: Springer, 2016.

[47] M. Shovon and M. Nirupama, "Microalga Scenedesmus obliquus as a potential source for biodesel production," *Appl Microbiol Biotechnol,* vol. 84, no. 2, pp. 281-291, March. 28.

[48] G. Iyer, Y. Gupte, P. Vaval, and V. Nagle, "Uptake of potassium by algae and potential use as biofertilizer," *Indian Journal of Plant Physiology,* vol. 20, no. 3, pp. 285-288, 2015.

[49] M. M. El-Sheekh, A. A. Farghl, H. R. Galal, and H. S. Bayoumi, "Bioremediation of different types of polluted water using microalgae," *Rendiconti Lincei,* vol. 27, no. 2, pp. 401-410, Dec. 2015.

[50] E.-S. Salama *et al.*, "Recent progress in microalgal biomass production coupled with wastewater treatment for biofuel generation," *Renewable and Sustainable Energy Reviews,* vol. 79, pp. 1189-1211, 2017.

[51] H. El Arroussi, R. Benhima, I. Bennis, N. El Mernissi, and I. Wahby, "Improvement of the potential of Dunaliella tertiolecta as a source of biodiesel by auxin treatment coupled to salt stress," *Renewable Energy,* vol. 77, pp. 15-19, 2015.

[52] T. Wang *et al.*, "Salt stress induced lipid accumulation in heterotrophic culture cells of Chlorella protothecoides: Mechanisms based on the multi-level analysis of oxidative response, key enzyme activity and biochemical alteration," *J Biotechnol,* vol. 228, pp. 18-27, Jun 20 2016.

[53] S. Tebbani, R. Filali, F. Lopes, D. Dumur, and D. Pareau, "CO2 Biofixation by Microalgae: Automation Process," in *Modeling, Estimation and Control*, F. Castine, Ed. Great Britain and the United States: ISTE Ltd and John Wiley & Sons, Inc, 2014.

[54] Y. K. Lee, Y. Chisti, and J. Pruvost, "Algae Biotechnology," in *Green Energy and Technology*, F. Bux and Y. Chisti, Eds. (Microalgae Cultivation Fundamentals, Switzerland: Springer, 2016, pp. 1-47.

[55] J.G.J. Olivier, K.M. Schure , and J. A. H. W. Peters, "Trends in global CO2 and total greenhouse gas emissions," PBL Netherlands Environmental Assessment Agency, The Hague, Dec. 2017.

[56] "Quarterly Update of Australia's National Greenhouse Gas Inventory:," *Australia's National Greenhouse Accounts*, Available: http://www.environment.gov.au/system/files/resources/7b9824b8-49cc-4c96-b5d6-f03911e9a01d/files/nggi-quarterly-update-dec-2017-revised.pdf

[57] K. L. Kadam, "Environmental implications of power generation via coalmicroalgae cofiring," *Energy*, vol. 27, pp. 905–922, 2002.

[58] M. G. d. Morais and J. A. Costa, "Biofixation of carbon dioxide by Spirulina sp. and Scenedesmus obliquus cultivated in a three-stage serial tubular photobioreactor," *J Biotechnol*, vol. 129, no. 3, pp. 439-45, May 1 2007.

[59] J. B. Guckert, "Triglyceride Accumulation and Fatty acid profile changes in Chlorella (Chlorophyta) during high pH-induced cell cycle inhibition," *Journal of Phycology*, vol. 26, no. 1, pp. 72-79, 1990.

[60] O. Avidan, "Regulation of triglyceride biosynthesis and accumulation by acetyl-CoA in green microalgae," Doctor of Philosophy Microbiology, Plant sciences, Scientific Council of the Weizmann Institute of Science Rehovot, Israel, Institute of Science Rehovot, Israel, East Eisenhower Parkway, 10904137, Feb 2015.

[61] M. L. Bartley, W. J. Boeing, B. N. Dungan, F. O. Holguin, and T. Schaub, "pH effects on growth and lipid accumulation of the biofuel microalgae Nannochloropsis salina and invading organisms," *Journal of Applied Phycology*, vol. 26, no. 3, pp. 1431-1437, 2013.

[62] N. R. Moheimani, "Inorganic carbon and pH effect on growth and lipid productivity of Tetraselmis suecica and Chlorella sp (Chlorophyta) grown outdoors in bag photobioreactors," *Journal of Applied Phycology*, vol. 25, no. 2, pp. 387-398, 2012.

[63] Z. Arbib, I. de Godos Crespo, E. L. Corona, and F. Rogalla, "Understanding the biological activity of high rate algae ponds through the calculation of oxygen balances," *Appl Microbiol Biotechnol*, vol. 101, no. 12, pp. 5189-5198, Jun 2017.

[64] T. M. Louw, "Algae Biotechnology," in *Green Energy and Technology*, F. Bux and Y. Chisti, Eds. Switzerland: Springer, 2016, pp. 123-125.

[65] C. C. Parl, *Photorespiration*, 2nd ed. (A dictionary of environment and conservation,). Oxford University Press, Jan. 2013.

[66] M. Sophie, M. D. Castets, and C. Jacques, "Primary production, respiration and calcification of the temperate free-living coralline alga Lithothamnion corallioides," *Aquatic Botany*, vol. 85, no. 2, pp. 121-128, 2006.

[67] Navid R. Moheimani, David Parlevliet, Mark P. McHenry, P. A. Bahri, and K. d. Boer, "Biomass and Biofuels from Microalgae," in *Advances in Engineering and Biology*, vol. 2, N. R. Moheimani, M. P. McHenry, K. d. Boer, and P. A. Bahr, Eds. Switzerland: Springer International Publishing, 2015, pp. 4-5.

[68] S. n. M. n. Asterio, C. G. m. Antonio, F. G. a. Camacho., M. G. Emilio, and C. Yusuf, "Comparative evaluation of compact photobioreactors for large-scale monoculture of microalgae," *Biotechnology*, vol. 70, no. 1-3, pp. 249-270, April. 1999.

[69] M. A. Borowitzka and N. R. Moheimani, "Algae for biofuels and energy," in *Developments in applied phycology*, vol. 5, M. A. Borowitzka and N. R. Moheimani, Eds. (Open Pond Culture Systems) New York: Springer International Publishing, 2013, pp. 133-148.

[70] L. Brennan and P. Owende, "Biofuels from microalgae—A review of technologies for production, processing, and extractions of biofuels and co-products," *Renewable and Sustainable Energy Reviews*, vol. 14, no. 2, pp. 557-577, 2010.

[71] C. Q. Lan and B. Wang, "Microalgae for biofuel production and CO_2 sequestration," in *Energy Science, Engineering and Technology Series*, C. Lan, B. Wang, N. Courchesne, and Y. Mu, Eds. New York: Nova Science Publishers, Inc, 2010, pp. 18-41.

[72] N. R. Moheimani, A. Isdepsky, J. Lisec, E. Raes, and M. A. Borowitzka, "Coccolithophorid algae culture in closed photobioreactors," *Biotechnol Bioeng*, vol. 108, no. 9, pp. 2078-87, Sep 2011.

[73] M. Leupold, S. Hindersin, G. Gust, M. Kerner, and D. Hanelt, "Influence of mixing and shear stress on Chlorella vulgaris, Scenedesmus obliquus, and Chlamydomonas reinhardtii," *Journal of Applied Phycology*, vol. 25, no. 2, pp. 485-495, 2012.

[74] Q. Huang, F. Jiang, L. Wang, and C. Yang, "Design of Photobioreactors for Mass Cultivation of Photosynthetic Organisms," *Engineering*, vol. 3, no. 3, pp. 318-329, 2017.

[75] A. Martinez, D. Astrain, A. Rodriguez, and P. Aranguren, "Advanced computational model for Peltier effect based refrigerators," *Applied Thermal Engineering*, vol. 95, pp. 339-347, 2016.

[76] N. J. M. Reddy, "A low power, eco-friendly multipurpose thermoelectric refrigerator," *Frontiers in Energy*, vol. 10, no. 1, pp. 79-87, 2015.

[77] A. Martínez, D. Astrain, A. Rodríguez, and G. Pérez, "Reduction in the Electric Power Consumption of a Thermoelectric Refrigerator by Experimental Optimization of the Temperature Controller," *Journal of Electronic Materials*, vol. 42, no. 7, pp. 1499-1503, 2012.

[78] M. D. Thakor, S. K. Hadia, and A. Kumar, "Precise Temperature Control through Thermoelectric Cooler with PID Controller," presented at the IEEE ICCSP, 2015.

[79] A. Martínez, D. Astrain, and A. Rodríguez, "Dynamic model for simulation of thermoelectric self cooling applications," *Energy*, vol. 55, pp. 1114-1126, 2013.

[80] Duninotech. *Duinotech Uno XC-4410* Available: https://www.jaycar.com.au/medias/sys_master/images/8961502969886/XC4410-dataSheetMain.pdf [Accessed, Oct. 8 2018].

[81] Adafruit. (2018). *DHT11, DHT22 and AM2302 Sensors* Available: https://cdn-learn.adafruit.com/downloads/pdf/dht.pdf [Accessed, Oct. 8 2018].

[82] T. Instruments. *LMx35, LMx35A Precision Temperature Sensors* Available: http://www.ti.com/lit/ds/symlink/lm235a.pdf [Accessed, Oct. 8 2018].

[83] D. Semiconductor. *Z6386 • Stainless Steel Housing Waterproof DS18B20 Temperature Probe* Available: https://www.altronics.com.au/p/z6386-stainless-steel-housing-waterproof-ds18b20-temperature-probe/ [Accessed, Oct. 11 2018].

[84] T. L. Company. (2009). *TSL2560, TSL2561 LIGHT-TO-DIGITAL CONVERTER* Available: https://cdn-shop.adafruit.com/datasheets/TSL2561.pdf [Accessed, Oct. 8 2018].

[85] M. Well. (2017). *125W Dual Output Switching Power Supply* Available: https://www.meanwell.com/webapp/product/search.aspx?prod=RID-125 [Accessed, Oct/ 9 2018].

[86] POWERTECH. (2018). *Open Framer switchmode powersupply* Available: http://www.designfx.com.au/jaycar/cat_pdfs/mobile/J16_power_m.pdf [Accessed, Oct. 9 2018].

[87] L. Petru and G. Mazen, "PWM Control of a DC Motor Used to Drive a Conveyor Belt," *Procedia Engineering*, vol. 100, pp. 299-304, 2015.

[88] STMicroelectronics. *MOSFET STP60NE06L-16/FP* Available: https://www.jaycar.com.au/medias/sys_master/images/9115105853470/ZT2450-dataSheetMain.pdf [Accessed, Oct. 8 2018].

[89] E. K. Trading. (2018). *Solid State relay SSR-25DD* Available: http://www.ekt2.com/pdf/42_SOLID_STATE_SSR-25DD.pdf [Accessed, Oct. 19 2018].

[90] *Thermoelectric Peltier* Available: https://www.jaycar.com.au/medias/sys_master/images/9113244729374/ZP9104-dataSheetMain.pdf [Accessed, Oct. 13 2018].

[91] C.-T. Hsu, G.-Y. Huang, H.-S. Chu, B. Yu, and D.-J. Yao, "An effective Seebeck coefficient obtained by experimental results of a thermoelectric generator module," *Applied Energy*, vol. 88, no. 12, pp. 5173-5179, 2011.

[92] H. S. Lee, "Thermal Design " in *Heat Sinks, Thermoelectrics, Heat Pipes, Compact Heat Exchangers, and Solar Cells*1 ed. Hoboken, New Jersey: John Wiley & Sons, Incorporated, 2010, pp. 100-179.

[93] Ramset™. *FomoFill™* Available: http://www.ramset.com.au/Product/Detail/62/FomoFill- [Accessed, Oct. 9 2018].

[94] J. H. L. IV and J. H. L. V, "A heat transfer Textbook," 4th ed. Cambridge, Massachusetts, USA: Dover Publications, 2011, pp. 640-661. [Online]. Available.

[95] Arduino. (2018, July). *Arduino IDE Software* Available: https://www.arduino.cc/en/Main/Software [Accessed, Oct. 9 2018].

[96] H. S. Lee, "Thermal Design " in *Heat Sinks, Thermoelectrics, Heat Pipes, Compact Heat Exchangers, and Solar Cells*1 ed. Hoboken, New Jersey: John Wiley & Sons, Incorporated, 2010, pp. 34-81.

[97] A. K. R. Sombra, F. C. Sampaio, R. P. T. Bascopé, and B. C. Torrico, "Digital Temperature Control Project Using Peltier Modules to Improve the Maintenance of Battery Lifetime," 2016 12th IEEE International Conference on Industry Applications (INDUSCON), pp. 1-7.

[98] L. I. Anatychuk and O. J. Luste, "Thermoelectrics Handbook," in *Macro to Nano*, D. M. Rowe, Ed. 6000 Broken Sound Parkway NW, Suite 300: Taylor & Francis Group, LLC.

[99] Y. A. Cengel and M. A. Boles, "Thermodynamics: An Engineering approach," 8th ed. New York: McGraw-Hill Education, 2015, pp. 52-97.

[100] Y. A. Cengel and M. A. Boles, "Thermodynamics: An Engineering approach," 8th ed. New York: McGraw-Hill Education, 2015, pp. 608-639.

[101] R. a. A.-C. E. American Society of Heating, "2015 ASHRAE handbook: heating, ventilating, and air-conditioning applications," Atlanta, Georga: ASHRAE, 2015.

[102] E. I, "Polyurethanes Today: Polyurethane insulation for building envelopes," *Cellular Polymers*, vol. 2, no. 32, 2013.

[103] R. a. A.-C. E. American Society of Heating, "2014 ASHRAE handbook: refrigeration," Atlanta, Georgia 2014.

[104] J. H. L. IV and J. H. L. V, "A heat transfer Textbook," 4th ed. Cambridge, Massachusetts, USA: Dover Publications, 2011, pp. 49-91. [Online]. Available.

[105] R. W. Serth, "Process Heat Transfer : Principles and Applications," 1 ed.: Elsevier Academic Press, 2007, pp. 44-65.

[106] R. H. S. Winterton, "Newton's law of cooling," *Contemporary Physics*, vol. 40, no. 3, pp. 205-212, 1999.

[107] W. Boyes, "Instrumentation reference book," 4th ed.: Butterworth-Heinemann/Elsevier, 2010, pp. 269-326.

[108] A. Inc. (2019). *Fusion 360 for startups and hobbyists* Available: https://www.autodesk.com/campaigns/fusion-360-for-hobbyists [Accessed, Jan. 8 2019].

[109] F. Thompson, "Coupled coils, magnets and Lenz's law," *Physics Education*, vol. 45, p. 173, 2010.

[110] C. Rivadulla, G. Foffani, and A. Oliviero, "Magnetic field strength and reproducibility of neodymium magnets useful for transcranial static magnetic field stimulation of the human cortex," *Neuromodulation,* vol. 17, no. 5, pp. 438-41; discussion 441-2, Jul 2014.

[111] B. A. Ogunnaike and W. H. Ray, *Process dynamics, modelling, and control* (Topics in chemical engineering). Oxford University Press, 1994, p. 1260.

[112] D. E. Seborg, T. F. edgar, D. A. Mellichamp, and F. J. D. III, "Process Dynamics and Control," 3rd ed.: John Wiley & Sons inc, 2011, pp. 134-149.

[113] T. K. Hareendran. (2018) Mini Fridge With Peltier Modules.

[114] R. A. Serway and J. John W Jewett, "Principles OF physics A calculus-Based Text," 5th ed.: Cengage Learning, 2011, pp. 546-573.

[115] R. A. Serway and J. John W Jewett, *Principles OF physics A calculus-Based Text*, 5th ed. Cengage Learning, 2011.

[116] A. R. Hambley, "Electrical Engineering Principles and Applications," 6th ed. Essex England: Pearson, 2014, pp. 269-351.

[117] R. C. P. Ltd. (2018). *PWM Programmable PID Controller* Available: https://au.rs-online.com/web/p/peltier-module-controllers/4901553/ [Accessed, Oct. 20, 2018].

[118] L. Zhang, X. Yuan, X. Wu, C. Shi, J. Zhang, and Y. Zhang, "Performance Evaluation of High-Power SiC MOSFET Modules in Comparison to Si IGBT Modules," *IEEE Transactions on Power Electronics,* pp. 1-1, 2018.

[119] F. G. Acien, J. M. Fernandez, J. J. Magan, and E. Molina, "Production cost of a real microalgae production plant and strategies to reduce it," *Biotechnol Adv,* vol. 30, no. 6, pp. 1344-53, Nov-Dec 2012.

[120] L. Michalski, K. Eckersdorf, J. Kucharski, and J. McGhee, "Temperature Measurement," 2nd ed.: John Wiley & Sons Ltd, 2001, pp. 361-378.

[121] C. Y. Chen, K. L. Yeh, R. Aisyah, D. J. Lee, and J. S. Chang, "Cultivation, photobioreactor design and harvesting of microalgae for biodiesel production: a critical review," *Bioresour Technol,* vol. 102, no. 1, pp. 71-81, Jan 2011.

[122] P. s. Instruments. (2018). *Photobioreactor FMT150* Available: http://psi.cz/download/document/manuals/photobioreactor/PBR_HW_Manual.pdf [Accessed, Oct. 29 2018].

[123] H. Power. *Pricing Standard residential* Available: https://horizonpower.com.au/connections/pricing/ [Accessed, Nov. 2 2018].

[124] C. J. L. Hermes, C. Melo, F. T. Knabben, and J. M. Gonçalves, "Prediction of the energy consumption of household refrigerators and freezers via steady-state simulation," *Applied Energy,* vol. 86, no. 7-8, pp. 1311-1319, 2009.

[125] R. M. Felder and R. W. Rousseau, *Elementary Principles of chemical processes*, 3rd ed. Hoboken, NJ: John WIley & Sons, Inc, 2005.

[126] K. Raznjevic, *Handbook of thermodynamic tables and charts*. Washington: Mcgraw Hill, 1976.

[127] J. H. L. IV and J. H. L. V, *A heat transfer Textbook*, 3rd ed. Cambridge, Massachusetts, USA: Dover Publications, 2011, pp. 1-679.

[128] Y. A. Cengel and M. A. Boles, *Thermodynamics: An Engineering approach*, 8th ed. New York: McGraw-Hill Education, 2015, p. 996.

Appendices

Appendix A. Design, calculation and construction

A.1 Magnet housing

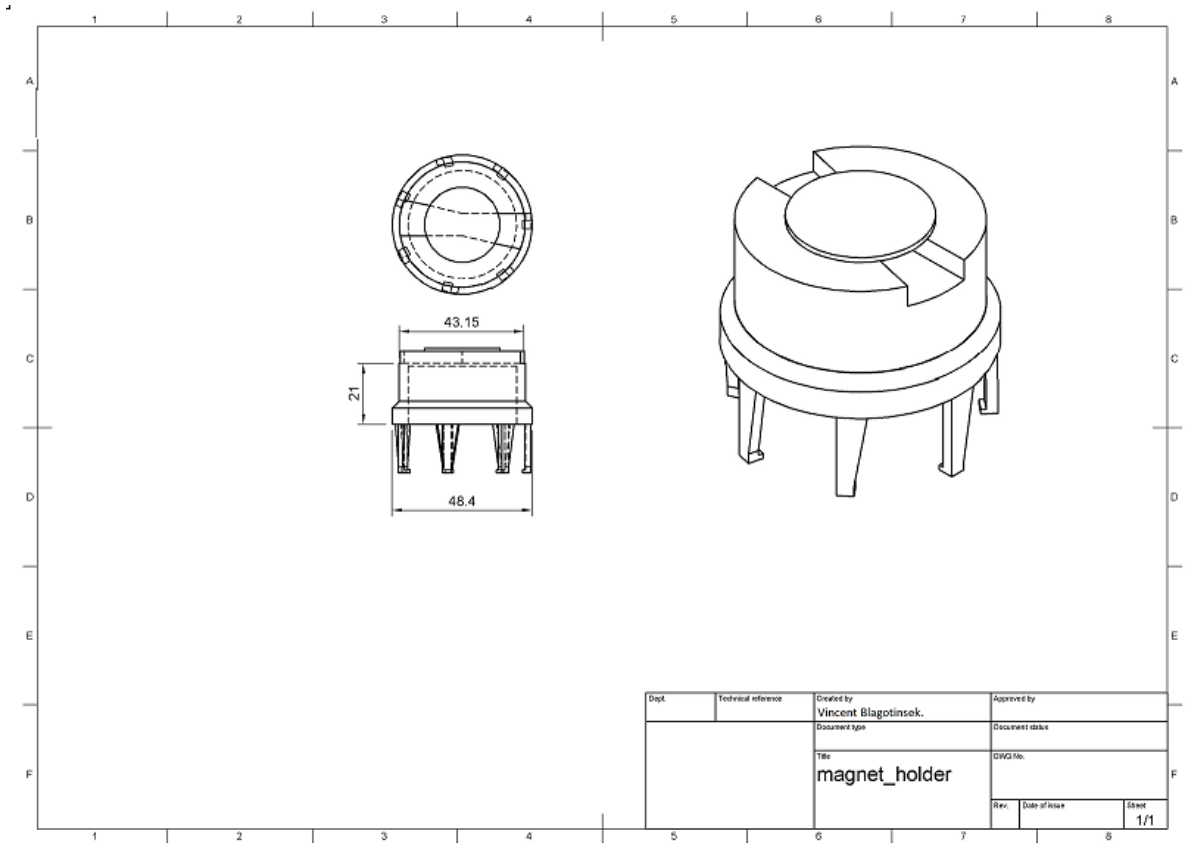

Figure 5-1 3D Printed Agitation motor, Magnet housing

Fusion360 is a free software that anyone with a email address can log into and begin designing their own ideas. The 3D magnet housing is designed to remove some of the eddy currents that may affect the speed of the fan.

A.2 TEC Peltier Module Datasheet

ZP9104 PELTIER MODULE 68W/8.5A 40X40MM W/LEADS
Imax=8.5A
DTmax=68degC
Vmax=15V
Qmax=68.09
Dimensions= 40x40x3.3mm

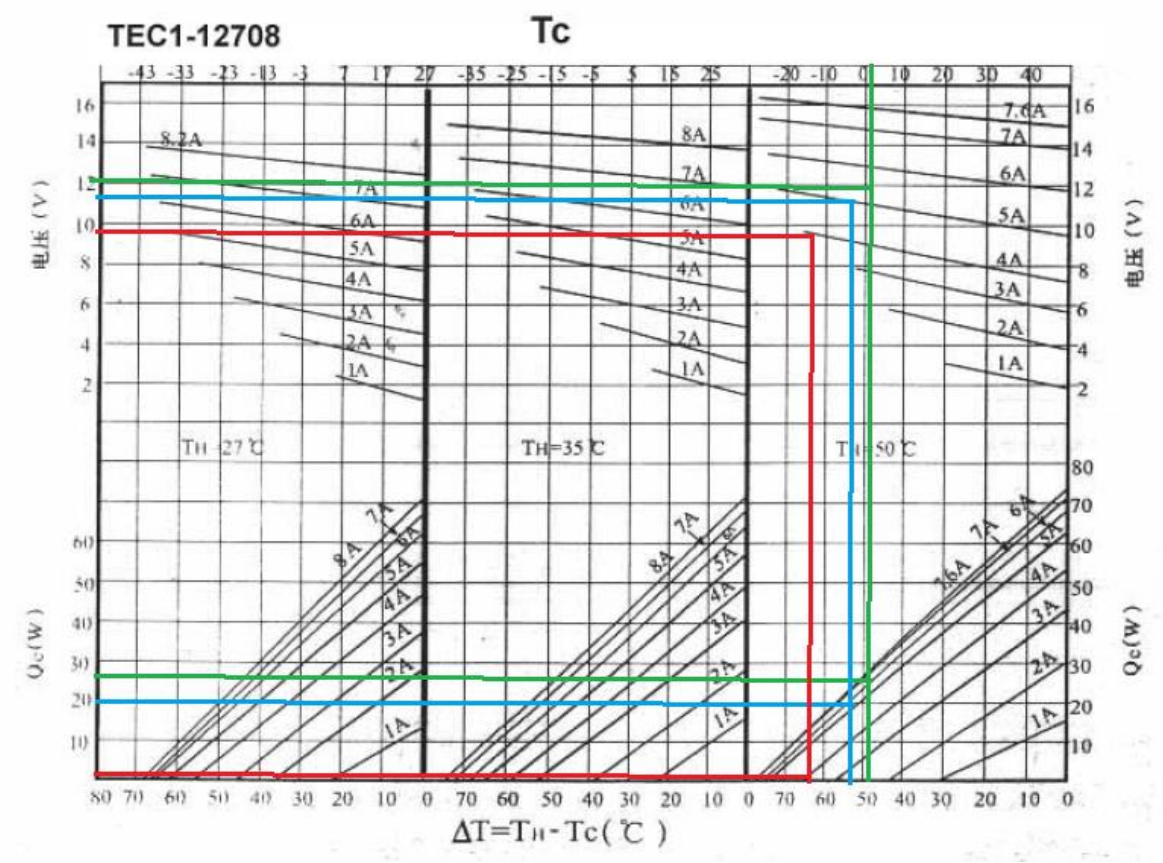

Figure 5-2 TEC datasheet
3 separate conditions of Q_c have been calculated: Green: 25 W. Blue: 20 W. Red: 0 W. Notice from the below table as ΔT_{TEC}**(°C)** increases the ability for Q_c to remove heat is reduced and the COP is reduced.

Table 5-1 TEC Datasheet values

The values below are extracted from the TEC datasheet

Description	Equation	Reference
Two-Point linear interpolation	$y = y_1 + \frac{x - x_1}{x_2 - x_1}(y_2 - y_1)$	[125]
TEC Data sheet	$\Delta T_{TEC} = (64 - 15) = 49\ ^{\circ}C$	Figure 5-2
Qc Data sheet	$Q_c = +25\ W$	Figure 5-2
Power input Datasheet	$P_W = VI = 71.5W$	Figure 5-2

Table 5-2 Heat added to thermal housing

Values used to calculate the thermal housing and references for the constants are provided.

Constants	Reference	Constants	Reference
Volume (V): 0.6229 m^3	Measured	Coefficient of performance (COP)	[100]
Specific heat Aluminium (C_p): 0.905 kJ / kg ºC.	[94]	$Q_{aluminium}$	[128]
Specific volume of air ($C_{v,air}$): 0.7578 kJ/kg ºC.	[126]	Q_{air}	[128]
Density of Air (ρ_{air}): 1.2928 kg /m^3	[126] [94]	$water$	[128]
Density of aluminium (ρ): 2,707 kg / m3.	[127]	Q_{total}	[128]

Coefficient of performance

$$COP_{TEC} = \frac{Qc}{P_W} \quad (31)$$

To remove heat from the micro environment and keep the system at steady state value of 15 ºC the amount of work heat removed from the system is illustrated below using MATLAB.

A.3 Heat energy calculations

Table 5-3 Total amount of Q for water

Description	Variable	Reference
Volume of water	0.0005 m^3	Measured
Specific heat of water	4.18 kJ / kg ºC	[128]
Temperature difference	(25-15) = 10 ºC	Measured
Density	1000 kg/ m^3	[128]

$$Q_{water} = \rho_{water} \cdot V_{water} \cdot C_{water} \cdot \Delta T \quad (32)$$

$$Q_{aluminium} = \rho_{aluminium} \cdot V \cdot C_p \cdot \Delta T \quad (33)$$

$$Q_{air} = \rho_{air} \cdot V \cdot C_v \cdot \Delta T \quad (34)$$

Below the MATLAB calculations

```
clc
clear
format shortEng

%specific heat
%If the aluminium core is 25 C and we would like to keep the temperature
%set point at 15 C then the amount of work required Qair to do so.
%refer to chapter 6.4.7 table  6.14 page 309
%Refer to the user manual of TEC to find correct sizing of peltier
%to determine the amount of Q to take water from 25 - 15 C
Vwater =0.5/1000; %volume of water
pwater = 1000; %density of water
Cpwater = 4.18; %specific heat of water
dtwater= (15-25); %temperature difference water is at room temperature 25

r1 = 0.087; % aluminium inner (radius inner)
Pal = 2700; %Density Kg/m3 alloy
A1 = pi*r1.^2; %Area of Aluminium
L = 0.265; %Length of the compartment
V = A1*L; %Volume of cylinder
Cp = 0.91; %Aluminium cp alloy
TF = 15; %ambient
TI = 30; %Initial temperature
DT = (TF-TI); % Change in temperature
pair = 1.225; %density of air
CVair = 0.7578; %specific heat of air kJ/kg
Voltage = 12;
I = 5.5;
Pw = Voltage*I
Qc = 20;



Qwater = pwater*Vwater*Cpwater*dtwater*0.2778%(KJ) to Wh
Qaluminium = Pal*Cp*V*DT*0.2778%(KJ) to W
Qair = (V*pair*CVair*DT)*0.2778%(KJ) to W
Qtot = Qaluminium+Qair+Qwater

COPtec = Qc/Pw

Qwater =

    -5.8060e+000


Qaluminium =

   -64.5153e+000


Qair =

   -24.3752e-003


Qtot =

   -70.3457e+000
```

A.4 Heat sink

Table 5-4 heatsink Variables

Type	**MATLAB Variable**	**Variable**
Number of fins	n	15
Convective heat transfer	h	25 w/m^2
T_{base}	T	65 °C
T_{∞}	T	25 °C
Thermal conductivity	k	195 W/m °C
Height of find from base	b	0.025 m
Fin thickness	t	0.001 m
Boundary condition	m	16.0128 °C
Fins Heat transfer	**MATLAB Variable**	**MATLAB calculated**
Fin efficiency	Nf	984.4720e-003
Length of fin (m)	Lf	200.0000e-003
Width of fin (m)	Wf	2.0000e-003
Area of fin (m^2)	Af	400.0000e-006
Single Heat dissipated (W)	Qf	334.7205e-003
Base Heat transfer	**MATLAB Variable**	**MATLAB calculated**
Length of base (m)	Lb	200.0000e-003
Width of base (m)	Wb	100.0000e-003
Area of base (m^2)	Ab	20.0000e-003
Single Heat dissipated (W)	Qb	17.0000e+000

Below the MATLAB calculations

```
clc
clear
%To calculate the amount of Q in watts the Heatsink can remove: Written by
%Vincent Blagotinsek

%variables common to the heatsink of interest
n = 15; %number of fins
h = 25; %Convective heat transfer coefficients (PAGE 93 THERMO DYNAMIC
ENGINEERING BOOK)
z = 10e-3; %air gap between fins
Tbase = 64; %Hot temp base
Tinfinity = 30; %ambient
k = 237; %thermal conductivity aluminium
b = 15E-3; %Height of fin from base of heatsink
t = 1E-3; %Fin thickness;
m = sqrt(2*h/(k*t)); %Calculated heat transfer from a single fin
Ob = Tbase - Tinfinity; %Boundary conditions

%Fins heat transfer
Nf = tanh(m*b)/(m*b);%Fin efficiency (usually lie between 0.7-0.7)
Lf = 200E-3; %Length of 1 fin
Wf = 2E-3; %Width of fin
Af = Lf*Wf; %area of fin
Qf = Nf*h*Af*Ob; %Single fi

%Base heat transfer
Lw = 200E-3; %Length of base
```

```
Ww = 100e-3; %Width base
Aw = Lw*Ww; %Area of base
Qw = h*Aw*Ob;

%overall Q dissipated
Qtotal = n*(Qf + Qw) %(W)
Qtotal =

   260.0208e+000
```

A.5 Energy requirement of thermal housing

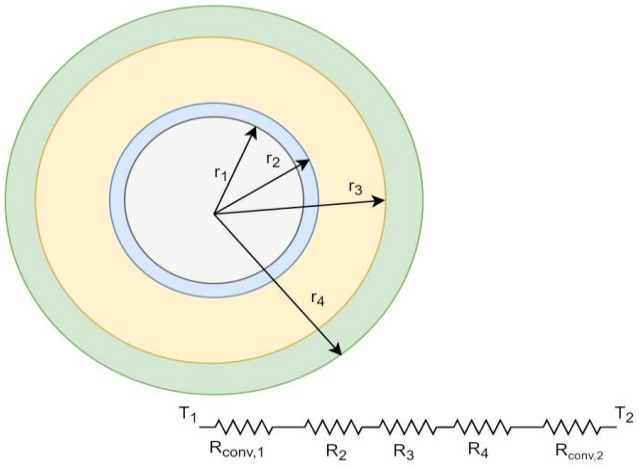

r_1: Inner chamber radius
r_2: Aluminium section radius
r_3: Polyurethane Insulation radius
r_4: Bucket radius
$T_{\infty,1}$: Inside temperature
$T_{\infty,2}$: Outside temperature

R2, R3, R4: Thermal resistances.

Figure 5-3 Thermal Housing profile. TOP view

Table 5-5 Thermal profile values

Constants	Reference		Constants	Reference
$R_{conv,1}$:	$1/h_1A_1$		h_1: 25 W/m^2	[99]
(Aluminium) r_2: 0.865 m	Measured		k_1: 237 W/m ºC	[94]
(Fomofill) r_3: 0.133 m	Measured		k_2: 0.04 W/m ºC	[93]
(Polyurethane) r_4: 0.133	Measured		k_3: 0.33 W/m ºC	[94]
$R_{conv,2}$:	$1/h_2A_2$		h_2: 25 W/m^2	[100]
$T_{\infty,2}$: 30 ºC	Inner Temp		A_1: 0.0235 m^2	Measured
$T_{\infty,1}$: 15ºC	Ambient temp		A_2: 0.0581 m^2	Measured
L: 0.265 m	Measured			

Below is the equations that determine the conduction and convection variables between each section of the thermal housing.

$$R_{Total} = R_{conv,1} + R_{cyl,1} + R_{cyl,2} + R_{cyl,3} + R_{conv,2} \tag{35}$$

$$R_{conv} = \frac{1}{h_1 A_1} \tag{36}$$

$$R_{cyl} = \frac{ln\left(\frac{r_o}{r_i}\right)}{2\pi L k_1} \tag{37}$$

$$Q_{in} = \frac{T_{\infty 2} - T_{\infty 1}}{R_{Total}} \tag{38}$$

$$Q_{in} = \frac{T_{\infty 2} - T_{\infty 1}}{\frac{1}{h_1 A_1} + \frac{ln\left(\frac{r_2}{r_1}\right)}{2\pi L k_1} + \frac{ln\left(\frac{r_3}{r_2}\right)}{2\pi L k_2} + \frac{ln\left(\frac{r_4}{r_3}\right)}{2\pi L k_3} + \frac{1}{h_2 A_2}} \tag{39}$$

Below the MATLAB calculations

```
clc
clear
clc
clear
%To calculate the Q lost to atmosphere and insulation effectiveness

T1 = 15+273.15; %TEMPERATURE OF INNER K
T2 = 30+273.15; %TEMPERATURE OF OUTER K
%radius of each segment
r1 = 0.0865; % aluminium inner m
r2 = 0.0875 ; % aluminium outer m
r3 = 0.133; % Fomofill m
r4 = 0.136; %Plastic m

A1 = pi*r1.^2; %Area of Aluminium m2
h1 = 25; %Heat transfer coefficient of inner (W/m2)
h2 = 25; %Heat transfer coefficient of outer W/m2
A2 = pi*r4.^2; %area of outer m2

L = 0.265; %Length of the compartment m

%Thermal conductivities 1W/m C = 1W / m K
k1 = 237;       %Aluminium
k2 = 0.04;      %Fomofill
k3 = 0.33;      %Polyethylene (HDPE)

%Convective transfers
Rconv1 = 1/h1*A1; %inner to aluminium
Rconv2 = 1/h2*A2; %outer to atmosphere

%Thermal resistances
R1 = log(r2/r1)/(2*pi*L*k1); %Aluminium
R2 = log(r3/r2)/(2*pi*L*k2); %Fomofill
R3 = log(r4/r3)/(2*pi*L*k3); %Plastic

disp('Steady state heat transfer rate through the three layer cylinder')
Qlost = (T2-T1)/(Rconv1+R1+R2+R3+Rconv2) %W

Steady state heat transfer rate through the three-layer cylinder
Qlost =

     2.3694e+000
```

A.6 Heat transfer through microenvironment

PBR has been calculated using the area of a cone equation while it is not the most accurate representation of a PBRs geometry it resembles a similar shape.

$$A_{PBR} = \pi \cdot r_{PBR} \cdot \left(r_{PBR} + \sqrt{{h_{PBR}}^2 + {r_{PBR}}^2} \right) = 0.03\ m^2 \qquad (40)$$

Assumptions of the mathematical model: The area of a cone is assumed to be similar to that of the PBR flask used. The temperature of the internal environment T_s has already reached steady state so the water temperature is assumed to have reached the same temperature. The worst-case scenario heat transfer coefficient of 25 W/m^2 is adopted.

Table 5-6 Mathematical model of PBR

Variable	Constants	Description	Variable		Description
Tw	calculated	Temperature Water	**A**	0.03	Area
Tal	calculated	Temperature Aluminium	**Kal**	235	
Tf	calculated	Temperature Fomofill	**Kf**	0.04	
Tp	calculated	Temperature plastic	**Kp**	0.02	
Ts	calculated	Temperature surrounding	**rpbr**	0.08 m	
TTEC	-5 ºC	Temperature TEC	**hpbr**	0.06 m	
Tinfinity	30 ºC	Temperature Outdoor	**h**	25 W / m^2	
Cpw	4.18	Specific heat water			
Pw	1000	Density water			
Qw	5.8	Heat energy water			

$$\frac{dT_w}{dt} = -h \cdot C_{pw} \cdot (T_w - T_s)$$

$$\rho \cdot C_{pw} \cdot Q_w \cdot V \cdot \frac{dT_w}{dt} = -h \cdot A_{PBR} \cdot C_{pw} \cdot (T_w - T_s)$$

Water
$$\frac{dT_w}{dt} = -\frac{h \cdot A_{PBR} \cdot C_{pw} \cdot (T_w - T_s)}{\rho \cdot C_{pw} \cdot Q_w \cdot V} \qquad (41)$$

Aluminium
$$\frac{dT_{al}}{dt} = -k_{al}(T_{al} - T_s) - k_f\left(T_{al} - T_f\right) - T_{TEC} \qquad (42)$$

Polyurethane
$$\frac{dT_f}{dt} = -k_f\left(T_f - T_{al}\right) - k_p\left(T_f - T_p\right) \qquad (43)$$

Polyethylene
$$\frac{dT_p}{dt} = -k_p\left(T_p - T_f\right) - k_p\left(T_p - T_\infty\right) \qquad (44)$$

Below the MATLAB calculations

```
function xdot = funfile(t,x);

%Using Newtons Law of cooling to solve for the temperature
%Written by Vincent Blagotinsek
%x(1) = water: Tw k1 water
%x(2) = aly: Tal k2 ally
%x(3) = fomo: Tfomo kf = Fomofill
%x(4) = plastic: Tplastic k4=poly

h= 25;
A= 0.03;
pwater= 1000;
V= 0.0005;
cp=4.18;
Qwater = 5.8;

Kal = -235;
Kfomo = -0.04;
Kpoly = -0.02;
Ts = 15;
Ttec = -5;
Toutside = 30;

xdot(1) =   -h*A*cp*(x(1)-Ts)/(pwater*V*cp*Qwater);
xdot(2) =   Kal*((x(2)-Ts)) + Kfomo*((x(2)-x(3)))-5;
xdot(3) =   Kfomo*((x(3)-x(2))) + Kpoly*((x(3)-x(4)));
xdot(4) =   Kpoly*((x(4)-x(3)))+ Kpoly*((x(4)-Toutside));

xdot = [xdot(1) xdot(2) xdot(3) xdot(4)]';


%Heat transfer through the  micro environment.
clear
clc
t0 = 0; tf = 200; span = [t0, tf];

%Initial conditions
x0 = [25 15 20 30]';
options =[];

[t,x] = ode45('funfile',span,x0,options);


plot(t,x(:,1),'b:')
title('Change in Water temperature');
ylabel('Temperature (C)');
xlabel('Hours');

plot(t,x(:,2),'m:')
title('Change in Aluminium temperature');
ylabel('Temperature (C)');
xlabel('Hours');
%
plot(t,x(:,3),'r:')
title('Change in Fomofill temperature');
ylabel('Temperature (C)');
```

```
xlabel('Hours');

plot(t,x(:,4),'k:')
title('Change in Plastic Mould temperature');
ylabel('Temperature (C)');
xlabel('Hours');
```

Appendix B. Calibration curves

B.1 Agitator Motor

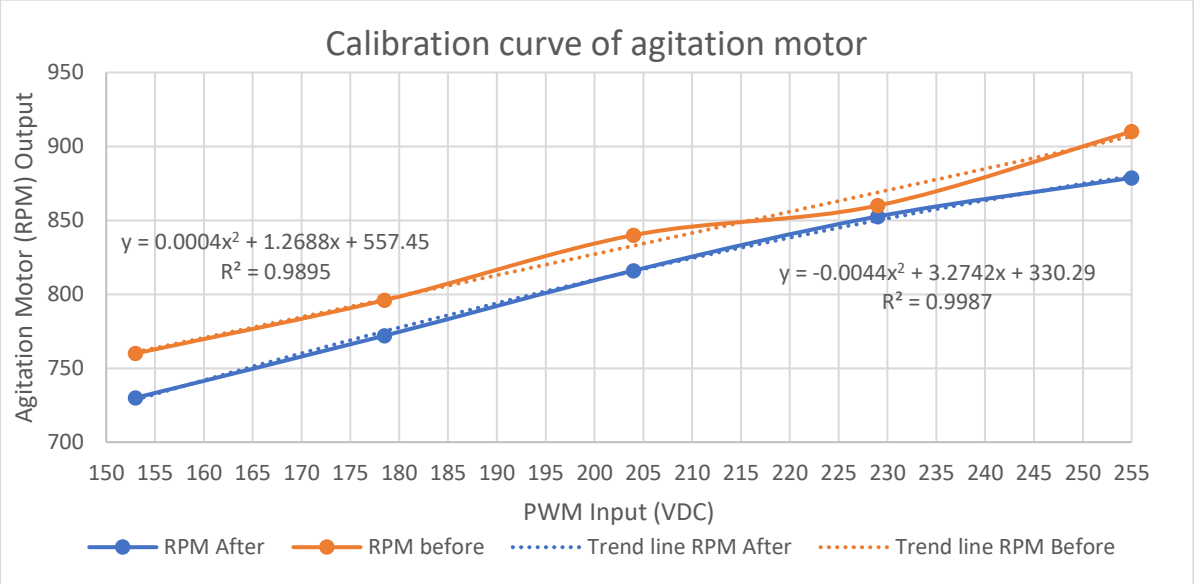

Figure 5-4 Calibration curve of agitation motor before and after
The calibration curve illustrates that the magnet housing has a small effect on the overall output of the agitation motor. After a PWM signal of 153-255 is sent to the motor different RPMs are observed

The RPM values are obtained using a Digital Tachometer DT-48 has the accuracy of ± 0.05%. RPM measurements are obtained before and after the magnet housing is attached. This is done to observe the RPM loss and the effect that an induced magnetic field has on the RPM. Evidently there is a distinguishable difference that can be explained. The 3D printed housing and the two magnets increase the mass of the on the fan.

B.2 PI manipulated variable output

Calculation of the PWM output calculated by slope of a straight line 255/5 Eq. (45). Arduino microcontrollers PWM reads between 0 and 255. Using the calibration curve amplifies the PM signal.

$$PWM_{out} = 51 \times (\Delta v_k) \quad (45)$$

Appendix C. Temperature control design

C.1 PI controller design

The values chosen are based off the behaviour of the PI controller MV. It is understood that too much aggressive switching of the PWM will cause overheating of the MOSFET.

Table 5-7 Qualitative PI Controller values

Kc	Taui	Dt
3	0.03	1

Appendix D. Electrical and Power

D.1 Power consumption and cost

Below illustrates the power consumption to keep 500mL of water at a constant temperature of 19 ºC. **Example 1**: Assumes the worst-case scenario: The power supplies are considered to operate 24 hours per day, 8760 hours in 1 year. **Example 2**: Assumes the best-case scenario: The auxiliaries are only operating.

Table 5-8 Energy consumption of micro environment

Device	Total	Volts (VDC)	Current (A)	Power (W)
Power supplies 1	1	12	3.5	42 W
Power supplies 1	1	CH1 12, CH2 5	CH1 9.2A CH2 3A	125.4 W
Fan	3	12	80 mA	2.88 W
TEC	66	12	5.5	66 W
RGB	3m	12	0.6A per metre	21.6 W

First example: Assuming the total power supply is P1 + P2 and the cost of electricity per kW is 28.33 cents/kWh.

$$E_{total} = 1466.24 \frac{kWh}{year} \quad (46)$$

The total cost per year

$$Cost\ per\ year = \$415.39 \quad (47)$$

Second example: Ignoring the power supplies allows for a better idea of what the devices are consuming alone. If the axillaries such as the lights, TEC, heatsink cooling fans and agitation motor, then total power consumed is 90.48 W and will cost $224.55 to run this system.

D.2 Electrical Schematic diagram

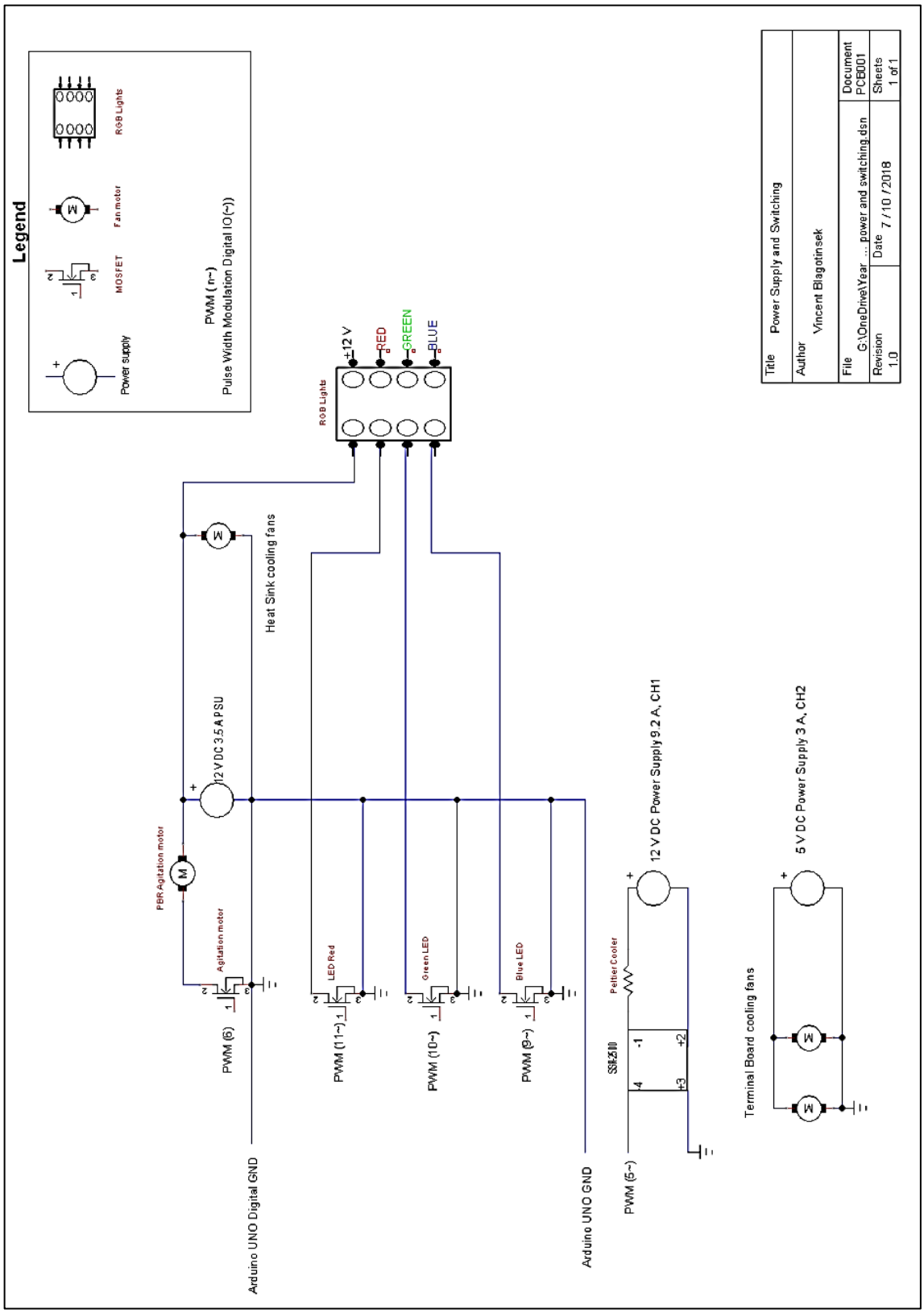

Figure 5-5 Electrical Schematic diagram

D.3 PCB Schematic drawing 001

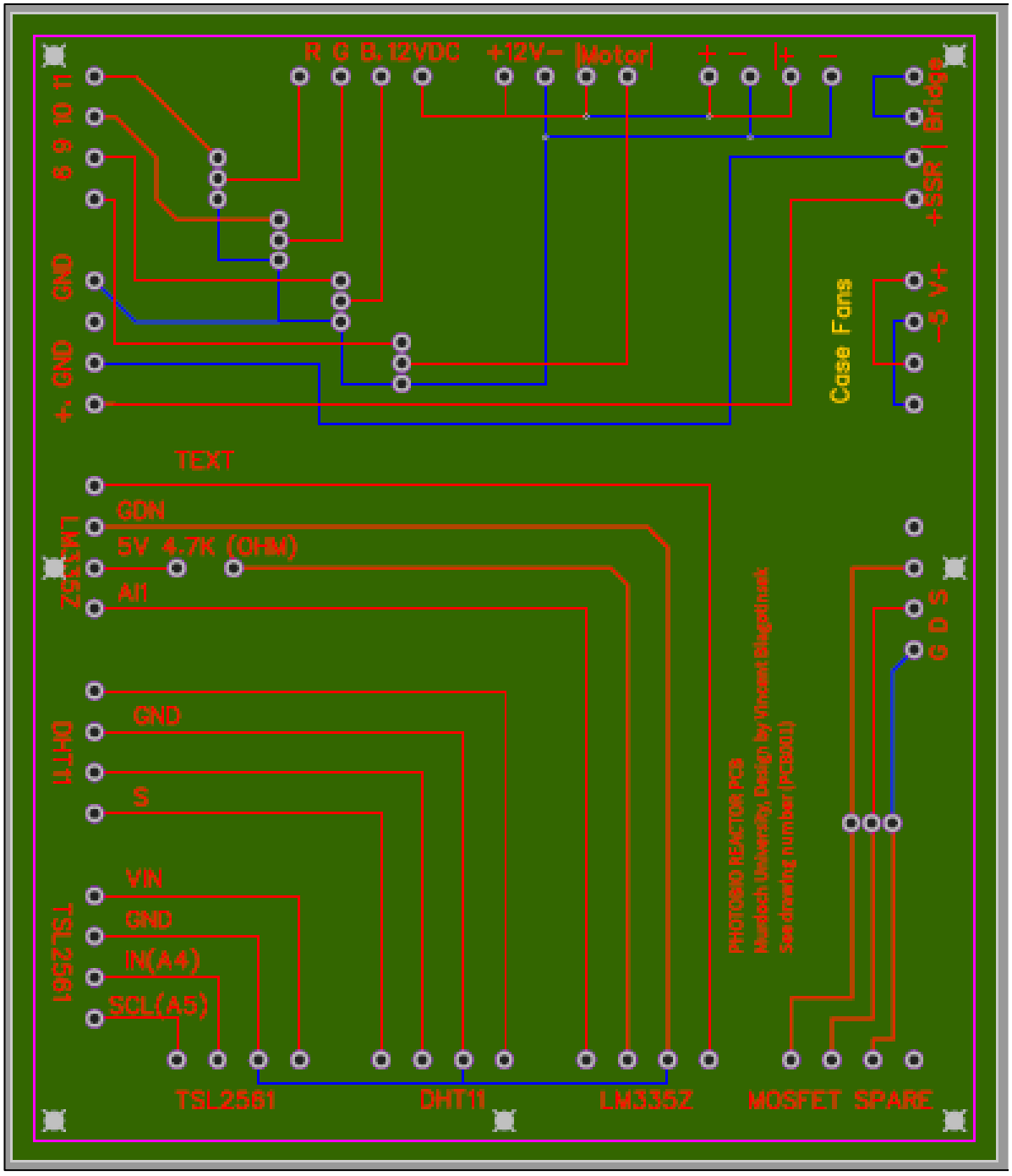

Figure 5-6 PCB 001 Drawing
This is a two layered PCB board. The red is top surface while the blue is the second surface. The grey holes are the drill holes which are used to mount the board. Photo credit (The Author)

Appendix E. Arduino Sketch

Written By Vincent Blagotinsek: 29 October 2018

```
#include <DallasTemperature.h>
#include <OneWire.h>
#include <dht.h>
#include <Wire.h>
#include "BlueDot_BME280_TSL2591.h"
BlueDot_BME280_TSL2591 bme280;
BlueDot_BME280_TSL2591 tsl2591;
#define dht_apin A0
float tempK=0, tempC=0, tempF=0;
dht DHT;
#define ONE_WIRE_BUS 2
OneWire oneWire(ONE_WIRE_BUS);
DallasTemperature sensors(&oneWire);
void setup(){
  Serial.begin(9600);
     tsl2591.parameter.I2CAddress = 0x29;
        Wire.begin();
   tsl2591.parameter.gain = 0b00;
   tsl2591.parameter.integration = 0b000;
   tsl2591.config_TSL2591();
   bme280.parameter.IIRfilter = 0b100;
   sensors.begin();
 }
 void loop(){
tempK = analogRead(1) * 0.004882812 * 100;
tempC = tempK - 273.15;
DHT.read11(dht_apin);
sensors.requestTemperatures();
   Serial.print((DHT.temperature+tempC)/2);
   Serial.print("\t");
      Serial.print(DHT.humidity);
   Serial.print("\t");
       Serial.print(tsl2591.readIlluminance_TSL2591());
   Serial.print("\t");
     //Serial.println(tempC);
  //Serial.print("\t");
    Serial.print(sensors.getTempCByIndex(0));
    Serial.println();
 delay(250);
}// end loop()
```

E.1 LUX sensor calibration

Higher gain values are better for dimmer light conditions but lead to sensor saturation with bright light.

0b00: Low gain mode

0b01: Medium gain mode

0b10: High gain mode

0b11: Maximum gain mode

Longer integration times also helps in very low light situations, but the measurements are slower

0b000: 100ms (max count = 37888)

0b001: 200ms (max count = 65535)

0b010: 300ms (max count = 65535)

0b011: 400ms (max count = 65535)

0b100: 500ms (max count = 65535)

0b101: 600ms (max count = 65535)

The IIR (Infinite Impulse Response) filter suppresses high frequency fluctuations In short, a high factor value means less noise, but measurements are also less responsive You can play with these values and check the results! In doubt just leave on default

0b000: factor 0 (filter off)

0b001: factor 2

0b010: factor 4

0b011: factor 8

0b100: factor 16 (default value)

Appendix F. Hybrid refrigerator

Figure 5-7 Hybrid Refrigeration
Stirring and agitation beds can be constructed to save costs while already established photobioreactors with nutrients and pH could be supplied in from an insulated compartment. Refrigeration units are not expensive to run and can help maximise the microalgae close to its optimal growth conditions. Photo credit: The Author

F.1 Job safety analysis form

Murdoch UNIVERSITY

Job Safety Analysis

Work Request: 1

Permit Number: 1

1 To be completed by the Work Team Lead

1a	Date / Date Range:	June 2018-November 2018	Contractor Company Name:	Thesis project
1b	Name of Work Team Lead:	Vincent Blagotinsek	Work Team Lead contact number:	na
	Name of Responsible officer:	Vincent Blagotinsek	Responsible Officer contact number:	na
1c	Work Area Location:	Home use		
	Building:	Home	Floor(s): 1	Room(s): 4
				Number of Workers: 1
	Work to be undertaken:	Design and contstruct PBR, connect 12VDC to auxilleries and power supply 240 VAC		
1d				
1f	Attached list of Safe Work Method Statements or Procedures:			

2 Personal Protective Equipment Requirements

All boxes must be checked with either a YES (☑) or Not Applicable (⊟)

2a	☑	Eye Protection	☐	Half face mask respiratory protection	☐	Full face mask respiratory protection	☐	Head Protection	☐	High Visibility Clothing	☐	Working at Heights	☐	Hand Protection	☑	Chemical Suits				
2b	☑	Foot Protection	☐	Protective Body Clothing	☑	Face Protection	☑	Hearing Protection	☐	Fall Arrest with Harness	☐	Other (Specify):								

2c Hazard Identification

The hazards indicated below are only a prompt and not an complete table of hazards you may encounter.

2d	☑	Electrical	☐	Laser Risk	☐	Non-Ionising Radiation	☐	Biological	☐	Flammable Materials	☐	Poisons	☐	Radiation	☐	Chemical				
2e	Responsible Officer	By signing off on the JSA we agree that the hazards have been identified, and the control measures assigned, as being able to mitigate the identified hazards.		Signature:						Office/ School:	Home				Date:	June 2018				
2f	Work Team Lead	By signing off on the JSA we agree that the hazards have been identified, and the control measures assigned, as being able to mitigate the identified hazards.		Signature:											Date:	June 2018				

3 Work Team Sign On

	Role	Name	Signature	Date	Role	Name:	Signature	Date
	Student	Vincent Blagotinsek		June 2018				

JSA – JOB SAFETY ANALYSIS

A JSA is a tool for managing and recording the hazards associated with work tasks and identifies the tasks required to do a job, identifies the hazards associated with those tasks, and identifies controls to mitigate those hazards. The J&A is simply taking the time to: Plan the job, have I got right tools and equipment, correct materials, right people to assist me where required, have I got right personal protective equipment, identify hazards associated with the job and record job steps for safety-Do not assume that all those involved know what to do and how to do it in a safe manner.

STEPS INVOLVED IN DEVELOPING J&A'S

- Select the job/task.
- Break down task/job into sequential steps and record on JSA.
- Identify hazards within each step and record on JSA.
- Develop appropriate control solutions to eliminate or minimize the hazard and record on JSA.

How many steps depends on the complexity of the job/task (some will break down into 3-4 steps some may require more than a dozen steps).

Step	Significant Task Activity (What are we going to do?)	Identified Hazards (What can hurt us or someone else?)	Control Measures or Action Required (What are we going to do about the hazards?)	Assigned Person Specific JSA-Assigned Workgroup member the implement control	
				Name	Initial when complete
1.	Connect wires into power supply	Electric shock	use certified tools and correct electrical workers number	Vincent	VB
2.	Design and build PBR housing	Power tools not suitable for task	Ensure correct tools for the jo	Vincent	VB
3.		Cuts from sharp edges	Wear gloves when working	Vincent	VB
4.		Other people in area	Communicate with people in area to notify them of hazards	Vincent	VB
5.		Trips on untidy work surfaces	Ensure all tools are put away correctly and no hazards on floor	Vincent	VB
6.	Commissioning of equipment	Incorrect connections to PCB board	Confirm all connections from electrical drawing	Vincent	VB
7.		Not site compliant	Before taking to Murdoch university get PBR certified by staff	Vincent	VB
8.	Clean work area	Tools and equipment left inside PBR	Ensure PBR is tidy and no tools left around	Vincent	VB
9.		Tools and equipment left laying around	Put all tools and equipment away	Vincent	VB
10.				Vincent	VB

Notes

Total words: ~14,720.

Not including table of contents, endnotes, equations, headers, tables, figures, dedication and acknowledgements.

Total document word count is 24,420